RACE for 2030

RELIABLE
AFFORDABLE
CLEAN
ENERGY

N2 Research Report

Investigation into Voltage Management Technologies for Future Australian Suburban Distribution Networks

Final Report

Australian Government
Department of Industry, Science and Resources

AusIndustry
Cooperative Research Centres Program

RACE for Networks

Research Theme N2: Low voltage network visibility and optimising DER hosting capacity

ISBN: 978-1-922746-46-7

Industry Report

Investigation into Voltage Management Technologies for Future Australian Suburban Distribution Networks

September 2023

Citations

Razzaghi, R., Burstinghaus, E., Gerdroodbari, YZ., Hibbert, M., and Liu, J. (2023). Investigation into Voltage Management Technologies for Future Australian Suburban Distribution Networks. Prepared for RACE for 2030 CRC.

Project partners

Project team

Monash University

- Dr Reza Razzaghi
- Dr Edward Burstinghaus
- Yasin Zabihinia Gerdroodbari

eleXsys Energy Pty Ltd

- Dr Jiannan Liu
- Mark Hibbert

Acknowledgements

The authors would like to thank the stakeholders involved in the development of this report, in particular the interviewees and the industry reference group members who have given so generously of their time, including Monash University, EleXsys Energy, Western Power, CSIRO, Climate-KIC, Energy Queensland, Ausgrid and Energy Consumers Australia. Whilst their input is very much appreciated, any views expressed here are the responsibility of the authors alone.

Acknowledgement of Country

The authors of this report would like to respectfully acknowledge the Traditional Owners of the ancestral lands throughout Australia and their connection to land, sea and community. We recognise their continuing connection to the land, waters and culture and pay our respects to them, their cultures and to their Elders past, present and emerging.

What is RACE for 2030?

RACE for 2030 CRC is a 10-year cooperative research centre with AUD350 million of resources to fund research towards a reliable, affordable and clean energy future. racefor2030.com.au

Disclaimer

Contents

List of Acronyms

ABS – Australian Bureau of Statistics

AEMO – Australian Energy Market Operator

AER – Australian Energy Regulator

BAU – Business as Usual

BESS – Battery Energy Storage System

CECV – Customer Export Curtailment Value

CSIRO – Commonwealth Scientific and Industrial Research Organisation

DAPR – Distribution Annual Planning Report

DER – Distributed Energy Resource

DNSP – Distribution Network Service Provider

dSTATCOM – Distribution Static Synchronous Compensator

EV – Electric Vehicle

HEMS – Home Energy Management System

ISP – Integrated System Plan

LDC – Line Drop Compensator

LVR – Low Voltage Regulator

MEN – Multiple Earthed Neutral

NER – Neutral Earthing Resistor

OLTC – On-Load Tap Changer

PV – Photovoltaic

QDSL – Quasi Dynamic Simulation Language

STATCOM – Static Synchronous Compensator

Executive Summary

This report investigates voltage management and curtailment issues in Australian distribution networks that contribute to DER hosting capacity challenges for these networks. A highly detailed and realistic power system model, including 11 kV and 433 V levels of the network for a suburb in Brisbane, Queensland has been assembled in the program DIgSILENT PowerFactory. Representations of the low voltage connections to individual households and businesses in this suburb were incorporated into the model, so that an unprecedented clarity of modelling insight into these issues could be gained. The network model was also baselined using real-world transformer monitor and SCADA measurements provided by Energy Queensland, so that the study would commence from an accurate representation of current network conditions.

Components which implement the volt-watt and volt-var algorithm that are mandated by AS4777.2 were developed and incorporated into the network model so that the phenomenon of curtailment could be measured. Projections in the growth of both rooftop PV inverter installations and electric vehicles out to 2050 were also incorporated into the study. The projections spanned 2025 – 2050 and were sourced from two of AEMO's 2022 ISP scenarios: Slow Growth and Step Change. Their inclusion in the study facilitated an assessment of the credible range of possible levels of impact on the voltage management of the network that DER may have in future. Export limits were applied only to the existing PV generators for which records indicated they were in place; export limits were not applied to future PV installations.

The overall level of curtailed solar energy across all years of both scenarios was found to be negligible when viewed as a proportion of delivered solar energy. For subsets of the customers at the fringe areas of the studied network however, the levels of curtailment are significant in both scenarios and exhibit substantial year on year growth in Step Change. Violations were identified affecting both the upper and lower voltage limits across the network at noon and during the evening peak respectively; violations exist in both scenarios but are more severe and only exhibit significant year on year growth in Step Change. Voltage unbalance throughout the LV network was also found to be a relatively significant issue in the future, even though it appears to be well within limits at present.

A simplified hosting capacity assessment, considering voltage management requirements, was performed using the criterion that not more than 5% of the low voltage buses in the network model should exhibit voltages exceeding either of the upper or lower statutory limits on any of their phases. Despite the voltage support provided by the volt-watt and volt-var functions, the network was found to reach its hosting capacity at noon due to solar PV induced overvoltages shortly after 2030 in the Step Change scenario. During the evening peak however, the network was not found to reach hosting capacity in either scenario despite voltages being gradually pushed downwards by increased volumes of electric vehicle charging at this time of day. This indicates that overvoltages caused by PV are likely to become a pressing issue sooner than are undervoltages due to EV charging.

A sensitivity analysis with respect to the volt-watt and volt-var control functions was also performed. It was found that the assumption of universal absence of these functions lead to dramatically higher overvoltages at noon which would see inverter level protection functions activate across the network in practice. This highlights the effectiveness of AS4777.2 in managing voltage and the importance of compliance with it.

An assessment into the effectiveness of distribution-scale static synchronous compensators at addressing curtailment and overvoltage due to PV penetration at noon was performed for the 2035 Step Change version of the network model. Out of the 229 low voltage areas represented, six specific areas exhibiting the worst

curtailment were selected for this assessment. The more traditional network augmentation strategies of low voltage distribution line re-conductoring as well as employment of more recently developed on-load tap changers on distribution transformers were also simulated for comparison. A third traditional network augmentation strategy of altering the zone substation LDC settings was considered but eventually discarded, owing to the fact that the existing LDC voltage settings at the modelled zone substation are already relatively low.

It was found that re-conductoring exhibits the poorest performance while on-load tap changers exhibit the best performance, followed closely by static synchronous compensators. With only one static synchronous compensator per LV area, the curtailment in the six areas assessed is alleviated more than for re-conductoring, but the proportion of LV buses violating the upper limit is not significantly improved. With multiple static synchronous compensators equivalent to the number of LV feeders in each LV area installed however, the improvement in the latter metric almost matches the improvement that is achieved by the on-load tap changer solution. The effectiveness of on-load tap changers is, however, limited by the fact that it can only furnish uniform upward or downward translation of the three low voltage phase voltages. The severe voltage unbalance in the futuristic state of the network therefore means that two out of the six low voltage areas assessed cannot have on-load tap changers installed, lest the voltage on their minimal phase be pushed below the lower limit in the attempts to lower the phases in overvoltage. The outcomes reported for the on-load tap changer solution are therefore highly dependent on which low voltage areas are selected. The static synchronous compensator on the other hand can correct low voltage phase unbalance; the utility of this functionality would therefore make it a more robust solution than the tap changer. With widespread deployment, although not modelled in this study, the impact of reactive power flowing through the MV system would also improve voltage management at that level, thus producing a two-tier impact that no other studied solution could provide.

A cost-benefit analysis was also conducted which found that the multiple static synchronous compensator option would outperform the other options considered both in terms of having lower cost and high annual benefit as measured by the customer export curtailment value metric. This demonstration of the superior cost-effectiveness of the static synchronous compensator as a solution for distribution network voltage management issues indicates that it will be useful in maximising the value of investments in the distribution network in a lot of cases. It is therefore likely that this technology will play an instrumental role in future urban renewable energy zones.

This study also identified an abundance of thermal limit violations on distribution lines and transformers in the future states of the area studied during noon under high solar day conditions. Significantly smaller levels of overloads were identified during the evening peak when EVs had been assumed to be maximally charging. The thermal overload trends for distribution transformers in particular were the highest in all years of both ISP scenarios, indicating that this type of distribution network equipment will be likely to be the one that requires the most frequent and immediate upgrades in the years ahead. The thermal overload issues were actually found to be more significant than the over and undervoltage issues in terms of their severity and upgrades to line and transformer ratings were found to be inadequate in addressing them in the 2035 Step Change version of the model. It is suggested that a BESS solution may be more effective at addressing these issues.

1 Introduction

This report details the findings of a fast-track project within the RACE for 2030 research program under the sub-theme N2b; assessing and mapping the DER hosting capacity of energy networks. Australia is undergoing an energy revolution, in which the landscape of energy technologies will change drastically. One of the unanswered questions in this area is the extent to which different sections of Australian power distribution networks will be able to host distributed energy resources (DER); their so-called "hosting capacity".

Distribution networks in Australia were originally designed to facilitate the transfer of power only in the direction from transmission networks down into households and businesses. Their voltage regulation facilities therefore do not cater for the occurrence of voltage rise at the load end. Given the steady rise in the penetration of photovoltaic (PV) generating systems on Australian rooftops in recent years, voltages in some areas of the distribution networks have started to exceed statutory limits during high solar generation periods [1], [2]. This level of voltage rise can damage or shorten the usable lifespan of consumer appliances, cause spurious over-voltage protection tripping if it is sufficiently severe and result in the loss of renewable energy through the mechanism of curtailment. As the trend in residential, commercial and industrial PV uptake is set to accelerate in the coming years, this problem can be expected to worsen if no remedial measures are taken.

Electric vehicles (EV), the charging load of which could drastically increase peak loads on distribution networks, also sits just over the horizon. The under-voltage events that could be caused by this technology, especially if its adoption proves to be more rapid than that of home battery systems, could also cause significant operational issues for Australian distribution networks. The default industry solution to these problems includes upgrading conductor and/or transformer sizes or splitting existing LV areas by the addition of new distribution transformers and reconfiguration of open points. The cost of this solution would be all but prohibitive however, especially over the relatively short timescale over which it would have to occur.

The purpose of this study is to investigate the effectiveness of new solutions to the expected voltage management issues that are likely to occur in Australian distribution networks. Such new solutions will potentially constitute alternatives to the status quo of conductor upgrades and the addition of new transformers.

1.1 Background

One of the most challenging aspects of assessing hosting capacity in Australian distribution networks is that these networks are largely invisible to network operators at present [3]. This is attributable to the fact that activity within them was sufficiently limited by their design and by the predictable behaviour of consumer loads, such that adherence of the voltages within them to the statutory limits could generally be inferred by investigation of the voltages and currents at the nearest distribution substation alone. For this reason, detailed records of the topology, length, impedance, and distribution of customers on distribution networks are not necessarily maintained by Australian network utility companies in formats that facilitate rapid estimation of the state of the consumer end of the network. Monitors which measure and record currents, voltages and power flows have also historically not been installed at this end of the system.

Now that Australian distribution networks contain significant volumes of rooftop PV and are expected to host larger volumes of this and other forms of DER in the coming years, the range and direction of power flows along them are changing at a pace much faster than they have at any other time in their history. The lack of monitoring facilities available to network operators, when it comes to the consumer end of distribution

networks, has meant that industry efforts to manage the effects of rapid PV uptake have been limited to placing uniform export limits across all connected customers and mandating the activation of volt-watt and volt-var control functions across all newly installed PV inverters. While these export limits and control functions appear to be effective at mitigating the over-voltages that would otherwise be caused by rooftop PV, due to a degree of energy curtailment associated with the volt-watt and volt-var control functions, they also prevent the renewably sourced energy that would have been injected into the network from being put to good use. This implies both an opportunity cost for the Australian economy as well as a direct cost for energy consumers trying to offset rising energy prices and pay off their investment in rooftop PV.

Solutions that will address the underlying voltage management issues that influence the hosting capacity in Australian distribution networks are drastically needed. These solutions will need to be more cost-effective than conductor upgrades and do a better job of exploiting the potential utility of DER than export limits and volt-var and volt-watt functions. One existing study in this area identified that installing residential battery systems will not provide an effective mitigation strategy for this problem if they are installed with the sole intention of maximising self-consumption at an individual customer level [4]. This is because operation of the batteries in this manner will mean that they finish charging at some point in the morning before the peak solar irradiance and corresponding over-voltages occur. This study also investigated the effectiveness of uprating of distribution transformers, replacing distribution transformers with upgraded versions that include two additional buck taps on their off-load tap changers or on-load tap changers (OLTCs), reconductoring of LV networks, installation of low-voltage regulator (LVR) devices and upgrades of existing PV inverters to include volt-watt and volt-var functionality in improving network hosting capacity. However, the installation of distribution-scale static synchronous compensators (dSTATCOMs) was not investigated. Furthermore, hosting capacity was assessed using gradual elevation of the volume of installed PV capacity on the LV networks studied, but no investigation of expected future trends in solar PV or EV growth was made.

Another study performed by Endeavour Energy, the distribution network operator for Greater Western Sydney and other regions of New South Wales, quantified the economic benefit of avoided future PV curtailment after applying a sequence of interventive strategies involving a variety of solutions [5]. These solutions included re-connection of customer phases in areas of heavy imbalance, transformer tapping where possible, transformer tap-changer upgrades, installation of LV dSTATCOMs and/or network batteries, reconductoring and splitting the LV networks between old and new distribution transformers. This study also included explicit modelling of curtailment as a result of volt-watt and volt-var functionality for future growth of PV inverters and EVs that can be expected if the most likely of the scenarios in AEMO's 2022 ISP eventuates [6]. The studies performed in [5] reveal a hierarchy of curtailment reduction from the different successive solutions investigated. For example, in the particular distribution network owned by Endeavour Energy, significantly larger improvements to future expected curtailment levels can be made by changes to existing off-load tap settings than by LV network augmentations. This study determines which of the LV augmentation solutions should be applied in each of the LV networks it investigates. Because it presents an optimised business case consisting of a mixture of several solutions, it offers no direct comparison between the technical or financial performance of different distribution network voltage management solutions. It also doesn't include LVRs or upgrades of distribution transformers to include OLTCs.

The relative effectiveness of dSTATCOMs for improving the management of voltages across distribution networks compared to conventional network solutions such as re-conductoring and OLTC installation has not yet been assessed on a per-installed-unit basis, however. Furthermore, the extent of the positive effect which these technologies can have on network voltages is dependent on the details of the distribution network to

which they are connected. A useful comparison of their performance must therefore be performed in studies on a variety of realistic distribution networks.

1.2 Study objectives and overview

The aim of this study was to demonstrate the effectiveness of dSTATCOMs as solutions to the voltage management problem which is one of the major factors that is expected to determine hosting capacities in Australian distribution networks in the coming years. It was also an aim to compare this effectiveness to that of re-conductoring and OLTC installation, which are two conventional network augmentation strategies. A detailed investigation using a realistic distribution network model encompassing a variety of actual feeder types was undertaken. The model included the entirety of a zone substation area within the network owned by Energy Queensland (EQ) down to the customer connection level. The identity of this particular zone substation has been omitted from this report. The network model, which will ultimately be made available, has also been de-identified to protect the identity of customers supplied from this system. The software package chosen for the study was DIgSILENT PowerFactory.

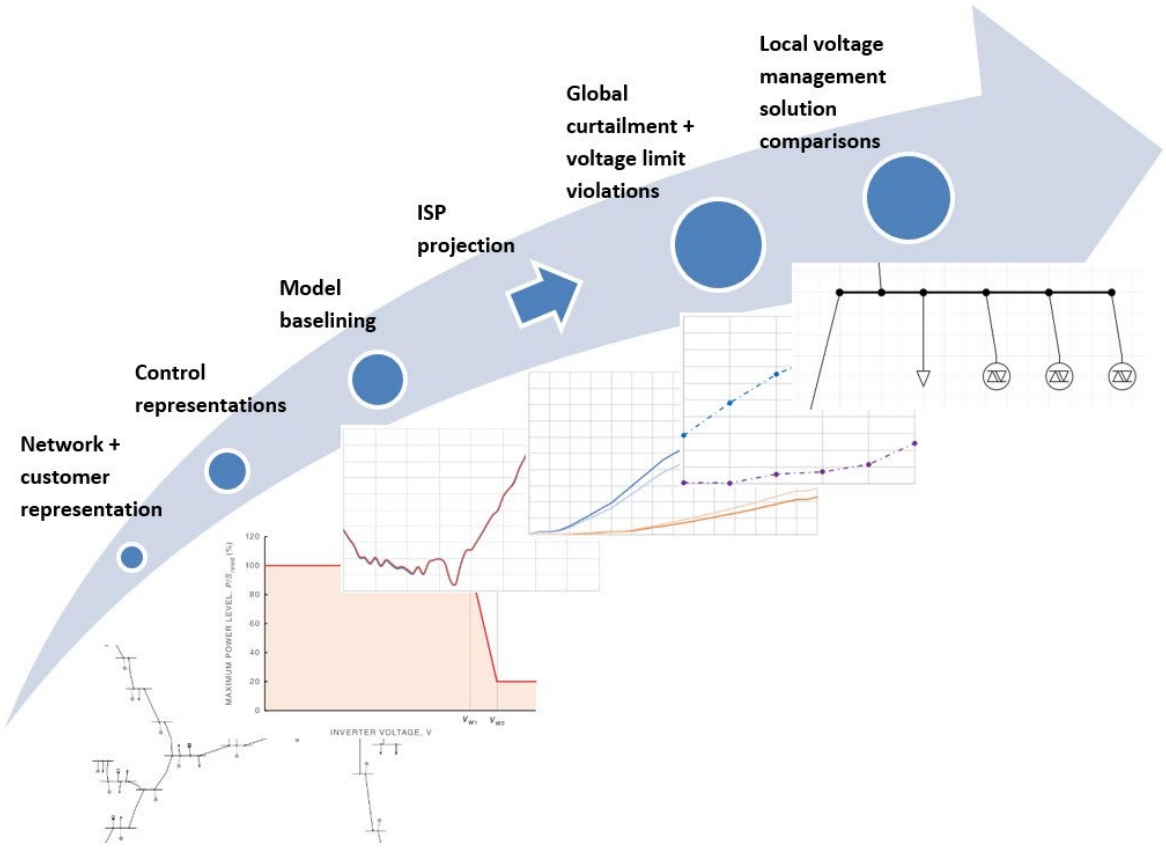

Figure 1 – High level overview of the study

A high-level overview of the studies presented in this report is shown in Figure 1. Low and medium voltage network and customer data was used to generate a network model. Representations of the important control mechanisms acting within that system, namely the volt-watt and volt-var functions on each of the solar inverters and the line drop compensator (LDC) algorithm in operation at the zone substation, were then incorporated into the model. Following this the model was baselined against real-world measurements of the voltages and power flows in the system being represented, then projections of the rate of growth in PV and EVs from AEMO's 2022 ISP [6] were applied to the model. The multiple versions of the model representing

hypothetical future states of the network against which baselining was performed were then used to develop global curtailment and voltage management results, as well as local results of the same sort in areas of the network identified as exhibiting relatively high levels of curtailment. These local results were then re-generated for multiple cases involving applications of different voltage management solutions, one of which included STATCOMs.

2 Network Data Gathering and Analysis

The study period chosen for baselining of the model was 30/04/2021 - 30/10/2022. A particular zone substation in the Energex network, which has been de-identified for the purposes of this report, was modelled in detail from the 33 kV level down to the LV level in PowerFactory.

2.1 Input data

Input data for the study provided by Energex included:

- PowerFactory MV (11 kV) network model for the modelled zone substation.
- Route length and conductor type data for all buried and overhead conductor routes in the LV (433 V) networks connected to modelled zone substation.
- Load location and phasing connection data for all loads (where known) in the modelled zone substation area. Phasing connections where this data was not known have been assumed.
- Rooftop PV location, size and phasing connection data for all rooftop PV installations in the modelled zone substation area. Phasing connections for solar PV systems where this data was not known have been assumed.
- Transformer monitor data for 153 of the 259 distribution transformers in the modelled zone substation area upon which monitors were found to be installed – this data consisted of phase to ground voltages, phase currents and voltage-current phase angles, as well as negative sequence voltage and total harmonic distortion, recorded every 10 minutes for the period of 30/04/2021 – 30/10/2022.
- SCADA data, consisting of B phase currents and BC phase line to line voltages, for each of the 11 kV feeders connected to the modelled zone substation.
- Control system setpoints and operating principles for the line drop compensator (LDC) algorithm in operation at the modelled zone substation, as well as the upstream bulk supply substation and other connected 33 kV substations in the area.
- On-load tap changer step sizes and range for the 33/11 kV transformers at modelled zone substation.
- Size and control system setpoints and operating principles for the 11 kV capacitor banks at modelled zone substation.

2.2 Existing network description

The existing network in the modelled area consists of 11 kV (MV) and 433 V (LV) feeders supplying 13,535 residential customer connections, as well as a further 785 connections to customers that would be classified as either commercial or light industrial. The modelled area is a typical suburb in Queensland and as such, the commercial customer connections are largely represented by small businesses such as restaurants, fuel stations, aged care homes, schools and shopping centres. The even smaller subset of the latter category of customer connections is mostly made up of warehouse facilities. Due to the lack of available transformer monitor data, the sizes of the loads representing the larger customers in the MV network model that was provided by Energex were left unchanged during the dynamic studies that were performed with the model in this study. Figure 2 provides a topological overview of the modelled network area.

Figure 2 – Topological overview of the modelled network area

The zone substation supplying the network in the modelled area consists of ten MV feeders which have been re-named as “Feeder 01” through to “Feeder 10” in line with the area de-identification previously mentioned. Several attributes which characterise these feeders are listed in Table 1. The different types of MV and LV overhead distribution lines and buried cables in the modelled area, as well as the cumulative installed lengths of each are further detailed in Table 2 through to Table 5. Note that the cumulative installed lengths indicate the relative prevalence of the different conductor types in the network.

Table 1 – Data characterising the ten MV feeders in the modelled area

Feeder	Feeder 01	Feeder 02	Feeder 03	Feeder 04	Feeder 05	Feeder 06	Feeder 07	Feeder 08	Feeder 09	Feeder 10
Total backbone length (m)	9029	4197	6254	3908	5808	3061	4848	4170	4804	2110
Total conductor length (m)	17141	6404	14958	8140	12931	9755	10501	10897	11246	2813
Proportion of MV that is underground (%)	87.16	4.5	19.15	33.27	75.33	25.9	20.5	40.8	35.48	41.46
Proportion of MV that is overhead (%)	12.84	95.5	80.85	66.73	24.67	74.1	79.5	59.2	64.52	58.54
Peak load kVA	3025	1124	2595	2269	3259	2596	2603	2125	3560	1640
No. of distribution transformers	39	15	36	27	25	29	25	15	34	14
Transformer installed capacity (kVA)	14938	4085	8371	10285	10603	9220	6755	10295	11370	6900
No. of LV feeders	95	28	54	56	63	63	51	23	78	19
Total LV feeder length (m)	37912	10115	21424	22564	31856	27839	23819	10589	29842	5790
Proportion of LV that is underground (%)	95.19	2.22	38.49	69.17	96.22	26.99	14.19	61.65	50.06	16.84
Proportion of LV that is overhead (%)	4.81	97.78	61.51	30.83	3.78	73.01	85.81	38.35	49.94	83.16

Table 2 – MV overhead conductor types and cumulative installed lengths within the modelled area

MV Overhead Line Type	Cumulative Distance in Model (km)	Proportion of all MV Overhead Line Distance in Model (%)
11 kV O/H - Other	0.103	0.3
HDBC 7/.08_100°C_11kV_A_SEQ	0.071	0.2
Pluto_75°C_11kV_B_SEQ	0.128	0.4
7/.186 AAC_100°C_11kV_A_SEQ	0.187	0.6
HDBC 7/.08_75°C_11kV_A_SEQ	0.210	0.6
Banana_75°C_11kV_B_SEQ	0.359	1.1
Moon_55°C_11kV_A_SEQ	0.473	1.4
Apple_75°C_11kV_B_SEQ	0.473	1.4
Libra_75°C_11kV_A_SEQ	0.847	2.6
Moon_75°C_11kV_A_SEQ	0.879	2.7
11kV120CCT75A	1.135	3.5
Apple_55°C_11kV_A_SEQ	1.218	3.7
Mars_75°C_11kV_A_SEQ	1.301	4.0
Libra_55°C_11kV_A_SEQ	1.384	4.2
Libra_100°C_11kV_A_SEQ	7.551	23.1
Mars_100°C_11kV_A_SEQ	7.976	24.4
Moon_100°C_11kV_A_SEQ	8.372	25.6

Table 3 – MV buried cable types and cumulative installed lengths within the modelled area

MV Buried Cable Type	Cumulative Distance in Model (km)	Proportion of all MV Buried Cable Distance in Model (%)
11kV UG - Other	0.224	0.5
11kVUG185cuPLYHDPDU	0.390	0.9
11kVUG185cuPLYDU	0.502	1.1
11kVUG25cuPLYHDPEDU	0.535	1.2
11kVUG95alXLDB	0.628	1.4
11kVUG300alPLYDU	1.005	2.3
11kVUG240cuPLYDU	1.055	2.4
11kVUG240alXL70DU	1.292	3.0
11kVUG95alXLDU	1.531	3.5
11kVUG240cuXL90DU	2.824	6.5
11kVUG240cuTRPX90DU	3.830	8.8
11kVUG400alTRPX90DU	4.901	11.2
11kVUG240alTRPX90DU	12.218	28.0
11kVUG240alXL90DU	12.755	29.2

Table 4 – LV overhead conductor types and cumulative installed lengths within the modelled area

LV Overhead Line Type	Cumulative Distance in Model (km)	Proportion of all LV Overhead Line Distance in Model (%)
LV - O/H - Other	0.061	0.1
LV - LIBRA	0.548	0.6
LV - BANANA	1.094	1.2
LV - MINK	1.386	1.5
LV - MARS	15.239	16.6
LV - 95 ABC	19.967	21.8
LV - MOON	53.420	58.2

Table 5 – LV buried cable types and cumulative installed lengths within the modelled area

LV Buried Cable Type	Cumulative Distance in Model (km)	Proportion of all LV Buried Cable Distance in Model (%)
LV - UY/G - Other	0.105	0.1
LV - 150 Cu 3C+NS	0.245	0.2
LV - 25 Cu 4C XLPE	0.367	0.3
LV - 300 Al 3.5C	0.479	0.4
LV - 25 Cu 3C+NS PVC	0.496	0.4
LV - 120 Al 3C+NS	0.656	0.5
LV - 240 Cu 4C XLPEPVC	0.764	0.6
LV - 25 Cu 4C PLY-HDPE-PVC	0.878	0.7
LV - 120 Cu 4C XLPEPVC	0.908	0.7
LV - 240 Al 3C+NS	1.506	1.2
LV - 16 Cu 4C PVC	1.553	1.3
LV - 16 Cu 4C XLPE	18.793	15.1
LV - 120 Al 4C XLPEPVC	24.769	19.9
LV - 240 Al 4C XLPEPVC	72.637	58.5

2.3 Native load curve and PV generation curve estimation from transformer monitor data

The following methodology was used to estimate native load and PV generation curves for each of the distribution transformers for which at least 50 days' worth of transformer monitor data was available in each season. The intention of this methodology was to identify load curves that are reasonably typical in that they don't represent once-per-year peak loads or unusual events like load transfers or network outages, but which are still also representative of relatively high levels of load for normal operation of the modelled network during the evening peak and relatively low levels of effective load during midday for high solar day conditions. The motivation for representing the network in this way was that it is expected to produce conservative estimates of both the severity of undervoltage events during the evening peak and of the severity of overvoltage events at midday for high solar day conditions respectively but will also remain relevant for system normal conditions.

A description of the methodology is provided below:

1. The dates and times of maximum load on each 11 kV feeder in the study in each season were identified.
2. For each season *S* and distribution transformer *Tx*, the load absorbed by that individual distribution transformer at the date and time of peak feeder load was calculated; let this value be denoted $P_{S,Tx}$. Note that this value may not correspond to the peak in distribution transformer peak load on that date.

3. For each season S and distribution transformer T_x, the set of dates with daily peak load values within ±5% of $P_{S,Tx}$ were identified. From these sets, the dates for which the daily peak load was more than two standard deviations away from the average daily peak load in that season were removed. Let the remaining sets of dates be denoted by $D_{S,Tx,n}$. If the number of members of any one of these sets was less than three, additional dates with daily peak load values that were less than $P_{S,Tx}$ by more than 5% were gradually added to the set until the set had at least three members. Note that this implies that dates having peak loads more than 5% higher than $P_{S,Tx}$ were not added to the sets D_{S,Tx_n} in general.
4. The night-time (6pm – 6am) portions of the native load curves for each season S and distribution transformer T_x were calculated by taking the daily average of each set $D_{S,Tx,n}$ over those hours.
5. For each season S and distribution transformer T_x, the set of dates with summated load between the hours of 6am and 6pm that were above the average summation of load between these hours was identified. These dates were then sorted in order of cumulative daily solar irradiance and all but the three with the lowest irradiance were discarded. Let the sets resulting from this step be denoted by $D_{S,Tx,d}$.
6. The day-time (6am-6pm) portions of the native load curves for each season S and distribution transformer T_x were calculated by taking the daily average of each set $D_{S,Tx,d}$.
7. For each season S and distribution transformer T_x, the set of dates on which the daily cumulative solar irradiance exceeded the 90th percentile was identified. These dates were then sorted in order of summated load between the hours of 6am-6pm and all but the three with the lowest summated load were discarded. Let the sets resulting from this step be denoted by $I_{S,Tx}$.
8. The daily peak PV generation values for each season S and distribution transformer T_x were then calculated by subtracting the daily averages of each respective set $I_{S,Tx}$ from daily native load curves calculated in step 6 for the hours between 6am and 6pm inclusive. Generic solar generation curves for small residential PV systems in the locality of the modelled zone substation and for each season were then rescaled by these peak PV generation values to formulate the PV generation curves for each season S and distribution transformer T_x. The specific shapes of the normalised solar generation curves used in this process were sourced from [7].

Important features of this methodology are that:

- Estimation of each portion of each load curve (i.e., day-time and night-time) and each PV generation curve using averaging of at least three days-worth of data ensures some removal of noise due to cloud cover, intermittent use of loads etc.
- Steps 1-3 ensure that dates with evening peak load approaching the maximum for that distribution transformer in that season are used to construct the night-time portion of the daily native load curves, but that the diversity in the timing of their peak loads relative to the peaks of other transformers on the same 11 kV feeder is also accounted for i.e., that the dates with maximal evening peaks for each transformer are not the only dates utilised.
- Removal of the dates with daily peak load more than two standard deviations away from the average daily peak load in step 3 also ensures that outliers corresponding to load transfers or other highly atypical events do not distort the load curves.
- Separation of the daily native load curve construction into averages over separate sets of dates for separate halves of the day (i.e., day-time and night-time) ensures that dates with high solar irradiance, which would be more likely to produce high evening peak load values, do not need to be removed from the estimates of load during the evening.
- The condition on solar irradiance in step 5 ensures that the day-time portions of the daily native load curves are constructed from dates with relatively low solar irradiance.

- The condition on summated load between the hours of 6am and 6pm in step 5 ensures that the daily native load curves are not distorted by data from dates on which unusually low load occurred during the day for reasons other than solar PV generation such as network outages or other unusual events e.g. dates on which several customers connected to that transformer were away on holidays. This condition is relatively lenient because the solar irradiance condition also applied in step 5 is already relatively restrictive.
- The condition on cumulative daily solar irradiance in step 7 ensures that the daily PV generation curves are constructed using dates with the highest solar irradiance so that distortion due to cloud cover and other factors is minimised.
- The condition on summated load between the hours of 6am and 6pm in step 7 ensures that the daily PV generation curves are not constructed from dates with day-time load that is abnormally high due to load transfers or other atypical network events. This condition is relatively restrictive because the set of dates produced by the condition on solar irradiance in this step should already have relatively low cumulative daily load to begin with i.e., because the high solar irradiance will produce high solar generation and offset apparent load readings to a higher extent degree.
- Active power data was utilised in application of the above methodology in general as apparent power is non-directional i.e., does not indicate a direction with its sign.

For five of the 153 distribution transformers with monitor data available, the estimation process outlined above produced an amount of PV generation large enough to imply PV inverter utilisation factors higher than 100%. Since utilisation factors as high as this cannot occur in practice, it was assumed that additional PV inverter capacity not listed in the PV record data would exist on the LV networks connected to these transformers. Additional PV inverters were therefore added to those buses in the LV networks connected to these transformers which had records of connected load data until the implied PV utilisation factors were reduced to 100%. Note that the estimated PV generation curves themselves were not altered; these were simply divided up between installed inverters on their corresponding LV networks according to PV inverter capacity in general. The assumption here was that new PV systems may have been added (as growth is still reasonably significant), but that the new data had not found its way into the records at the time the records were accessed.

2.4 Native load curve and PV generation curve estimation for transformers without usable monitor data

For some of the distribution transformers in the zone substation area modelled for this project, monitor data had gaps which resulted in less than 50 days' worth of data for one or more seasons. The transformer monitor data for these transformers was declared unusable. Furthermore, for 106 of the transformers, no transformer monitor data was available.

Using observation of the surrounding buildings shown on Google Maps, the distribution transformers in the project were categorised into either residential or commercial/industrial load types. A small subset of these were found to be located either in sparsely populated bushland, or beside highways, without being in close proximity to any buildings. These transformers were categorised as having unknown load types. Distribution transformers with ratings below 100 kVA were mostly found to be situated in locations of this description also, hence these were also designated as having unknown load types. For the transformers with unknown load types and no usable monitor data, loads were sized according to the static load sizes that were present in the initial MV PowerFactory model received from Energex and were not dynamically altered throughout the day.

As the number of transformers in this category is small, this approach is not expected to have a noticeable impact on the results of this study.

The daily native load and PV generation curves for the transformers with unusable or non-existent transformer monitor data which were categorised as having residential or commercial/industrial load types were then constructed by taking averages of the normalised load and PV generation curves for the five geographically closest distribution transformers of the same load type for which usable transformer monitor data was available respectively. In the case of the load curves, the normalisation was performed by dividing by the transformer apparent power capacities and the average load curves were then rescaled using the apparent power capacity of the transformer for which the curve was being estimated.

For the PV generation curves on the other hand, the normalisation was performed by dividing the curves for the five nearest transformers with usable monitor data by the installed volume of PV inverter apparent power capacity. The averages of these PV generation curves were then rescaled using the installed volume of PV inverter apparent power capacity for the transformer for which the curve was being estimated. In the case of 24 of the 259 distribution transformers in the modelled area in particular, records indicated zero PV installations on the LV area connected to the transformer and monitor data was also not available. In these cases, PV inverter capacity was added to the LV network for that transformer until implied PV peak utilisation factors of 100% were realised i.e. inverter capacity equivalent to the peak of the average PV generation curves identified was added.

3 Network Model Development

3.1 Representation of zone substation line drop compensator

The zone substation modelled in this project is also equipped with line drop compensator (LDC) algorithms that control the OLTCs on each of its three power transformers. These algorithms are implemented with piecewise linear voltage-power characteristics that are determined by upper and lower voltage settings V_H and V_L and corresponding upper and lower active power flow settings P_H and P_L as depicted in Figure 3.

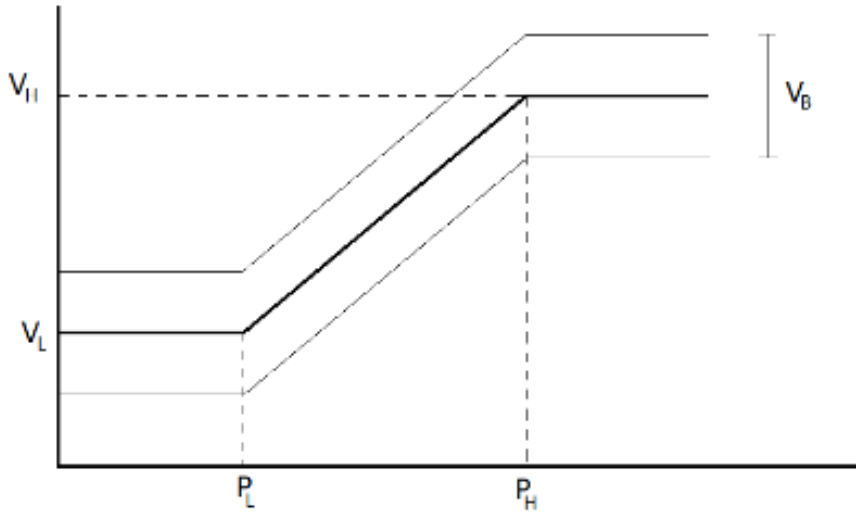

Figure 3 - LDC algorithm characteristic

If the voltages measured on the 11 kV terminals of each of these transformers differ from their corresponding characteristics by more than half of their voltage bandwidth settings V_B, which are equal to 270 V, then a tap-changer operation is initiated to try and correct the 11 kV voltage and bring it closer to the characteristic. The values for the LDC settings at the zone substation modelled for this project are shown in Table 6.

Table 6 - LDC algorithm settings

Power Transformer	P_L (MW)	P_H (MW)	V_L (kV)	V_H (kV)	V_B (V)
1	0.0	7.3	10.80	11.20	270
2	0.0	16.4	10.80	11.20	270
3	0.0	21.9	10.80	11.20	270

The power flows on which these characteristics are implemented are the total active power flows into the sets of 11 kV feeders sourced from each of the three buses that the transformers feed respectively. The high and low active power settings for the three power transformers are based on the typical division of active power flows through the three 11 kV buses at this substation under system normal conditions. The intention therefore is that they will all tend to execute the same tap-position changes at similar times under their independent LDC control systems. The way in which the LDC algorithms are implemented also ensures insensitivity of the

11 kV voltages to voltage variations in the upstream 33 kV network. Any effect that these variations would have would result in OLTC tapping operations to bring the 11 kV voltage back as close as possible to the power-voltage characteristics.

The LDC algorithms at the zone substation studied in this project were modelled in PowerFactory by adding additional code to the Python script running the simulations. The additional code approximates the LDC control systems described above by modelling only one aggregate power-voltage characteristic with P_H and P_L settings equal to the sum of the settings for each of the three individual power transformers and V_H and V_L settings equal to 11.2 kV and 10.8 kV respectively. The three transformers themselves are represented by a grid source component, the voltage setpoint of which is determined by the Python script.

The voltage bandwidths which trigger the operation of the real-world LDC algorithms weren't modelled. Instead, the switching behaviour of the LDCs was approximated by triggers which sit at the centre-points between the three active power points on their aggregate voltage-power characteristic which correspond to the discrete 11 kV voltage levels accessible by the OLTCs on the transformers. This approximation was deemed to be acceptable because the LDC-triggered tapping operations which would occur on a daily basis due to atypical voltages and power flows would not be captured by the simulation process in any case. The simulations were only intended to capture tapping operations which tend to occur at similar times on most days due to the typical trends in substation active power throughput; the level of accuracy of the modelling approximation described here was expected to be sufficient to capture this category of events.

Given the characteristics of the OLTCs, the three voltage levels which sit between the V_H and V_L settings of 10.8 kV and 11.2 kV that are accessible to each of the transformers are 10.8625 kV, 11 kV and 11.1375 kV; or 0.9875, 1.0 and 1.0125 respectively on a per-unit bases. The voltages which sit at the centre-points of these are 0.99375 pu and 1.00625 pu, and the active power levels on the aggregate power-voltage characteristic for the LDC algorithms were 14968.2 kW and 30643.2 kW respectively. Thus, the behaviour of the LDCs was approximated by switching the source component representing the 11 kV side of the parallel sum of the three transformers at the zone substation such that its voltage rested at 0.9875 pu for active power flows through the substation out towards the loads that were below 14968.2 kW (including negative power flows), at 1.0125 pu for active power flows that exceeded 30643.2 kW and at 1.0 pu for power flows between these two values. Figure 4 depicts the real-world active power versus voltage magnitude characteristic that is targeted by the LDC algorithm for the modelled zone substation in blue as well as the three discrete voltage levels that were used to represent this in the studies for this report in red.

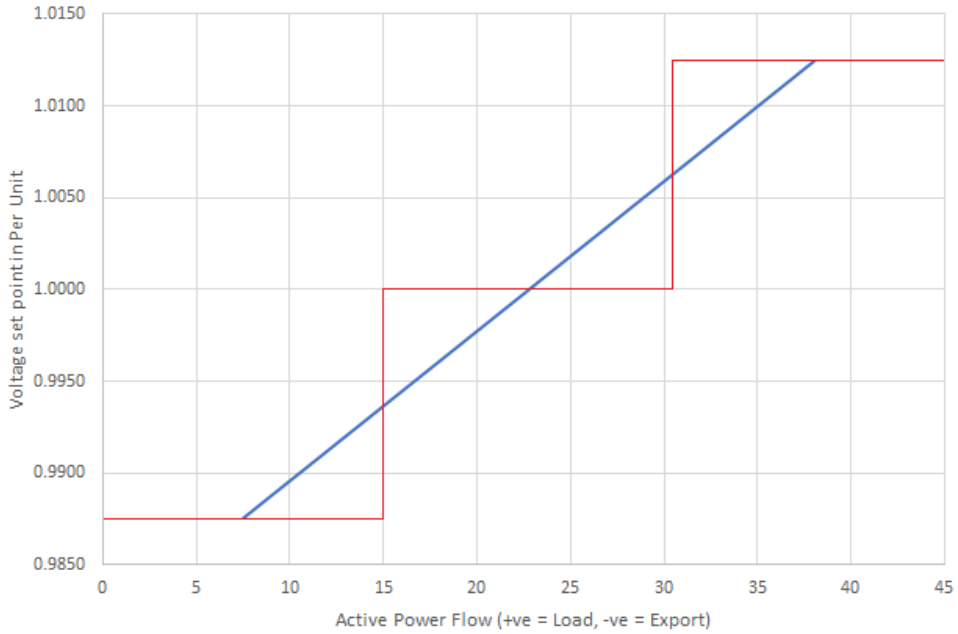

Figure 4 – Representation of the real-world LDC characteristic (blue) targeted by the LDC algorithm at the modelled zone substation and the effective representation of this characteristic (red) using three discrete levels used in this study.

3.2 Representation of volt-watt and volt-var functionality

Residential solar PV inverter systems installed in Australia after 2020 are equipped with both volt-var and volt-watt control functions as specified in the latest version of the standard AS4777.2 [8]. The volt-var function produces automatic changes to the reactive power output of the inverter when the connection point voltage approaches either of its its two voltage parameters V_{V2} or V_{V3}; reactive power is absorbed to try and arrest overvoltage events and injected to arrest undervoltage events. A. At voltages outside of the two lockout values V_{V1} and V_{V4} the volt-var algorithm ensures reactive power injection or absorption that is fixed at the two supplying and absorbing limits of 44% and 60% of capacity respectively. Refer to Figure 5 for a depiction of this and to Table 7 for the required volt-var voltage settings in Australia.

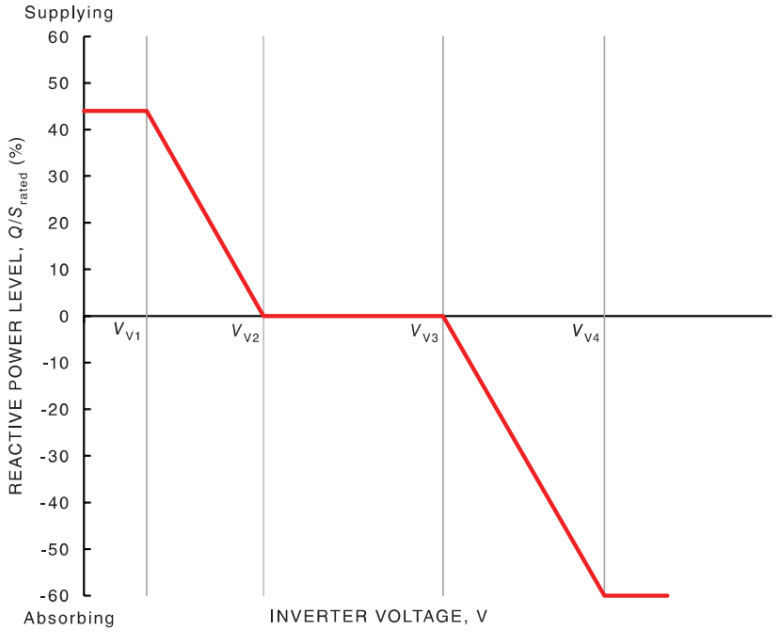

Figure 5 - Volt-var function [8]

Table 7 – Required volt-var settings in Australia [8]

V_{V1} (V)	V_{V2} (V)	V_{V3} (V)	V_{V4} (V)
207	220	240	258

The second of these control functions, known as volt-watt functionality, applies a limiter to the active power output of the PV inverter when the connection point voltage pushes into and exceeds the setting V_{W1}. Once the voltage exceeds the setting V_{W2}, the limiter locks out at 20% of rated inverter capacity. Refer to Figure 6 for a depiction of this and to Table 8 for the required volt-watt voltage settings in Australia.

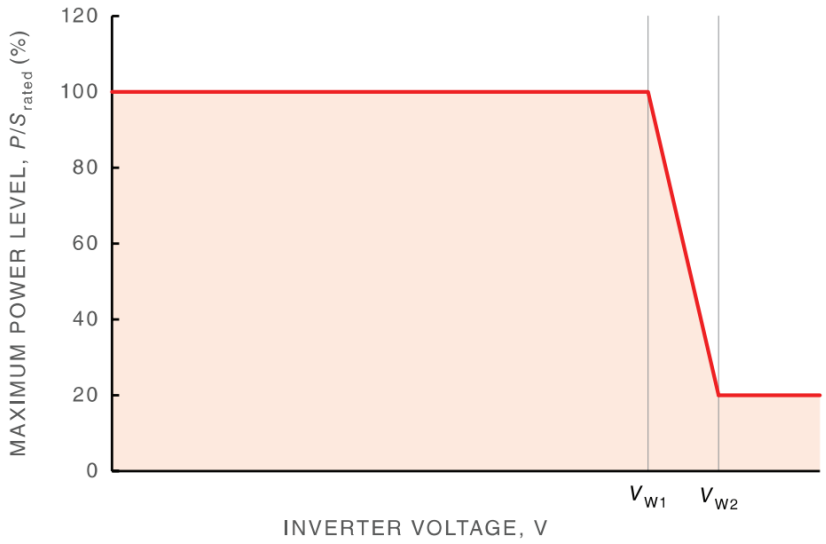

Figure 6 - Volt-watt function [8]

Table 8 – Required volt-watt settings in Australia [8]

V_{W1} (V)	V_{W2} (V)
253	260

The volt-watt and volt-var functions are implemented together in such a way that if the apparent power rating of the inverter is reached, the active power will be limited further to ensure that this rating is not exceeded. This is intended to ensure priority of the volt-var function in general.

The volt-var and volt-watt functions will have been affecting many of the PV generator systems present in the system studied in this project. These functions also constitute the mechanism by which PV curtailment, which is one of the central issues to be studied in this project, is realised in practice. It was therefore crucial to develop accurate modelling tools that were able to represent their influence. Standard components provided as part of the load flow simulation features of PowerFactory do not facilitate simulation of these control algorithms. It was therefore necessary to develop models for these control algorithms in the "QDSL" format provided as part of the PowerFactory interface.

Components in PowerFactory controlled using QDSL scripts facilitate a type of power system simulation known as "quasi-dynamic simulation", which is different to the steady state load flow simulation technique

employed in this project. Quasi-dynamic simulation is used to represent slow-varying dynamics in power systems by repeating a series of load flow solutions at a timestep specified by the user. Note that this type of simulation was not used in the studies for this project. QDSL scripts and components also facilitate an augmentation of the load flow algorithm that permits the solution to include the influence of feedback control systems such as the volt-var and volt-watt functions. A script in the QDSL language representing volt-var and volt-watt functions as employed on small-scale solar inverter installations in Queensland was therefore developed for this project. This script also modelled the additional reduction of the volt-watt limiter to ensure that the apparent power rating of each of the inverters are never exceeded and that the reactive power setpoints produced by the volt-var functions are always adhered to.

Many of the existing installed solar inverters and even those that will be installed in future are likely to include a reactive power capability limitation when available solar energy is low. For this reason, an assumption that volt-var functionality is de-activated once available solar irradiance falls below the level that would permit active power generation as high as 10% of the inverter rating, was also incorporated into the QDSL model.

Differences in previous revisions of the standard AS4777.2 mean that small-scale solar inverter systems installed between 2016 and 2020 were expected to have only the volt-watt function active and systems installed prior to 2016 had neither volt-watt nor volt-var active. The QDSL models controlling the solar inverters in the baselined version of the network model for this study have been configured so that the expectations of the version of AS4777.2 applicable at the time of installation of that particular inverter are adhered to. QDSL models assigned to the PV inverter components created for studying future scenarios have also been assumed to adhere to the 2020 version of AS4777.2 in particular with both of the volt-watt and volt-var functions active for all future inverters. It is noted that significant amounts of non-compliance with AS4777.2 have been identified in existing solar inverter installations in Australia [9]. Although this is the case, it is impossible to predict the extent of the non-compliance in the existing inverters installed in the area of Energex's network modelled in this study or in the solar inverters which will be installed here in future. Compliance with AS4777.2 has therefore been assumed in general in the modelling for this report.

For details on the validation process for the QDSL script, refer to Appendix A of this report. It is noted here that while over and undervoltage protection functions are also present on small-scale solar inverters installed in Australia, these functions were not modelled in this study.

3.3 LV line modelling

Transmission and distribution lines in the modelled LV area were represented using coupled buried cables and coupled tower geometry models, rather than with sequence network-based models. Refer to Appendix B for justification for this decision.

3.4 Representations of MEN neutral earthing resistances

Neutral earthing resistors (NERs) were added to each of the LV buses in the PowerFactory model for this project. These resistances were added to represent typical neutral earthing resistances in Queensland residential and commercial buildings, which are implemented using multiple earthed neutral (MEN) systems. A typical resistance value of 2.5 ohms per NER was used. This value was considered suitable as the buses in the LV network data were found to be connected to anywhere from two to five customers, with an average of

four customers, and a neutral-earth resistance of approximately 10.0 ohms for one installation is considered common.

Inclusion of these NERs was found to have a significant influence on the levels of curtailment predicted by the volt-watt and volt-var QDSL script instances in general. This is attributable to the fact that the volt-watt and volt-var functions respond to phase-neutral voltages and that the NERs in turn exhibit significant influence on the neutral voltages. The NERs were implemented in PowerFactory using shunt RL components rather than the NEC/NER component provided in the "Grounding Elements and Surge Arresters" section of the component library because the former component is implemented as a zigzag transformer which only provides an earth return path under fault conditions.

3.5 Modelling assumptions

It is noted here that the Energex Distribution Planning Manual [10] outlines phase connection patterns that should be adhered to when connecting customers to LV distribution lines so that the loading of the network remains balanced even at the LV feeder level. The load data received from Energex however was found to exhibit many cases in which these connection patterns were not evident. Also, 6,428 out of 14,792 customer records in this dataset had no phase connection information available. Because the data received did not appear to indicate adherence to the phasing connection patterns outlined in the Energex Distribution Planning Manual and because the effort implied by doing otherwise would have been significant, no effort was made to ensure adherence to the phasing connection patterns when assigning loads for which no phase connection information was available to phases in the model.

The PowerFactory model for the zone substation studied in this project was constructed using the following assumptions. Where phase connection information for loads and PV installations were not available, assumptions were made based on the following sequence of checks:

- Total load and rooftop PV installation counts were calculated for each LV circuit connected to a distribution transformer in the zone substation area.
- Rooftop PV installations with an unknown phase connection were assigned to phases corresponding to one of the customer connections listed as being connected to that same node and also in such a way that the total number of PV installations connected to each phase on each LV circuit would be approximately balanced.
- The remaining loads with unknown phase connections were assigned to phases so that the total number of loads connected each phase on each LV circuit would be approximately balanced.
- Where a solar PV installation was listed as being connected across two known phases, the corresponding customer connections at that same node were distributed equally across these two phases.
- For rooftop PV installations for which the phase of connection was unknown:
    - Those with registered capacities of 10 kW and above were modelled as three-phase systems.
    - Those with registered capacities below 10 kW were modelled as single-phase systems.
- Assignment of those loads and rooftop PV installations for which phase information was unavailable to phases could have been performed in accordance with the phasing connection patterns outlined in the Energex Distribution Planning Manual [10]. Inspection of phase connection data for LV feeders in the zone substation area for which the phase of connection of most loads were known

however revealed that these patterns had not necessarily been followed in general during construction of the real-world network. Rigorous adherence to these patterns during the assignment of loads and rooftop PV installations to phases was therefore not enforced as the additional effort that this implies would not necessarily have added a commensurate level of realism to the model.

- Since the load information made available by Energex did not contain estimates of the size of each connection, loads were sized evenly across each LV circuit according to the ratio of peak distribution transformer load estimated using the methodology described in the previous chapter to the total number of loads connected to that LV circuit, with the added rule that two-phase loads were twice as large as the single-phase loads and three-phase loads were three times as large as single-phase loads.
- Using inspection of Google Maps data, each of the distribution transformers were classified as being connected to either residential or commercial/industrial loads.
- Where load types to which distribution transformers were connected could not be identified via inspection of Google Maps data (e.g. where the transformer was found to be situated beside a highway, or in sparsely populated bushland, with no buildings nearby), the loads were listed as having an unknown type.
- Distribution transformers having ratings below 100 kVA were also designated as having unknown load types.
- The four seasonal daily load and rooftop PV generation profiles for each of the distribution transformers for which monitor data was not available were estimated using averages of the five geographically closest distribution transformers of the same type i.e. residential or commercial/light industrial.
- The four seasonal daily load profiles for each distribution transformer were also updated subsequently during baselining of the model.
- Distribution transformers with ratings above 1 MVA were assumed to have impedances of 6%.
- Distribution transformers with ratings above 500 kVA and up to 1 MVA were assumed to have impedances of 5%.
- Distribution transformers with ratings equal to or below 500 kVA were assumed to have impedances of 4%.
- For distribution transformers which had usable transformer monitor data, and which also had apparent peak PV utilisation factors above 100%, additional three-phase PV generation capacity was added to each bus in the LV network connected to these transformers with loads already connected until the peak PV utilisation factor was reduced to 100%.
- In accordance with the 2020 revision of AS4777.2 (which came into effect in December of 2020), PV installations commissioned in 2021 or later were assumed to have both volt-watt and volt-var functionality activated.
- In accordance with an earlier revision of AS4777.2 which was applicable at that time, PV installations commissioned in 2017 – 2020 were assumed to have volt-watt functionality activated but volt-var functionality deactivated.
- In accordance with an earlier revision of AS4777.2 which was applicable at that time, PV installations commissioned in 2016 or years before this were assumed not to have volt-var or volt-watt functionality activated.
- Anti-islanding protection and frequency-watt control functions weren't modelled.
- No electric vehicles or BESS systems in the modelled network in the baselined state.

- Export limits on solar PV installations were only modelled for those installations for which Energex PV records indicated a value for the export limit, which is only 424 out of 5552 recorded installations.

4 Network Model Baselining

Following construction of the PowerFactory model for the zone substation studied in this project, the model was baselined using real-world measurements additional to the transformer monitor data that was already utilised in constructing the native load and PV generation profiles.

Voltage and current data measured on the outgoing 11 kV feeders at the zone substation were used to re-scale the seasonal native load curves developed for each distribution transformer in the model for both high and low solar irradiance conditions. Due to the absence of phase angle and reactive power data in the 11 kV feeder SCADA measurements, only apparent power flows could be calculated from them. Additional SCADA data recording the total active and reactive power flow through the power transformers at the zone substation modelled in this project was also available; the power factor in this data was used to infer the ratio of active to apparent power in the 11 kV feeder SCADA data. Note that the approximation that this implies is relatively small as different 11 kV feeders connected to the same zone substation are likely to exhibit similar power factors in general.

Due to the absence of phase angle information, the active power flows on each feeder indicated by the SCADA data did not come with an indication of power flow direction. Therefore, where the SCADA data active power flow curves hit values in the middle of the day that were below 10% of their peak value, or where their shape exhibited a clear and obvious "bounce" characteristic during the hours from approx. 8am through to 2.30pm noon, as shown for Feeder 4 in spring in Figure 7, it was assumed that a reversal of the direction of power flow should occur in the typical day which this study was trying to capture in that season and on that feeder during high solar irradiance conditions. The bounce characteristic was much more pronounced and occurred much more frequently in spring and winter, perhaps due to a combination of lower average cloud cover and lower mid-day loads in those seasons. This may mean that some active power flow reversals during the midday period in summer and autumn were not captured.

The half-hour periods during which reversal of power flow was indicated by the original predictions of total load and PV volumes from transformer monitor and installed DER data were used as a guide to indicate the time at which the SCADA data should be multiplied by -1. Adjustments to these alterations were also made, via visual inspection of time series plots of the SCADA data, based on which reconfigurations of the gradient of each plot seemed more realistic. It is noted here that this method of estimating the times of active power flow reversal on each feeder and on a typical high solar day in each season is likely to be a source of error in this project; given the measurements available however it was unavoidable.

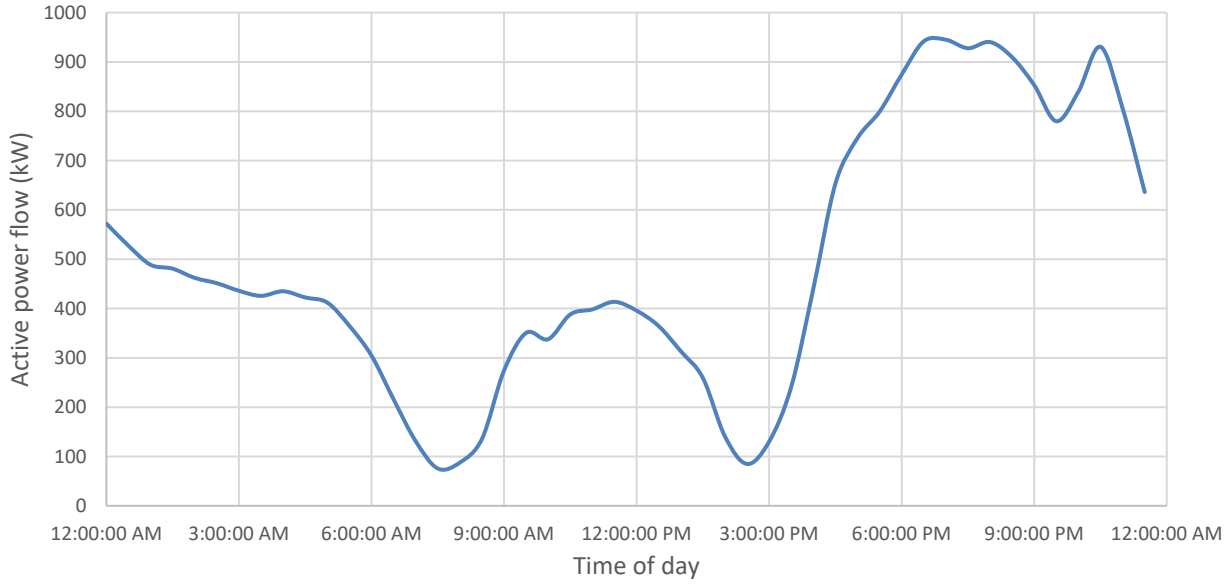

Figure 7 - Active power flow on Feeder 02 during high irradiance conditions in spring indicated by SCADA data.

The use of SCADA data recorded upstream of the distribution transformers to re-scale the seasonal native load curves for each of the distribution transformers, which were formulated using data recorded on specific dates unique to each of those transformers, also implies the introduction of further modelling error. At the same time however, it implies the reduction of several other more significant forms of modelling error, as well as a re-distribution of these so that they become more evenly spread across the distribution transformers connected to each feeder. This trade-off therefore justifies the application of the baselining process outlined in this section of the report. The other forms of modelling error improved on by the baselining process include:

- The error caused by approximations and assumptions made for the load consumed by those distribution transformers for which no usable transformer monitor data was available.
- The potential underestimation of day-time load on hot days in summer and spring caused by the fact that the methodology utilised in section 3.2 uses dates with low solar irradiance to estimate load throughout day-time hours, which will tend to exhibit lower load due to the lower temperatures on low solar irradiance days, which is likely to result in a reduced use of air-conditioning.
- The error caused by the use of generic solar generation curves for small residential PV systems in the locality of the modelled zone substation i.e. that the real profiles for the PV generators connected to each distribution transformer may have atypical shapes due to the pitch of the roofs on which they are installed, the direction which these roofs face and the shading by trees, mountains and other landscape features that they may be exposed to.
- Errors in the offline tap-changer settings recorded for each of the distribution transformers.

4.1 Transformer tap correction process

As alluded to in the previous section, the baselining process was used to correct errors in the offline tap-changer settings for the distribution transformers in the modelled zone substation area. The 11 kV voltages implied by the transformer monitor datasets and the simulated voltages at the same points along the 11 kV feeders were plotted against distance for a collection of paths intersecting all the distribution transformers in the model for which monitor data was available. Such plots were prepared for the minimum and maximum

load hours of the day in summer, for which the hours of 12pm and 7pm were selected respectively. An example of one of these plots is shown below in Figure 8. The simulations for these plots were carried out before the load corrections described in the next section.

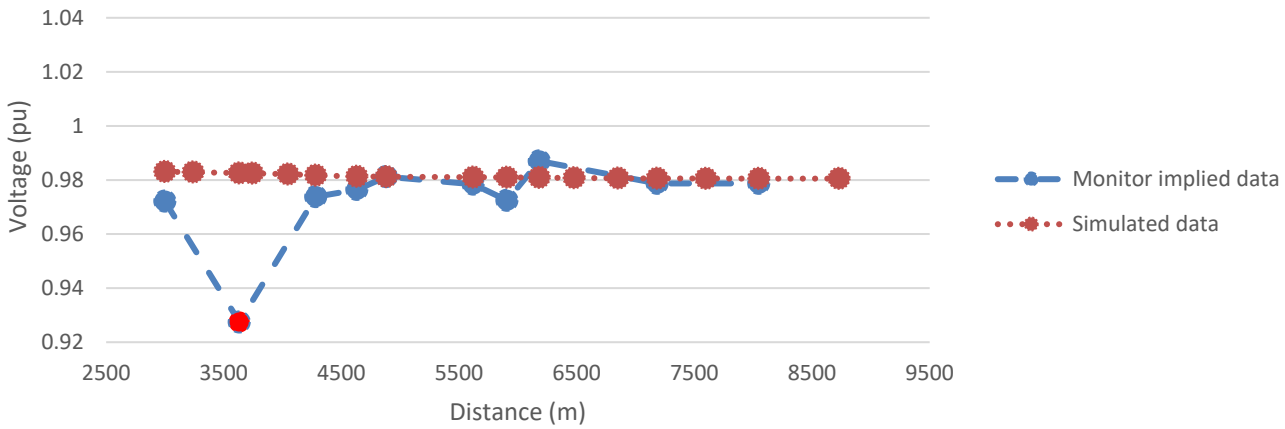

Figure 8 – Voltage-distance plot for one of the paths on Feeder 01 at noon on a high solar day in summer.

Each of the markers in Figure 8 represents the location of a particular distribution transformer. Note that some of the transformers for which simulated data is available did not have transformer monitor measurement implied data available. The distribution transformer represented by the second marker on the blue curve shows a difference in voltage from the simulated curve of more than 2.5%. Discrepancies like this that were larger than 1.25% when averaged across 12pm and 7pm were taken as indications of incorrect tap settings. The tap setting for such transformers was then increased if the monitor implied voltage was too high and reduced if the implied voltage was too low. This was done because the transformer monitor voltage measurements were recorded on the LV terminals and are hence fixed, but the implied 11 kV voltages will vary with the size of the turns ratio for each of the transformers, which itself reduces with increasing tap setting as per Table 9. Note that all distribution transformers in the modelled zone substation area are either 5 or 7 tap transformers.

Table 9 – Transformer ratios for different tap sizes for 5 and 7 tap distribution transformers in the modelled zone substation area

Buck/Boost Size	5 Tap Transformer	7 Tap Transformer	Turns Ratio
10% Buck		1	12100:433
7.5% Buck		2	11825:433
5% Buck	1	3	11550:433
2.5% Buck	2	4	11275:433
Nominal	3	5	11000:433
2.5% Boost	4	6	10725:433
5% Boost	5	7	10450:433

As a result of this process, tap settings for a subset of the transformers were left unchanged, and for an even smaller subset of them were increased; but for the majority of the distribution transformers, it was found that the tap setting needed to be reduced by one tap. The tap settings for the transformers for which no monitor data was available were also reduced by one tap, simply because the trend indicated by the rest of the population was that that this was likely to be necessary.

4.2 High solar and low solar expected feeder aggregate power curve formulation

For each 11 kV feeder at the zone substation, high solar day and low solar day expected feeder aggregate active power curves, were formulated using the methodology described below. This approach attempts to generate load curves representing the summation of load and PV generation on typical non-outlier days implied by SCADA data:

1. For each season S and 11 kV feeder F, the daily peak load in each day was identified and the dates for which the daily peak load was more than two standard deviations away from the average of daily peak load values in that season were removed. Let the remaining sets of dates be denoted by $D_{S,F,n}$.
2. For the dates in each set $D_{S,F,n}$, the load was summed across each hour of the day and the dates for which the summated load was more than two standard deviations away from the average summated load in that season were removed.
3. The dates remaining in each set $D_{S,F,n}$ were then ranked in order of daily cumulative solar irradiance and the three dates with the highest and lowest irradiance were averaged to formulate the high solar and low solar feeder aggregate load curves respectively.

This methodology is simpler than that which was applied to estimate native load and PV generation curves for each distribution transformer, which was described in section 3.2, for the following reasons:

- Because there was no need to isolate the PV generation from the load when formulating the feeder aggregate power curves, there was no need to identify dates with both high solar irradiance and relatively high day-time load to represent the underlying load curves throughout the middle of the day; hence there was no need to use separate dates to form the day-time and night-time portions of the curves.
- The criteria applied to daily peak load and daily summated load in this methodology are simply intended to remove outliers that would be likely to represent dates with unusual events (i.e. load transfers, outages, unusual absence of residents from their homes due to holidays etc.).
- The criteria applied to daily peak load and daily summated load in this methodology are more lenient than the corresponding criteria applied to these metrics in section 3.2 because of:
    - The reduced accuracy implied by approximating apparent power flows as active power flows.
    - The larger number of customers that is sampled by an 11 kV feeder relative to a single distribution transformer implies greater difficulty in isolating dates which would meet these criteria while simultaneously exhibiting the required high or low solar irradiance.

4.3 Load correction process

The following procedure, which was repeated for each 11 kV feeder in the model and in each season, was used to correct the load sizes in the PowerFactory model for each season and for high and low solar irradiance conditions.

Let the 11 kV feeder being baselined be denoted with F, let the season in which it is being baselined be denoted with S and let the set of distribution transformers connected to it in this season be denoted with Tx. Initial simulations using the load and PV curves estimated using the methodology described in section 3.2 were carried out so that first-pass simulated active power flows at the substation end of each of the 11 kV feeders in each season could be recorded. High and low solar versions of these simulations were carried out in each case i.e. for low solar day conditions, PV generator outputs were set to zero. Let these first-pass feeder simulated active power flows be denoted with $P_{F,S,sim,hi}(t)$ and $P_{F,S,sim,lo}(t)$, where the functional dependence on time indicates the variation throughout the typical day. Activation of volt-watt and volt-var functionality was found to produce variations in 11 kV feeder total active power flows of less than 2% in general; the QDSL models were therefore deactivated for these simulations to save computation time.

The distribution transformers on feeder F were then identified and the first pass simulated total load curves were calculated by summating the load curve points for each of them in each half-hour time interval of the day. Let these curves be denoted with $P_{\Sigma Tx,S,sim}(t)$.

High solar and low solar expected feeder aggregate active power curves for each feeder and in each season were then formulated from the 11 kV feeder SCADA data using the methodology described in the previous subsection. Let these curves be denoted with $P_{F,S,E,hi}(t)$ and $P_{F,S,E,lo}(t)$ respectively. The curves $P_{F,S,sim,hi}(t)$ and $P_{F,S,sim,lo}(t)$ were then subtracted from $P_{F,S,E,hi}(t)$ and $P_{F,S,E,lo}(t)$ respectively to calculate the active power error curves for high and low solar day conditions. Let these curves be denoted with $e_{hi}(t)$ and $e_{lo}(t)$ respectively.

The native load curves were then re-scaled uniformly in each half-hour interval of the day to effectively subtract the active power error curves $e_{hi}(t)$ and $e_{lo}(t)$ from the simulated total load curves $P_{\Sigma Tx,S,sim}(t)$. Note that compared to the simpler alternative of forcing $P_{\Sigma Tx,S,sim}(t)$ to match the expected feeder aggregate power curves $P_{F,S,E,hi}(t)$ and $P_{F,S,E,lo}(t)$, subtracting the active power error curves from them instead ensures that the active power losses in the 11 kV feeders are accounted for.

4.4 Baselining results

Following the load correction process described in the previous section, a relatively high level of agreement between the measured and simulated active power flows on each 11 kV feeder were achieved. The measured and simulated feeder aggregate active power flows were made to match within ±5% of the peak active power flow for the corresponding season, feeder and set of solar conditions in general. A plot showing the close agreement between the simulated active power flow on one of the 11 kV feeders and the SCADA measurements of that active power flow is shown in Figure 9.

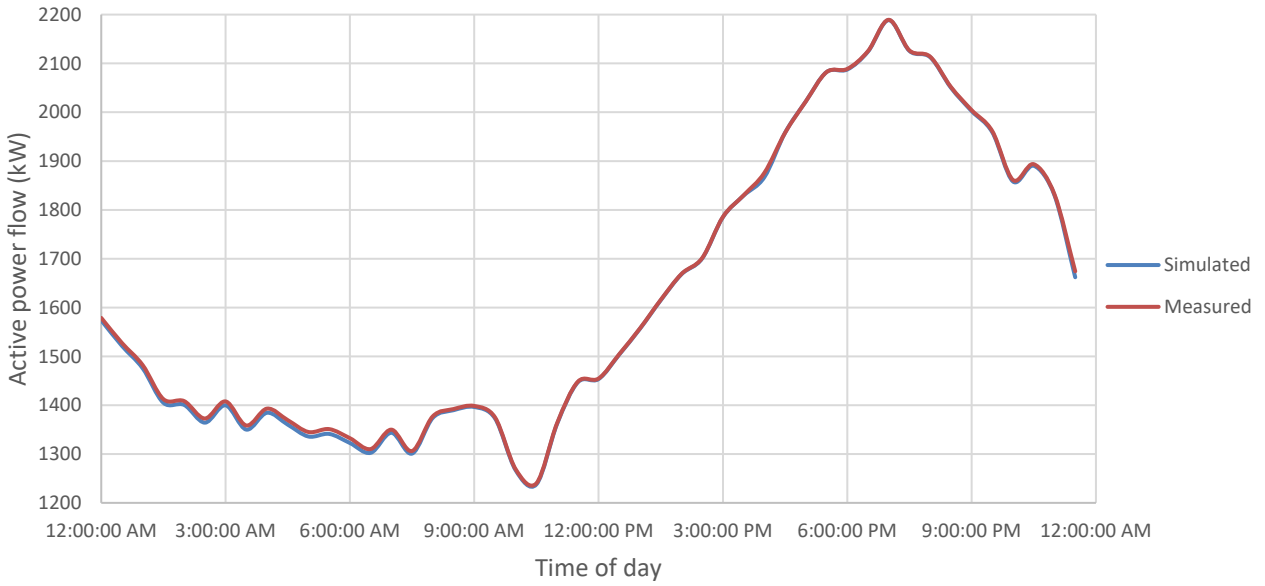

Figure 9 – Comparison of measured and simulated active power flows for Feeder 08 in summer with high solar irradiance conditions

It is clear from Figure 9 that the model reproduces the measured power flows well at the aggregate feeder level. This was an expected result as the load correction process enforced agreement at this level of the network. The agreement between measured and simulated active power flows, reactive power flows and voltages at the LV terminals of each of the distribution transformers on the other hand may have been reduced by this load correction process. This corresponds to the redistribution of modelling error caused by the baselining process as discussed at the beginning of this section of the report; it is likely that the error that would have been present at many of the distribution transformers for which transformer monitor data was unavailable was reduced as a result of the load correction process.

The quality of baselining at the LV terminals of the distribution transformers in the model was assessed by preparing a series of histograms for active power flows, reactive power flows and voltages; some examples for the latter of which are shown in Figure 10 and Figure 11. Note that 229 data-points were used to generate Figure 10 while only 146 data-points, which is equivalent to the number of transformer monitors with usable data for high solar day conditions in spring, were used to generate Figure 11. From Figure 10 and Figure 11 it is apparent that even though the load correction process has altered the sizes of the loads across the network model to force good agreement at the top of each of the 11 kV feeders, the level of agreement between simulated and measured voltages at the LV terminals of the distribution transformers is still reasonably high. The two-peaked shape of the distributions is caused by the fact that the two effective turns ratios of 11275:433 and 11550:433 are the dominant ones in use across the distribution transformers (following the tap corrections processed described earlier). The measured distribution shown in Figure 11 is more spread out and less concentrated in terms of its signal energy simply because of the random variations that are generally present in real-world measurements and that are impossible to capture in simulations.

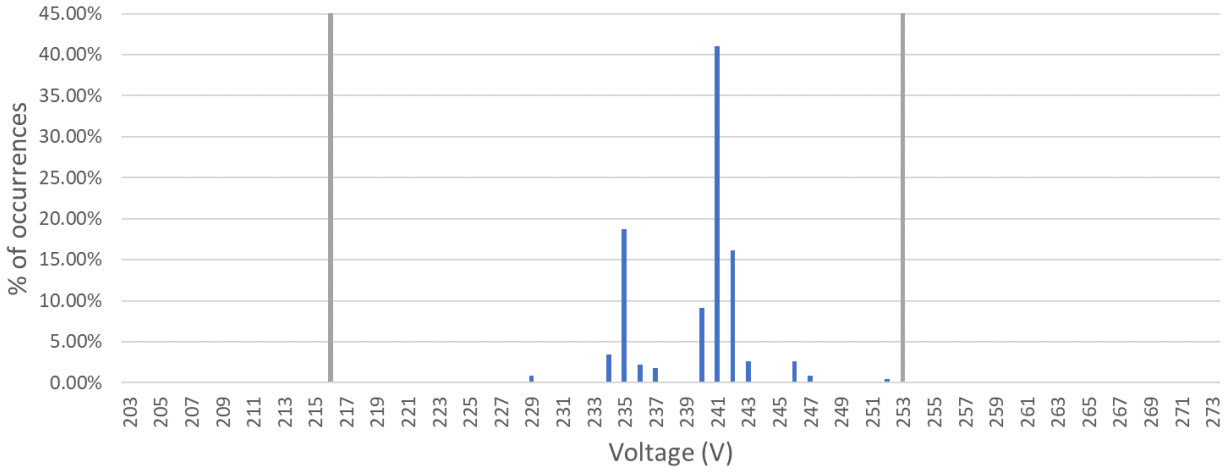

Figure 10 - Distribution transformer LV voltage histogram showing simulated voltages for high solar day conditions in spring at noon

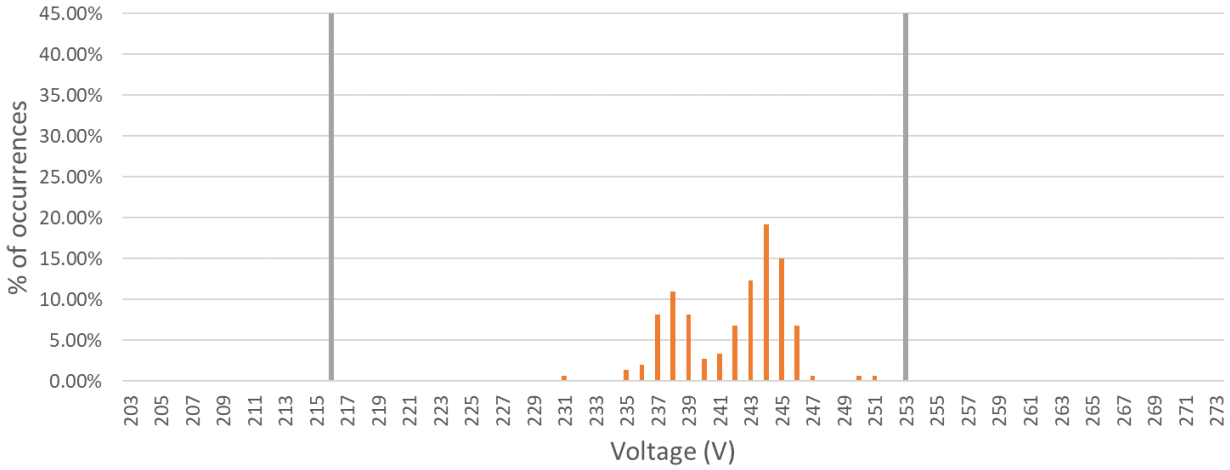

Figure 11 - Distribution transformer active power flow histogram showing measured power flows for high solar day conditions in spring at noon

The averages and standard deviations for the simulated and measured voltage distributions at the LV terminals of the distribution transformers in each season and for each set of solar irradiance and load conditions are summarised in Table 10. The results shown for maximum load conditions were recorded for simulations at 7pm, at which time the solar irradiance is negligible at all times of the year at the latitude of Brisbane. The results shown for minimum load conditions were recorded for simulations at 12pm for high irradiance conditions, at which point maximal PV generation has caused reversal of active power flows on many of the feeders in the studied network. Minimum load given low irradiance conditions was assumed to be reasonably well represented by simulations at 3am in the morning. The averages for the simulated and measured voltage distributions are within 1 – 2 V of each other for eight of the twelve set of conditions shown in Table 10. In some cases, however, the averages differ by as much as 4 V. Note that a distribution transformer tap size of 2.5% in the modelled system corresponds to approximately 6.3 V on the LV windings, indicating that the two distributions are within a half a tap setting of each other for eight out of twelve rows in Table 10 and within a tap setting of each other for the remaining four. This implies that improvement of the agreement between the two sets of distributions via further adjustments to the distribution transformer tap settings would not be possible. The standard deviations of the simulated voltage distributions also show good agreement with the measured ones, indicating distributions with similar shapes.

Table 10 - Statistics for measured and simulated voltages at distribution transformer LV terminals

Season	Solar irradiance and load conditions	Average LV voltage (V)		Standard deviation of LV voltages (V)	
		Simulated	Measured	Simulated	Measured
Spring	Max load	240.67	240.75	3.36	3.17
	Min load, high irradiance	239.97	241.90	3.56	3.38
	Min load, low irradiance	238.59	242.50	3.33	3.32
Summer	Max load	240.18	238.23	3.38	3.29
	Min load, high irradiance	239.01	239.73	3.19	3.35
	Min load, low irradiance	238.44	240.00	3.32	3.21
Autumn	Max load	240.29	238.69	3.37	3.21
	Min load, high irradiance	239.35	240.28	3.47	3.42
	Min load, low irradiance	238.58	240.31	3.33	3.29
Winter	Max load	240.63	241.06	3.37	3.22
	Min load, high irradiance	239.81	243.89	3.30	3.34
	Min load, low irradiance	238.58	241.31	3.34	3.07

The averages and standard deviations for the simulated and measured active power flow distributions at the LV terminals of the distribution transformers in each season and for each set of solar irradiance and load conditions are summarised in Table 11. It is clear that the simulated active power flows are generally in good agreement with the measured ones. Both the simulations and measurements indicate that the active power flow on the average distribution transformer in the modelled system reverses direction during high irradiance conditions at 12pm in spring, autumn and winter. The standard deviations of the active power flows on the distribution transformers exhibit significant variations depending on the time of day, solar conditions and season; the agreement between the simulations and measurements for these is nevertheless fairly high in general.

Table 11 - Statistics for measured and simulated active power flows at distribution transformer LV terminals

Season	Solar irradiance and load conditions	Average active power flow (kW)		Standard deviation of active power flow (kW)	
		Simulated	Measured	Simulated	Measured
Spring	Max load	66.98	63.76	48.32	45.79
	Min load, high irradiance	-24.61	-19.92	57.38	59.57
	Min load, low irradiance	30.59	29.15	23.25	22.09
Summer	Max load	85.63	98.87	61.61	70.64
	Min load, high irradiance	0.91	-7.26	65.43	58.49
	Min load, low irradiance	36.62	38.77	26.57	28.47
Autumn	Max load	80.00	83.16	57.74	57.28
	Min load, high irradiance	-4.21	-2.49	72.13	51.05
	Min load, low irradiance	31.16	33.07	22.06	24.39
Winter	Max load	69.55	67.60	47.83	45.57
	Min load, high irradiance	-35.34	-21.26	54.16	55.75
	Min load, low irradiance	31.83	29.56	22.87	20.25

The averages and standard deviations for the simulated and measured reactive power flow distributions at the LV terminals of the distribution transformers in each season and for each set of solar irradiance and load conditions are summarised in Table 12. The reactive power flows across the distribution transformers are relatively small in general when compared to the active power flows; for this reason, the apparent poor agreement between the simulated and measured reactive power flows indicated by Table 12 can be considered an overstatement. Improvement of this agreement would necessitate predictions of the time-varying power factors of each of the loads modelled in the network under study, which would be difficult and beyond the scope of this study. Furthermore, the relatively high agreement between the simulated and measured distribution transformer LV terminal voltage distributions shown in Table 10 indicates that the level of accuracy of the baselined system is sufficient, as accurate prediction of LV voltages is the primary objective of this study.

Table 12 - Statistics for measured and simulated reactive power flows at distribution transformer LV terminals

Season	Solar irradiance and load conditions	Average reactive power flow (kVAr)		Standard deviation of reactive power flow (kVAr)	
		Simulated	Measured	Simulated	Measured
Spring	Max load	-1.10	-3.07	3.81	11.17
	Min load, high irradiance	4.03	-3.61	14.00	12.65
	Min load, low irradiance	-2.05	-5.92	3.35	10.09
Summer	Max load	-0.37	1.04	3.99	13.88
	Min load, high irradiance	1.52	-0.96	11.13	14.19
	Min load, low irradiance	-1.95	-4.48	3.31	10.06
Autumn	Max load	-0.63	-1.21	3.82	12.56
	Min load, high irradiance	2.21	-3.49	13.12	15.26
	Min load, low irradiance	-2.06	-5.86	3.31	10.43
Winter	Max load	-1.01	-3.60	3.79	9.59
	Min load, high irradiance	5.13	-4.91	14.80	11.65
	Min load, low irradiance	-2.03	-6.05	3.34	8.87

4.5 State of the baselined network

For all seasons of the year, the baselined model representing the present-day state of the network exhibits negligible curtailment of PV generation throughout the daylight hours of peak solar irradiance. As the average capacity of installed solar generation is only approximately 2.6 kW per household[1] at this stage, this result is as expected.

The distributions of voltages on all LV buses of the network for high solar irradiance conditions at 12pm and 7pm in spring are shown in Figure 12 and Figure 13 respectively. It is clear that the voltage distribution does not violate the statutory upper limit of 253V or the lower statutory limit of 216V at this stage.

[1] *This average is taken across all households, not just those with installed solar PV systems.*

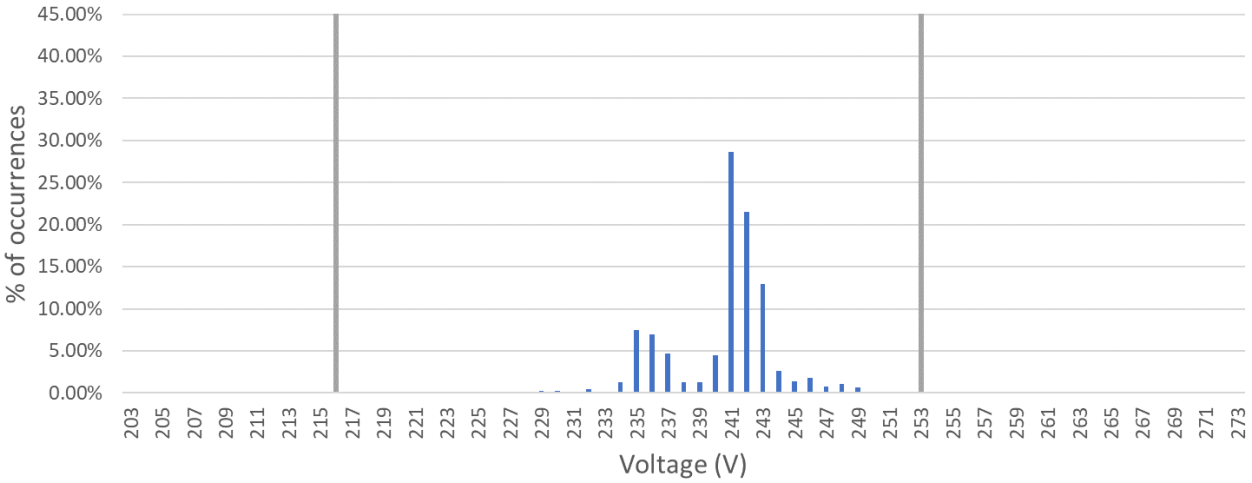

Figure 12 - Histogram showing distribution of simulated voltages for all LV nodes in network simulated voltages for high solar day conditions in spring at noon

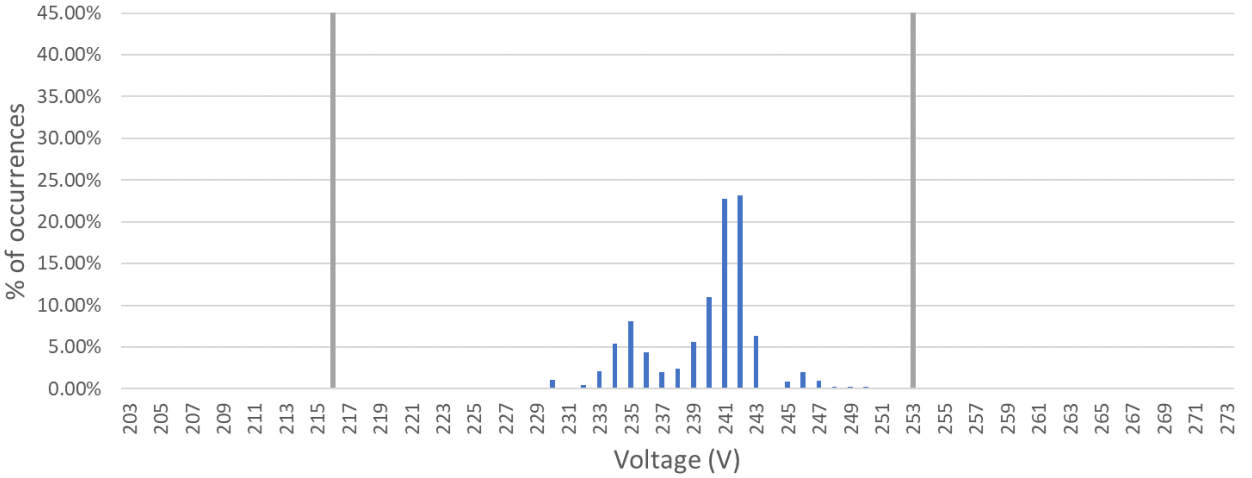

Figure 13 - Histogram showing distribution of simulated voltages for all LV nodes in network simulated voltages for high solar day conditions in spring at 7pm

The averages and 0.1st, 1st, 99th and 99.9th percentiles of the distributions for all LV voltages in the model under all seasons, load conditions and solar irradiance conditions are shown in Table 13. The lower statutory limit of 216V is not violated at any time of day or year. The upper statutory limit of 253V on the other hand is exceeded in winter during high irradiance conditions and minimum load (i.e., in the middle of the day at 12pm), but only in the 99.9th percentile. Given that the model contains 8382 LV buses, the 99.9th percentile corresponds to fewer than ten buses exhibiting voltages that exceed the upper limit. It is therefore clear that the existing network under study is, at present, neither overloaded nor overburdened with rooftop PV generation at any time of day or year.

Table 13 - Statistics for distributions of simulated voltages on all LV buses in the model

Season	Solar irradiance and load conditions	LV voltages 0.1st percentile (V)	LV voltages 1st percentile (V)	LV voltages average (V)	LV voltages 99th percentile (V)	LV voltages 99.9th percentile (V)
Spring	Max load	225.19	229.96	239.81	247.13	249.74
	Min load, high irradiance	228.78	232.52	240.58	248.35	249.73
	Min load, low irradiance	227.52	228.02	238.39	245.89	246.73
Summer	Max load	225.50	230.07	239.45	248.50	249.73
	Min load, high irradiance	228.30	232.45	239.47	246.68	247.95
	Min load, low irradiance	227.35	227.98	238.11	245.82	246.71
Autumn	Max load	226.17	229.98	239.69	248.36	249.72
	Min load, high irradiance	227.91	232.10	239.69	248.02	249.16
	Min load, low irradiance	227.48	227.95	238.36	246.12	247.06
Winter	Max load	224.47	229.82	239.33	246.69	249.57
	Min load, high irradiance	229.15	233.67	240.90	248.60	253.67
	Min load, low irradiance	227.41	227.96	238.34	245.84	246.96

4.6 Discrepancy between baselined load and Energex forecasts

The intent of the study was to capture the expected future levels of overvoltage and undervoltage events that will be expected to exceed the statutory limits for extended periods of time (i.e., more than a few minutes in one day of the year), rather than for only brief/transitory and rare outlier events. The former type of exceedances is more of interest because they correspond to consequences like lost energy and financial benefits due to curtailment, appliance degradation due to over voltages and poor service quality that customers would be likely to notice (i.e., brownouts). The more extreme but short and infrequent voltage limit exceedance events that could occur when peak or minimum load forecasts presented in Energex's Distribution Annual Planning Report (DAPR) for 2022 [11] are realised in practice however would result in different but more extreme consequences, such as unwanted protection system operation and outages. Although these consequences would also be of interest from a research perspective, they are more difficult to capture with a theoretical model and are also of less interest than the other consequences that would be observed during more sustained voltage exceedance events.

Due to the reasoning outlined above, the baselining methodology adopted in this study was intended to identify load curves for typical days with relatively high load in each season while simultaneously excluding load transfers, outages or other unusual events resulting in abnormally high or low load. As a consequence of this, the maxima and minima of the load curves used for the baselining in this study are less extreme than the maximum and minimum load forecasts shown in the DAPR. The substation peak load figures in particular are 10-15 MW lower than that shown in the DAPR. Note that this does not correspond to a modelling error, but rather a deliberate focus on expected future voltage violation events that would be more likely to drive investment in voltage management solutions. The selected data corresponds closely to the 98th percentile of load data, when considering the substation load-duration curve.

5 Future Scenario Development and Modelling

5.1 DER growth trajectories

For the studies of over and undervoltage issues that could be caused in future by DER in this report, a simplifying assumption was made that no BESS technology will appear either behind the meters of the homes in the modelled area or at the community level. Although it is inevitable that both of these types of BESS systems will eventually appear throughout Australian suburbs in the coming decades, the exact timing with which these technologies will appear, in sufficient numbers to be impactful, is difficult to predict. Projections of their growth presented in AEMO's 2022 ISP show slow growth relative to rooftop PV and EVs in general [6]. It is likely that these projections are somewhat dependent on the assumed cost trajectory for BESS systems, and the rate at which their costs change is likely to have a major impact on the growth trajectory. Since BESS systems will tend to support voltage management throughout the network when they appear, their inclusion in the studies for this report may result in an optimistic assumption that would lessen the severity of the energy curtailment, overvoltage and undervoltage results identified. On the other hand, their exclusion could be considered as a conservative assumption with associated error that is likely to be relatively small. Using the same reasoning; time of use tariffs, other tariff mechanisms, vehicle to grid discharging technology, EV reactive support services, home energy management systems (HEMS) that automate demand side management using smart appliances and underlying residential and commercial/industrial load growth have also all been omitted. The combination of residential demand tariffs and HEMS is likely to be a game changer for the networks as the impact is expected to be a flattening of the load curves. Unfortunately, the extent and timing of such changes is impossible to predict with any certainty, and hence, must be omitted from this study.

Projections of PV and EV growth that were studied in this project have been scaffolded from the Step Change and Slow Growth scenarios presented in [6]. The small-scale rooftop PV and EV projections from both of these scenarios have been downscaled to "per household" estimates as well as, in the case of part of the rooftop PV growth, "per business premises" estimates using average yearly population growth assumptions of 1.1% for Slow Growth and 1.3% for Step Change. These assumptions were sourced from the 2021 and 2022 EV Forecast reports released by the CSIRO respectively [12], [13]. Since the research done by the CSIRO was part of the source material which the AEMO uses to generate their ISP scenarios, these assumptions are applicable to the ISP scenarios.

Inclusion of the "Hydrogen Superpower" scenario, which involves faster growth in PV and EVs than does Step Change, was also considered. Since the general industry consensus at present is that Step Change is a more likely ISP scenario to eventuate, the decision was made to retain Step Change as the scenario in the study with the most rapid PV and EV projections and to simply add an additional tolerance of 20% to these, which results in projections beyond what is predicted by Hydrogen Superpower in any case. The tolerance of 20% was also subtracted from the projections in the Slow Growth scenario. It is noted here that the widening of the study projections by ±20%, which increases the range of future growth trajectories captured, is justified by the approximate nature with which the AEMO projections have been down-scaled from NEM-wide to per-household/per-business estimates.

The PV projections provided by the ISP were first sub-divided into residential and small business/light industry components using data provided in the 2021 CSIRO DER Forecast Report. A universal value of 0.75 was found to be a good approximation for this ratio across the years and scenarios for which it was calculable. The number of occupied private and non-private dwellings in Queensland at present was sourced from Australian

Bureau of Statistics (ABS) data [14]. The proportion of Queensland dwellings now and in the future which will be separate dwellings, rather than apartment complexes or townhouses which are unlikely to see significant future growth in rooftop PV, was also identified using separate dwelling data from the 2021 and 2022 EV Forecast reports released by the CSIRO [12], [13]. This starting pool of Queensland houses was then assumed to grow at the yearly average population growth rates associated with each of the two scenarios that were mentioned previously and the residential portion of the Queensland-wide PV projections from the ISP were then divided by this number in each future year of the study to obtain the average installed PV capacity per household. In the case of small-scale PV on businesses and light industrial buildings, since no statistics on the number of these in Queensland were available and since no need to distinguish between separate and non-separate buildings exists for these, the original installed capacity found on these types of buildings in the baselined model will simply be grown at the population growth rates attributable to each.

Data released by the ABS was also used to estimate the number of passenger vehicles garaged in or near to the typical Queensland household as 1.8 [15]. Projections for EVs were developed using the proportion of fleet share projections in these two reports, with the assumption that the eventual maximum size that the market for EVs in Queensland will grow to will correspond to a household average number of EVs equivalent to the 1.8 internal combustion engine-based passenger vehicles owned per household today. Note that this implies an exclusion of hydrogen-fuel-cell-based EVs, which is justified on the grounds that their growth trajectories in the ISP scenarios are significantly slower than the corresponding trajectories for battery-based EVs in general and that their inclusion would amount to an optimistic assumption in terms of future undervoltage severity. Figure 14 and Figure 15 depict the projections in average EVs per household and average installed capacity of residential PV per household respectively for the scenarios that have been chosen.

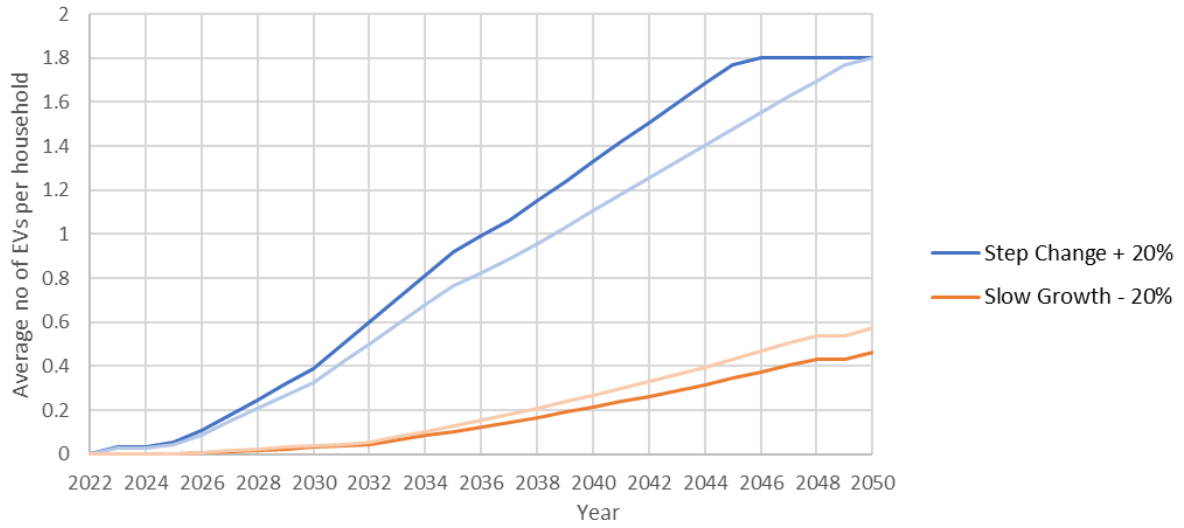

Figure 14 – Projections of EV growth in Step Change and Slow Growth scenarios with ±20% tolerance margins added

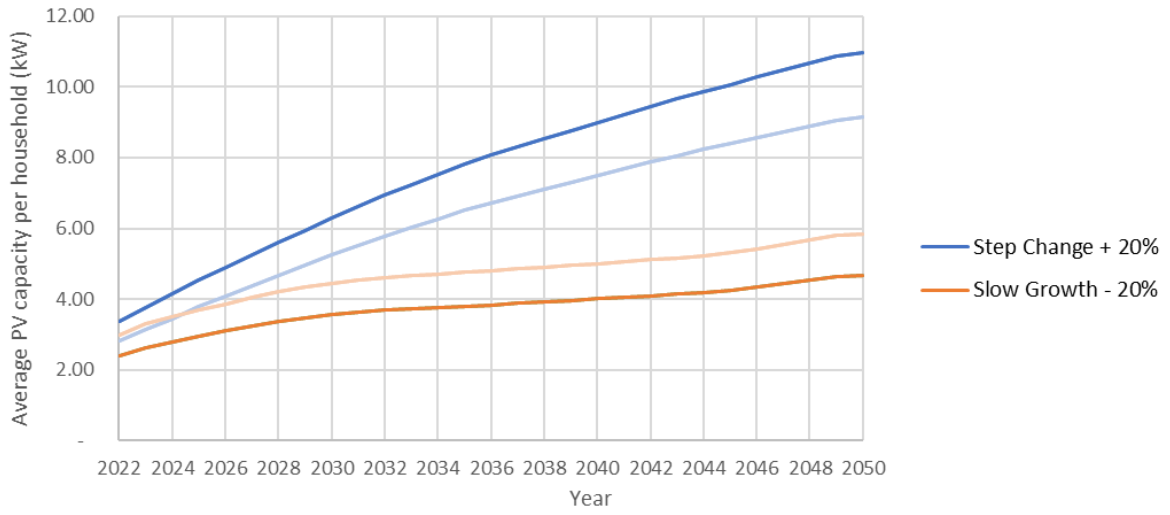

Figure 15 - Projections of residential PV inverter growth in Step Change and Slow Growth scenarios with ±20% tolerance margins added

Future states of the modelled area were constructed for each five-year interval from 2025 to 2050 inclusive. These future states of the model were realised by increasing the number of PV installations and EVs represented by sampling from uniform distributions to determine which customers connect new PV or EV systems. They were also realised in a successive fashion. However, versions of the model representing some of the points on the Step Change trajectories were created by increasing PV and EV volumes from versions of the model representing points on the Slow Growth trajectories and vice versa. In other words, each future version of the model in either of the two scenarios was created from whichever other version of the model in either scenario had the closest smaller amount of net PV and EV capacity. This was done to ensure that the areas of the modelled network exhibiting the most significant curtailment and voltage limit violation would emerge in both scenarios and all future states of the model in a consistent way, so that they could all be investigated consistently as well.

5.2 Modelling for PV installations

Since it would be unreasonable to assume that future solar PV installations should exhibit the same generation characteristics as existing PV systems installed elsewhere on the same LV feeder, annual solar generation data for a new installation in the modelled area was obtained using a commercial software tool known as "Helioscope". This annual generation data was used in conjunction with a DC-AC ratio of 1.2, which was assumed to be typical of future installations based on current Australian residential rooftop PV market trends [16], to formulate the peak PV inverter utilisation factors for each season of the year shown in Table 14. Note that these utilisation factors are applicable at noon on days with negligible cloud cover.

Table 14 – Peak PV inverter utilisation factors (%)

Summer	Autumn	Winter	Spring
100	97.62956	82.89305	100

It is noted here that the assumption of a uniform future DC-AC ratio of 1.2 was critical as it influences the amount of spare apparent power capacity that each PV inverter component has, which in turn it uses to support the network voltage via volt-var control. Using volt-var control to support the network voltage has the effect of staving off the need to activate volt-watt control and curtail active power output. Thus, the assumption around DC-AC ratio directly impacts the expected level of curtailment; higher values of the ratio will produce more expected curtailment and vice versa. A DC-AC ratio of 1.2 is a reasonably conservative assumption for this parameter that is in agreement with recent trends in the Australian rooftop PV market, but which does not hit the upper limit of 1.333, beyond which accreditation from the Clean Energy Council is no longer allowed and use of funding from government incentive schemes is no longer possible [17].

While there is a 5 kW export limit applicable to many PV installations across the Energex network at present, export limit values were shown for only a relatively small subset of PV installations in the existing network. It was therefore decided to assume that future PV installations added to the modelled network would not have an export limit applied. It was also assumed that the PV capacity owned by any one residential or commercial/ industrial customer should not have an upper limit, since available roof space possessed by different properties vary widely. Future PV installations were also assumed to be uniformly sized at 8 kW of inverter capacity in line with typical market trends [16]. While real-world rooftop PV systems will continue to be installed in a variety of sizes in practice, this assumption was made to simplify the augmentation of the model to include future growth in PV. Furthermore, this assumption will have had negligible impact on the curtailment results as the expected growth in average PV capacity per household has been adequately represented in the model and the volt-watt and volt-var algorithms are implemented on an installed capacity per-unit basis.

5.3 Modelling for EV charging

Two different sizes of EV charger were assumed in this study: 3.68 kW and 7.36 kW. It was assumed that all customers with a single or double phase connection to the distribution network would own the smaller size of charger, while all customers with three phase connections would have the larger size of charger. While some residential customers in the modelled area may choose to have their connections upgraded to three phase connections in future, it is expected that the proportion of these would be small. The populations of customers owning EVs and each of the two sizes of chargers were represented throughout the course of each daily simulation using two separate after-diversity charging curves sourced from the section on unmanaged EV charging in [18]. These charging curves were formulated from a trial in the UK and are thus expected to constitute reasonable representations of EV usage in dense suburban areas in Australia as well. They correspond to weekday EV charging trends. While weekend curves were also available, these were excluded from the present study in the interests of simplicity and based on the fact that the weekday curves were identified as having sharper, higher peaks and are also representative of conditions that occur more often.

For the future scenarios modelled, new EVs were assigned to residential customers represented in the model at random using sampling from uniform distributions. This process was applied until the average EV ownership per household corresponded to the values shown at particular points on the EV growth curves in Figure 14 or Figure 15 as appropriate. An upper limit of no more than two EVs per residential customer was enforced. While it is conceivable that some family households with a large number of occupants might own more EVs than this in future, it is more or less inconceivable that they would be likely to charge more than two EVs at any one time due to the large amount of secure garage space that this would require. The modelled area does represent power supply to a relatively small number of residential customers on large semi-rural properties at

the fringe areas of the suburb. For the most part however, the residential customers represented by the model own properties in the size range that is typical of middle and low-income Australians and the upper limit of two EVs charging at any one property is considered appropriate. It is also noted here that charging of electrified trucks and other types of vehicles that would be used by commercial and industrial customers has not been represented in this study, as it is assumed that this will take place mostly at large depots located elsewhere from the area represented by the model.

Charging of EVs in this study was modelled using a Monte Carlo approach. The EV representations in each future state of the model were activated randomly using uniform distributions until the cumulative amounts of active power drawn by each of the 3.68 kW and 7.36 kW charger populations corresponded to the points on each of their respective after-diversity charging curves from [18] when averaged across each of those populations respectively. It was also assumed that the population of the modelled suburb would not change significantly in future. In practice there may be some new high-rise apartment complexes built in the modelled suburb in future, which would impact the number of EVs purchased to some extent as EV ownership would be challenging to accommodate in such complexes. The growth of such complexes in the modelled suburb would be likely to be slow and is difficult to predict in general however, hence an assumption of no apartment complexes appearing in the modelled suburb over the modelling horizon was adopted for this study.

6 Modelling Results

6.1 Global curtailment and voltage trends

Global results are presented in the first two sections of this chapter. The term "global" is intended to imply solutions for the whole network model, except in several of the years of the Step Change scenario, for which it corresponds to solutions for the largest subset of 11 kV feeders for which the load flow algorithm could solve the model without non-convergence. More specifically, starting from the first version of the Step Change model in 2025, two specific 11 kV feeders must be deactivated for the model to solve for high solar day conditions at noon and must remain deactivated for it to solve for the same conditions for all years through to 2040 inclusive. Then in the year 2045, three specific 11 kV feeders must be deactivated for the model to solve for high solar day conditions at noon. Finally, in the final year of the Step Change scenario, six specific 11 kV feeders out of the ten such feeders in the model must be deactivated for the non-convergences to be avoided when running load flow simulations for high solar day conditions at noon. The non-convergences do not appear for the same simulations conducted with all MV feeders active at other times of day, such as at 7.30pm.

These non-convergences in the load flow algorithm are likely to have been encountered as a result of the model being close to the edge of its voltage magnitude – active power generation characteristics in some LV areas at noon in high solar day conditions. In other words, some regions of the LV system begin to exhibit solar-derived active power generation that is so high that it causes the voltage to approach a critical upper limit beyond which local voltage instability ensues. This form of voltage instability would be similar to the classical form of voltage instability presented in section 2.1.2 of [19], except that the "load" in this case is negative and the direction of active power flow is towards the fixed voltage source represented by the upstream network rather than away from it. Iterative load flow algorithms can often lose stability even when network instability thresholds such as these are approached but not traversed as such algorithms entail sequences of attempts at guessing the solution that oscillate either side of it before hopefully converging on a final correct answer. At any rate, the average values of electric vehicle count per household as well as the average values of solar inverter capacity per household and per business targeted in the 20%-inflated version of the Step Change scenario used in this study are still maintained even with the reduced number of 11 kV feeders active in all years of the study. In other words, the population size represented by using the maximal-solvable-subsets of MV feeders are more than sufficiently large in a statistical sense to produce results that are still generally applicable. Additional tests were also carried out with subsets of the MV feeders deactivated in the 2050 Slow Growth model to see if the results obtained from that version of the model with all MV feeders active would be recovered, which they were (noting that the results are percentiles across the populations simulated rather than total cumulative values).

Figure 16 shows the total energy that would be supplied by rooftop solar PV in the modelled network in the half-hour period around noon given high solar irradiance conditions in summer if the voltages across the LV network were lowered to a degree sufficient to prevent all curtailment. This trend has been plotted for both of the ISP scenarios. The cumulative amount of solar energy that would be supplied in the same time period and under the same conditions given the curtailment found to be occurring in the model has also been plotted with dashed curves. Even in the penultimate modelled year of the Step Change scenario, at which the installed PV inverter capacity has increased to 154.2 kVA, the ratio of energy curtailed to energy supplied is only as high as 2.3%.

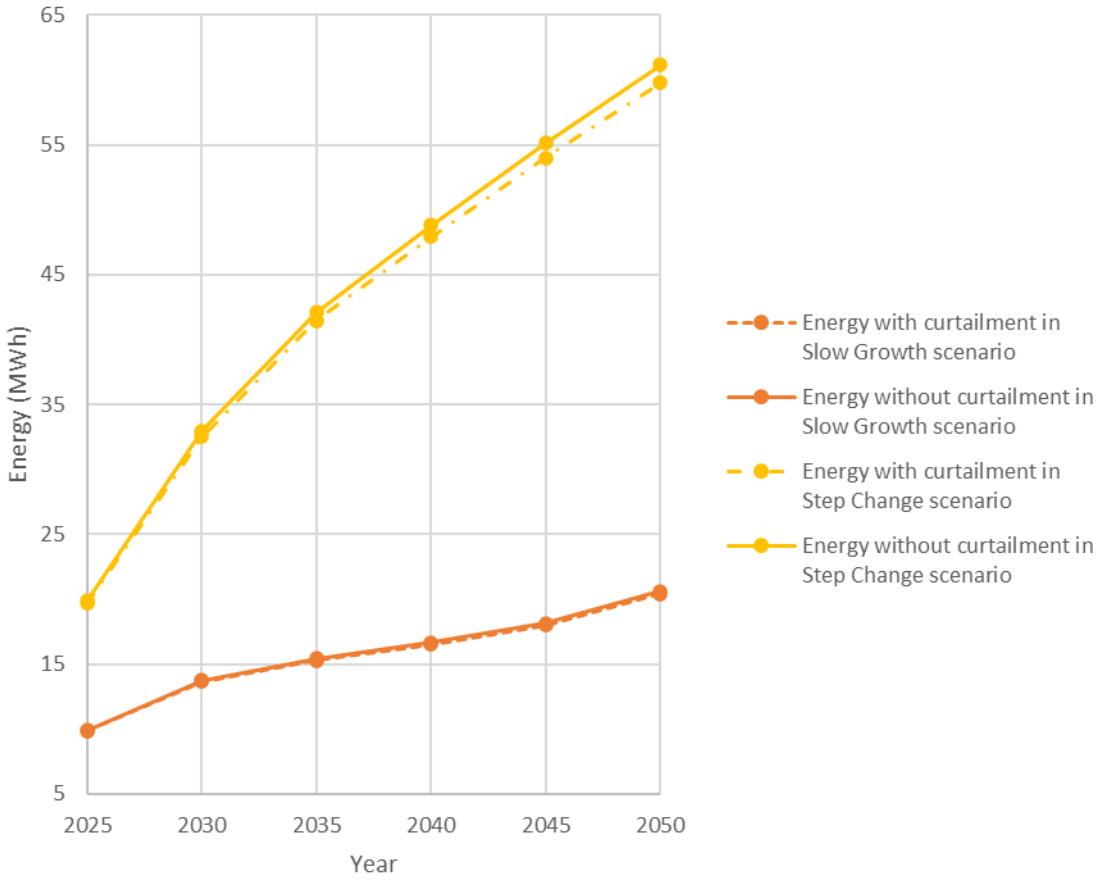

Figure 16 – Total energy that would be supplied by rooftop solar PV in the modelled network in the half-hour period around noon given high solar irradiance conditions in summer with and without curtailment

In Figure 17 on the other hand, the same metrics have been plotted for the same conditions as in Figure 18, except that the energy values have been calculated for only the top ten customers in the network model experiencing the worst curtailment. Although the units on the vertical axis have shrunk from MWh to kWh, it is clear that the curtailment being experienced by these customers is much worse on a relative basis. Note that the cumulative energy figures do not necessarily increase monotonically throughout all years in Figure 17 as the identity of the ten customers experiencing the worst curtailment is determined on a per-unit installed capacity basis, thus their identities change between some years. Comparison of Figure 16 and Figure 17 reveals that for the studied network at least, the economic opportunity cost of solar energy lost due to curtailment is unlikely to become significant, but the social inequity that it creates, is.

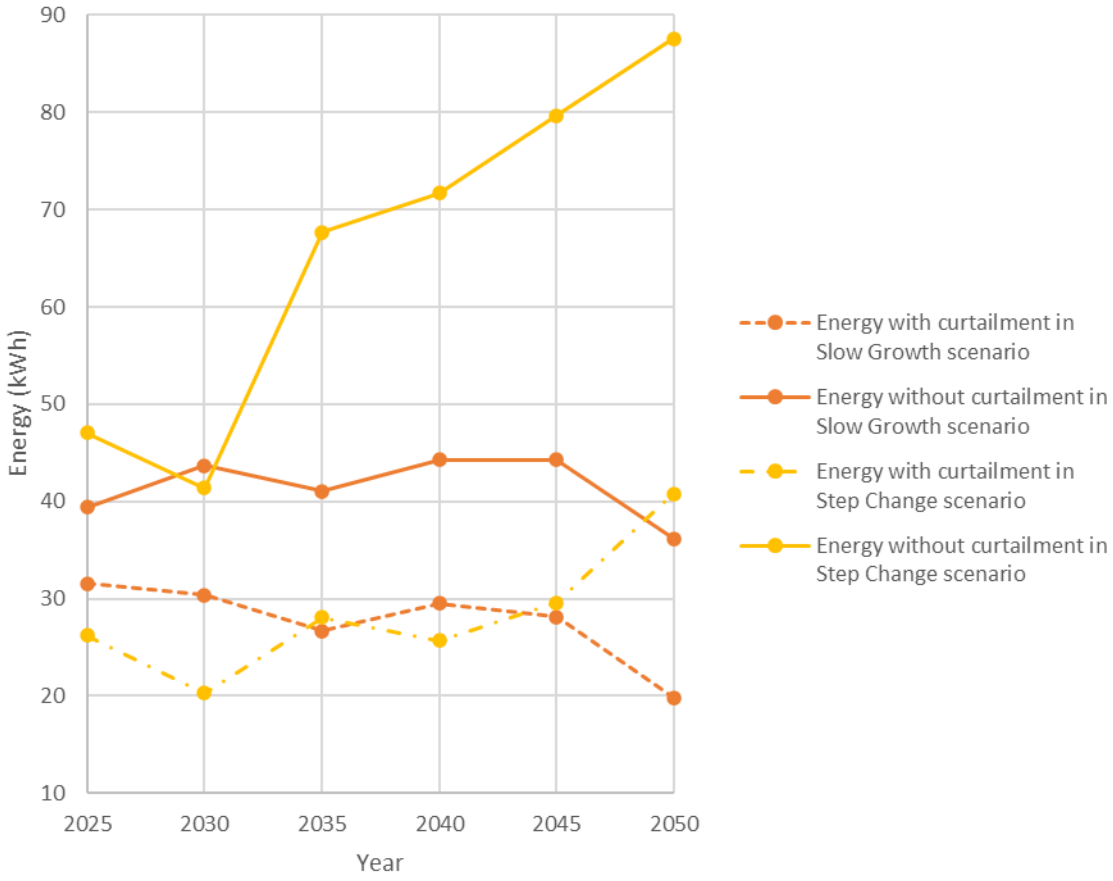

Figure 17 – Total energy that would be supplied by rooftop solar PV in the modelled network in the half-hour period around noon given high solar irradiance conditions in summer with and without curtailment

Several representations of results in this and other subsequent sections of this report have been made using the percentile calculation. The use of a few instances of this calculation furnishes efficient but concise representations of large distributions of data. In case the reader is not familiar with the meaning of this calculation; the n^{th} percentile of a distribution implies the value above which 100-n percent of the population lies. The 99^{th} percentile of a distribution for example thus represents the value above which precisely one percent of the population lies. The 50^{th} percentile on the other hand is representative of the middle of the distribution; while it is similar to the mean or average of the distribution if the distribution is fairly symmetric in shape, it is not the same as the latter metric in general. The 1^{st} percentile and 99^{th} percentile both represent values that are relatively rare in the population, but which lie at the two extreme regions at the edges of the distribution i.e. the lower and upper tails of the distribution respectively.

In Figure 18, the values for several percentiles of the global PV curtailment distribution for noon on high solar days in summer are presented for the six different five-year periods for which simulations have been carried out in the Slow Growth scenario. Note that the lines joining each of the points are merely interpolated and do not constitute the result of separate independent simulations. Note also that the curtailment data for which percentiles have been calculated here have been reported on a per-customer-installed-capacity basis; they therefore reflect trends in expected customer experience relative to the kVA of capacity on their solar inverter systems. It is clear that even in 2050, curtailment is relatively insignificant for all but the top 1% of customers in this scenario. This is expected however as the Slow Growth scenario from AEMO's 2022 ISP has been deflated by 20% in this study to capture the lowermost bounds of what can be expected to be likely to occur.

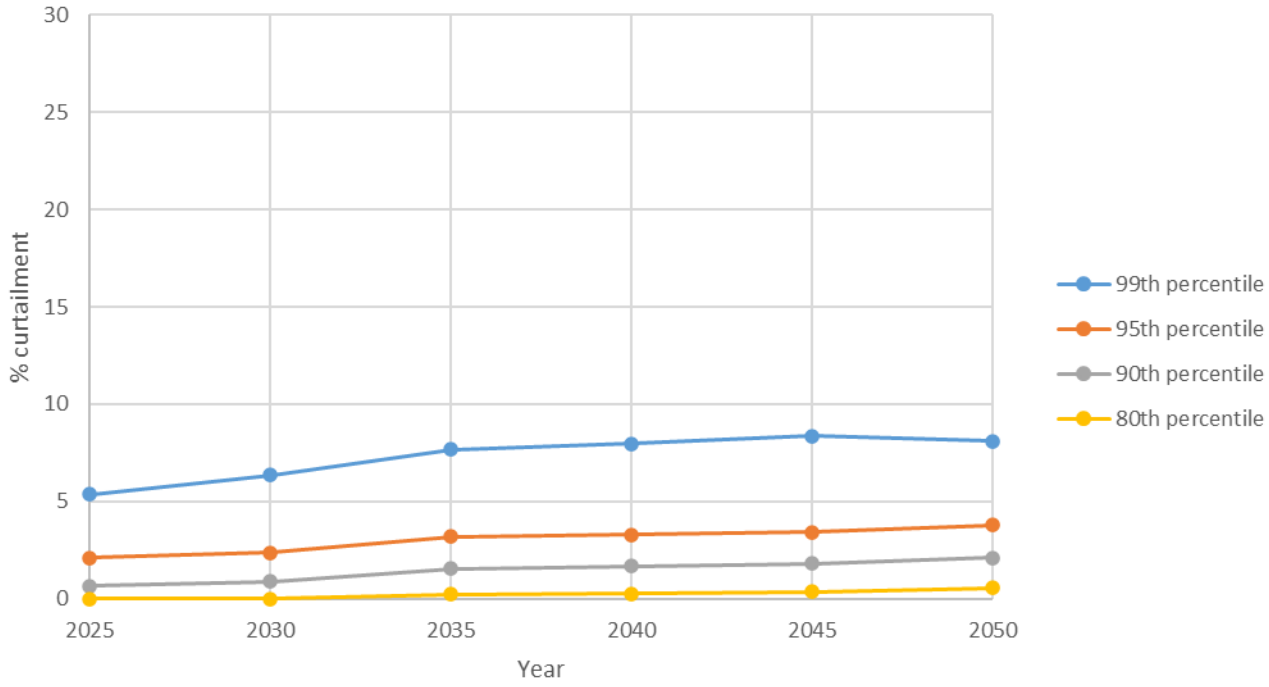

Figure 18 – Percentiles of the global curtailment distribution for noon in summer in the Slow Growth scenario under high solar day conditions

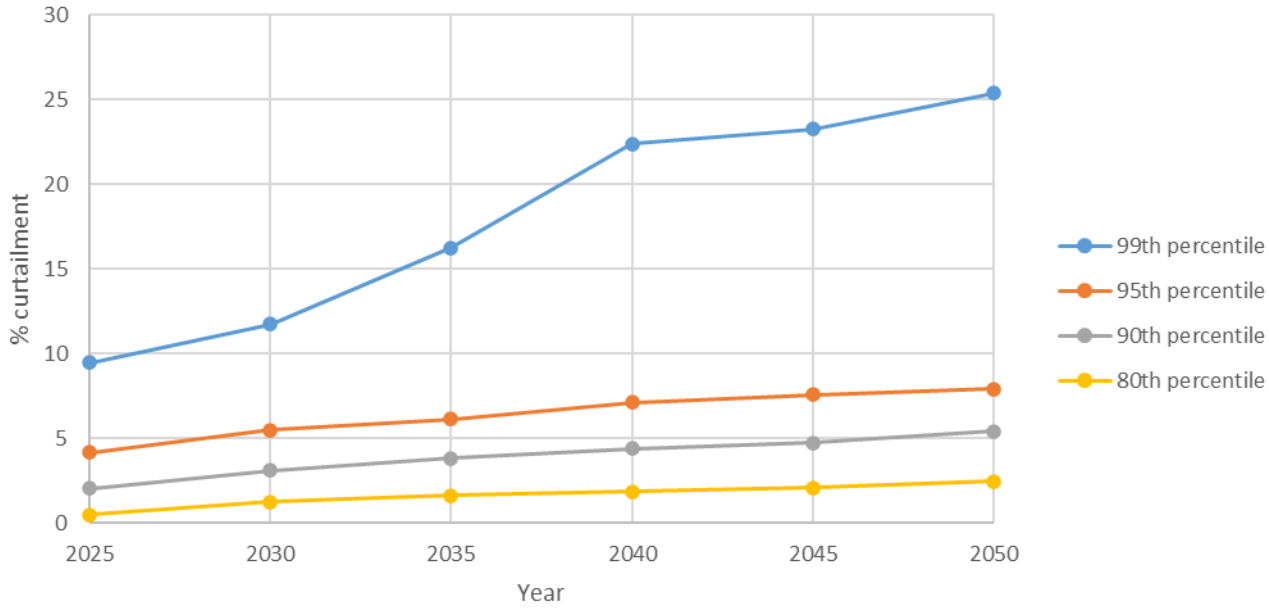

Figure 19 – Percentiles of the global curtailment distribution for noon in summer in the Step Change scenario under high solar day conditions

In Figure 18 and Figure 19, the values for several percentiles of the global PV curtailment distribution for noon on high solar days in summer are presented for the six different five-year periods for which simulations have been carried out in the Step Change scenario. The amount of curtailment is significantly higher; in 2050 the minimal amount of curtailment experienced by the top 5% of the population (i.e., the 95th percentile) is higher than the minimal amount of curtailment experienced by the top 1% of the population (i.e., the 99th percentile) in the same year in Slow Growth. Summer exhibits the most substantial growth in curtailment of the four seasons investigated due to the higher levels of assumed solar irradiance and thus peak PV utilisation.

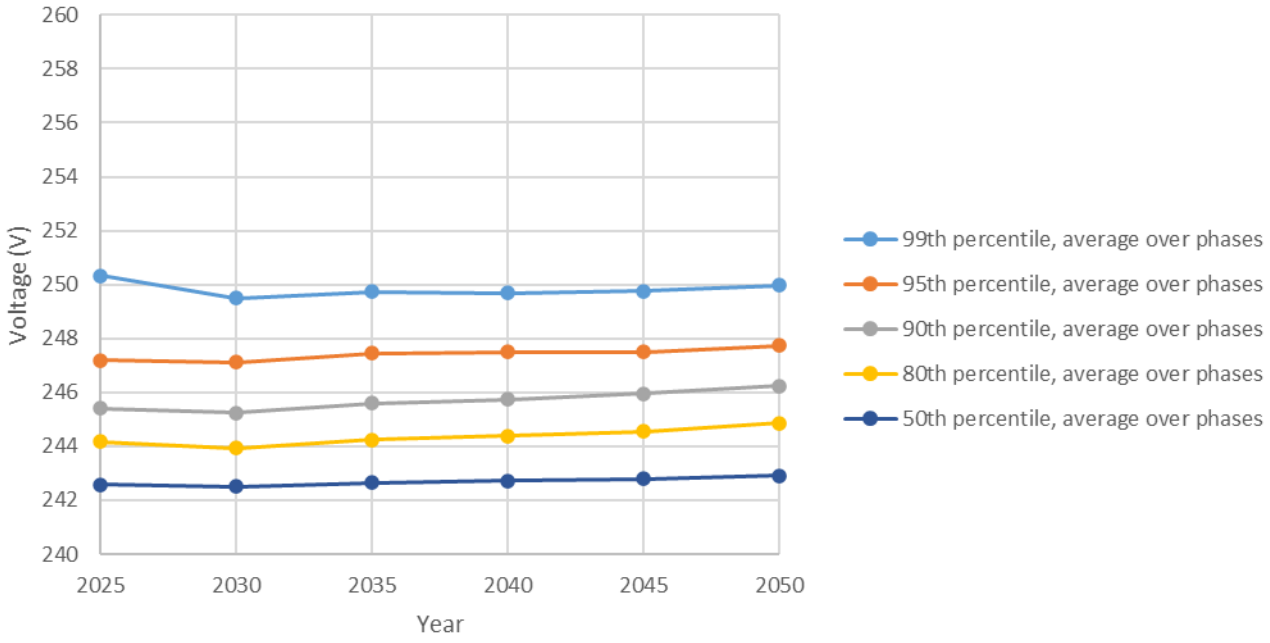

Figure 20 – Percentiles of the global LV bus voltage distribution for noon in summer for high solar day conditions in the Slow Growth scenario with the average of three phase-neutral voltages taken for each individual bus

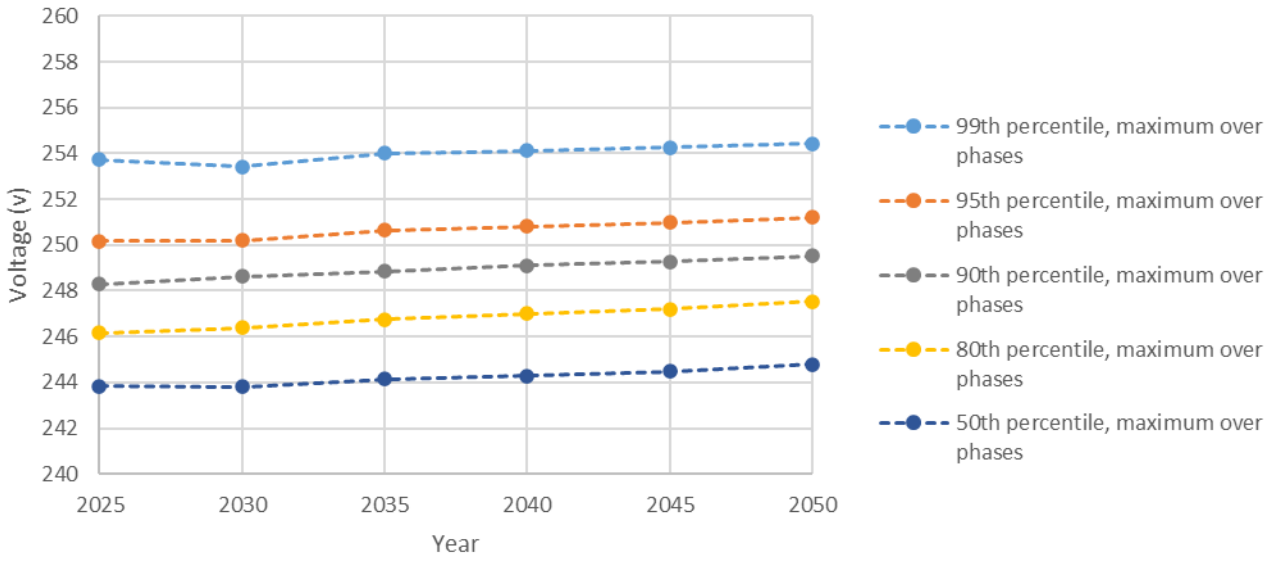

Figure 21 – Percentiles of the global LV bus voltage distribution for noon in summer for high solar day conditions in the Slow Growth scenario with the maximum of three phase-neutral voltages taken for each individual bus

Figure 20 and Figure 21 show percentiles for the global LV bus voltage distribution for Slow Growth at noon in summer for high solar day conditions. The percentiles do not change significantly throughout the years of the study. The first of these plots shows percentiles for the distribution of average bus voltages with averages taken across the three phase-neutral voltages of each bus. The second plot however shows percentiles taken from the distribution of maximal LV bus voltages wherein the maximum of the three phase-neutral voltages for each individual LV bus has been taken. Only the latter of these two metrics exhibits violation of the 253V statutory upper limit in the 99th percentile; it is important to consider however as customers can be connected to any given phase on a specific LV bus.

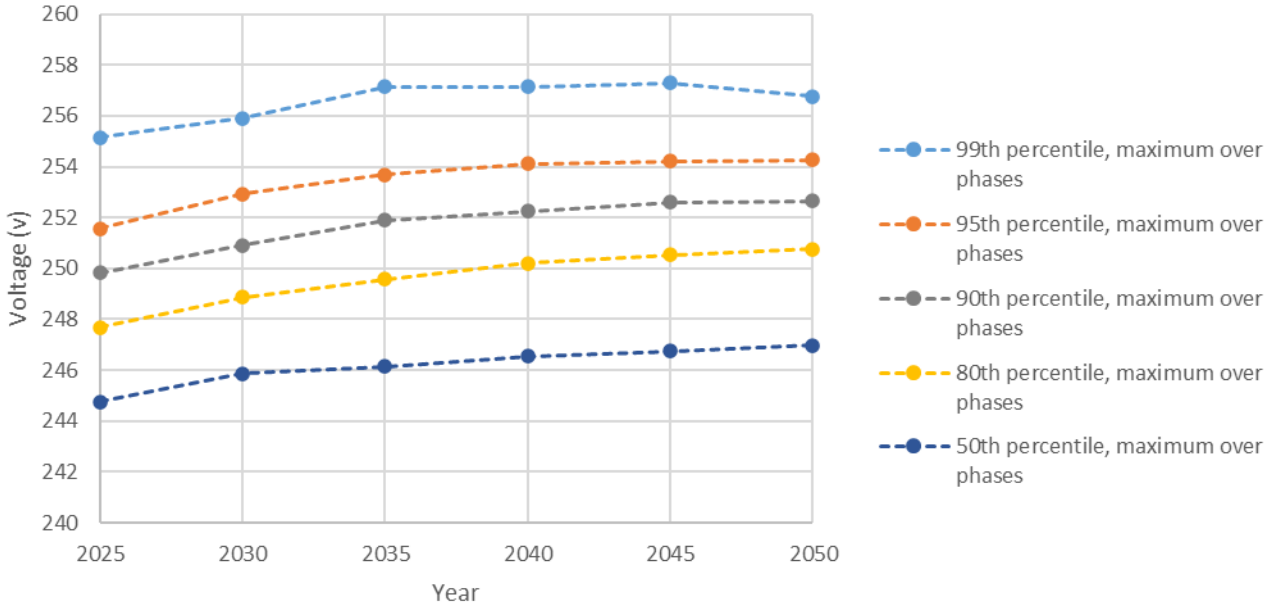

Figure 22 – Percentiles of the global LV bus voltage distribution for noon in summer for high solar day conditions in the Step Change scenario with the maximum of three phase-neutral voltages taken for each individual bus

Figure 22 shows the percentiles taken from the distribution of maximal LV bus voltages for Step Change at noon in summer for high solar day conditions. Note that the solar conditions are only relevant here because the high solar baselined load curve has a slightly higher evening peak in summer due to the implied greater residual heat and use of air-conditioning in the evening. The maximal LV bus voltage percentiles exhibit a slight upward trend through the years of the scenario. Significantly, the 253V limit is violated by both the 99th and 95th percentiles of the distribution in this scenario.

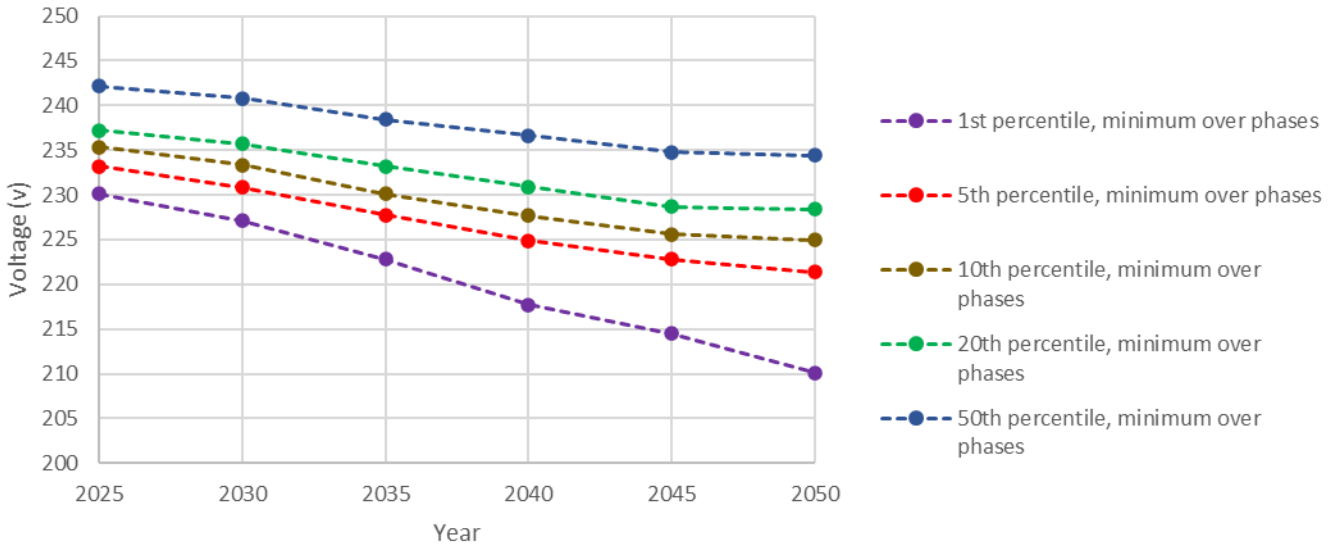

Figure 23 – Percentiles of the global LV bus voltage distribution for 7.30pm in summer for high solar day conditions in the Step Change scenario with the minimum of three phase-neutral voltages taken for each individual bus

In Figure 23, percentiles taken from the distribution of minimal LV bus voltages for Step Change at 7.30pm in summer for high solar day conditions are shown. As it is the time of peak load in the after-diversity load curve

for the most common of the two EV sizes represented, this is also the time of the evening load peak in general. Furthermore, since the baselined model load curves for high solar day conditions in summer exhibit the highest evening peak load when compared to the other seven combinations of seasons and solar conditions, this is the critical scenario for which evening peak load results have been presented in this report. The 1st percentile of the distribution falls below the lower statutory limit of 216V, however the 5th percentile doesn't. Comparison with Figure 22 implies that violation of the statutory LV voltage limits is generally more common for the upper limit, as the 95th percentile also exceeds the upper limit in that figure.

A depiction of one of the LV areas in the network model showing the variation of voltage magnitude across its length is shown in Figure 24. The colour yellow signifies voltage magnitudes at 0.96 pu, which is the threshold at which the absorbing section of the volt-var characteristic commences, while the colour red signifies 1.012 pu, which is the threshold at which the volt-watt characteristic commences and also the upper statutory limit. Figure 24 clearly demonstrates how the depth of overvoltages are more severe for customers situated at the remote ends of the LV feeders in their area. The MV bus on the HV side of the distribution transformer is also shown in red towards the bottom of the figure. This bus exhibits more severe overvoltage than the LV buses connected directly to the LV terminal of the transformer as it is a 7-tap transformer set to a reduced tap position of 4, which facilitates a drop in per unit voltage.

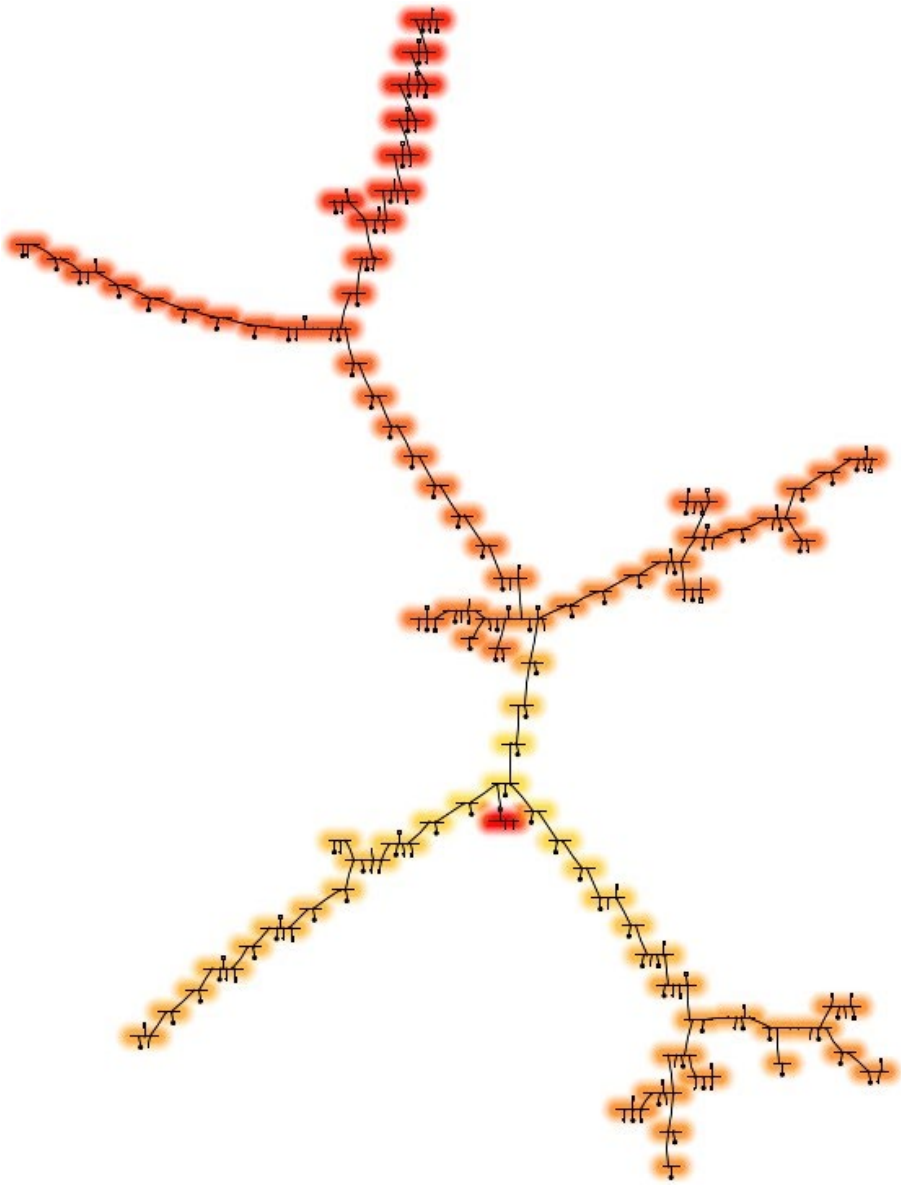

Figure 24 – Variation of voltage magnitude across the length of one of the modelled LV areas

Voltage unbalance was also found to be a problem of emerging significance for the network. A selection of percentiles for the distributions of voltage unbalance factors, which are given by the ratio of the negative sequence voltage magnitude over the positive sequence voltage magnitude, on all of the LV buses in the network is shown in for 2030 and 2050 in both of the ISP scenarios Table 15. Conditions for these results were high solar day conditions in summer. The differences between the voltage phase angles and the nearest member of the set [0°, 120°, -120°] to each were also calculated and the maximum of the three resultant angular error values for each LV bus was then taken into a distribution of maximal angular errors. A selection of percentiles for this distribution has also been added to Table 15. It is clear that the degree of unbalance in the LV sections of the modelled network tends to worsen with the progression of years in each scenario and that it is worse in the Step Change scenario than in the Slow Growth one in general. This clearly indicates that increasing levels of solar PV penetration will tend to worsen the level of voltage unbalance across the LV networks.

Table 15 – Percentiles of voltage unbalance factors and maximal angular errors for 2030 and 2050 in the Slow Growth and Step Change scenarios for high solar day conditions at noon in summer

Voltage unbalance factor/angular error metric	Slow Growth		Step Change	
	2030	2050	2030	2050
Voltage unbalance factor 99th percentile (%)	2.92	3.83	4.12	7.19
Voltage unbalance factor 95th percentile (%)	1.70	2.42	3.00	4.13
Voltage unbalance factor 90th percentile (%)	1.38	1.81	2.30	2.81
Voltage unbalance factor 80th percentile (%)	1.02	1.30	1.56	2.07
Voltage unbalance factor 50th percentile (%)	0.56	0.75	0.87	1.02
Maximal angular error 99th percentile (°)	9.00	12.19	15.56	27.82
Maximal angular error 95th percentile (°)	6.07	8.26	11.58	20.08
Maximal angular error 90th percentile (°)	4.93	6.80	9.63	16.75
Maximal angular error 80th percentile (°)	3.90	5.45	7.80	13.72
Maximal angular error 50th percentile (°)	2.40	3.71	5.41	9.81

In the present-day network that has been modelled for this study, voltage unbalance does not appear to be a significant problem. Figure 25 and Figure 26 show samples of measured positive sequence voltage magnitude and voltage unbalance factor data in one LV area in the network under consideration. The location considered is at the end of one relatively large LV area. As the data has only been collected since April, it cannot be regarded as indicative of peak solar conditions at noon in summer; it is expected that this snapshot is reasonably indicative of the current extent of voltage unbalance in the network, however. The voltage unbalance factor has been observed to reach as much as 2.5% on some days, but the average across the day is closer to 1% in general, which does not present any issues. This shows reasonable agreement with the Slow Growth 2030 unbalance factors predicted by simulation and shown in Table 15; the 99th percentile for which is 2.92% and the 50th percentile for which is 0.56%.

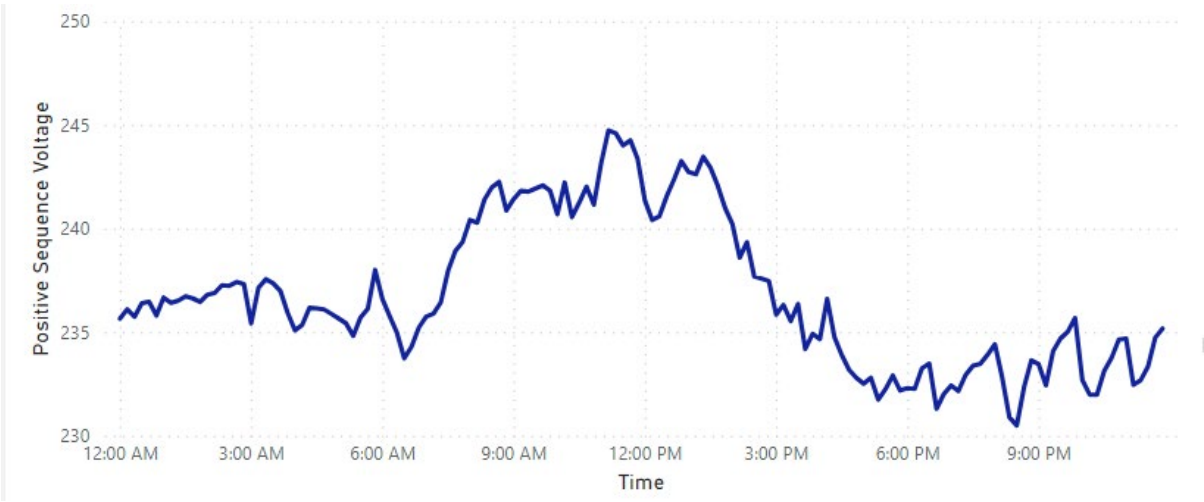

Figure 25 – Positive sequence voltage magnitude data measured on 03/05/2023 at the end of one of the LV feeders in the real-world network that has been modelled for this study

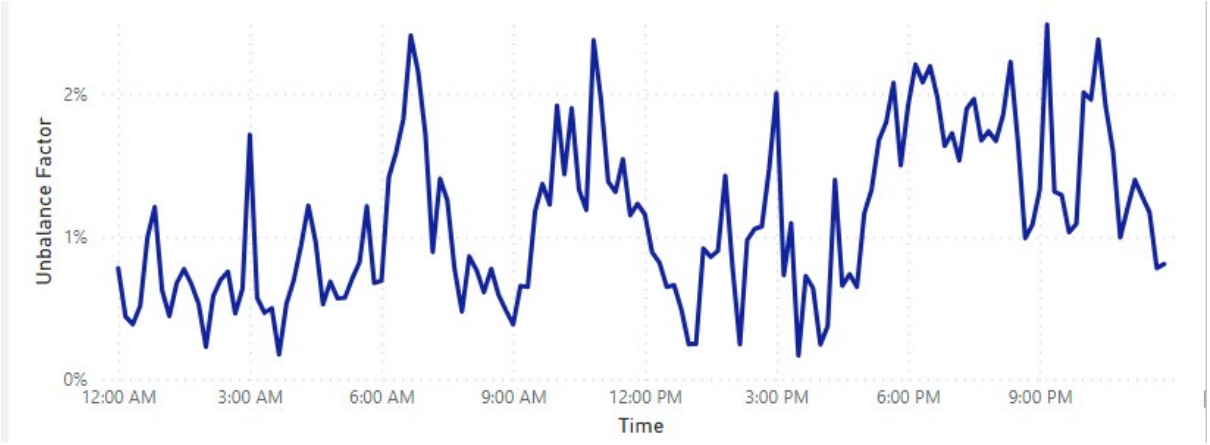

Figure 26 – Voltage unbalance factor data measured on 03/05/2023 at the end of one of the LV feeders in the real-world network that has been modelled for this study

6.2 Hosting capacity investigations

The hosting capacity of the network model is briefly investigated in a simplified fashion here. A simple criterion of not allowing more than 5% of the LV buses in the network to exceed their statutory limit is used to determine the point in time at which the hosting capacity of the network under study has been reached. Note that this criterion is not sourced from any established industry practice or literature on hosting capacity. It has merely been adopted in this study as an assumption that simplifies the complex gradual power injection elevation procedures simultaneous with constraint violation checking that a more detailed hosting capacity assessment would generally entail.

The proportion of LV buses exceeding the upper and lower statutory limits given use of their maximal and minimal phases respectively are shown in Figure 27 for the Slow Growth scenario and Figure 28 for the Step Change scenario. In the Slow Growth scenario, the hosting capacity of the network is not reached due to either PV or EV growth. In the Step Change scenario on the other hand, the hosting capacity is reached shortly after the year 2030 due to solar penetration at noon, though for EV charging at 7.30pm the hosting capacity is still not reached by 2050. The overall result therefore is that given the distribution transformer tap settings across the modelled area and the LDC algorithm settings currently in service at the zone substation for the modelled area, over-voltages throughout the middle of the day on high solar days are a more significant problem than are under-voltages during the evening peak.

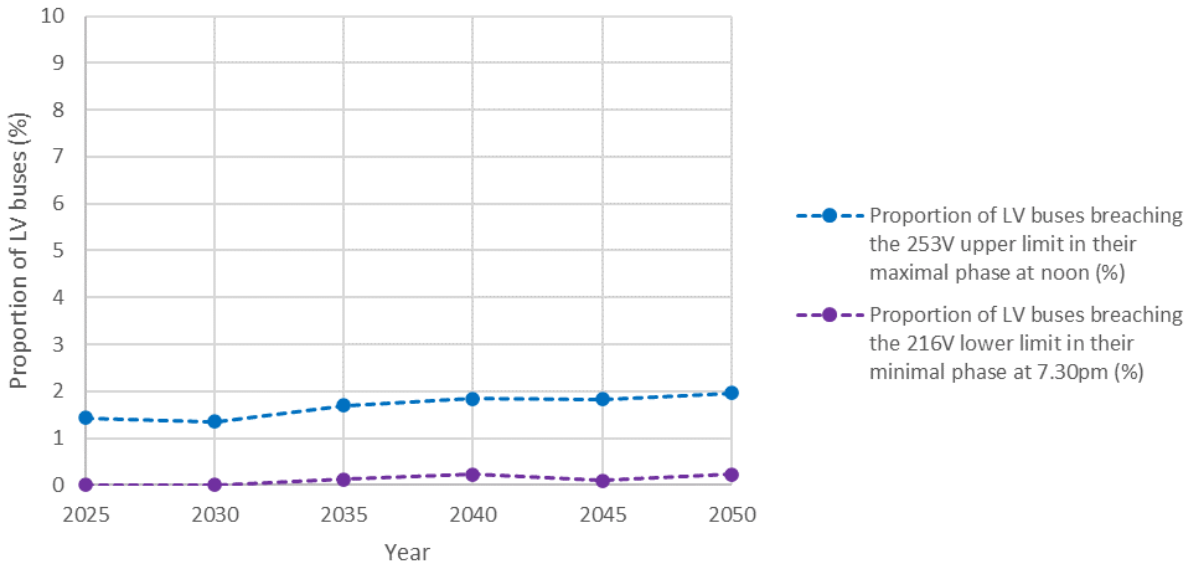

Figure 27 – Proportions of LV bus maximal and minimal phase voltages exceeding the upper and lower statutory limits at noon and at 7.30pm respectively in summer in the Slow Growth scenario for high solar day conditions

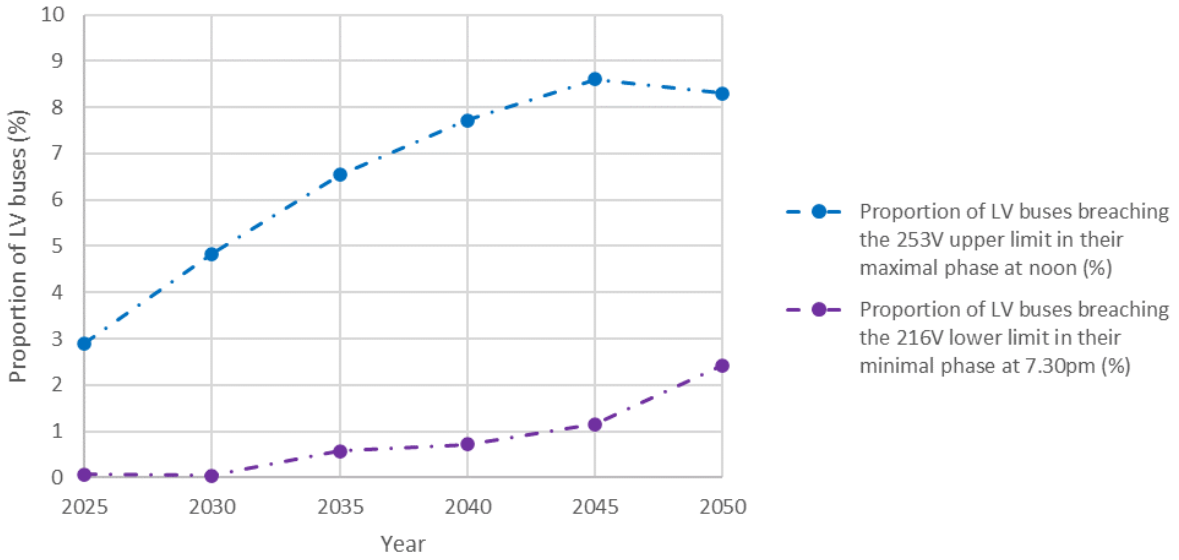

Figure 28 – Proportions of LV bus maximal and minimal phase voltages exceeding the upper and lower statutory limits at noon and at 7.30pm respectively in summer in the Step Change scenario for high solar day conditions

A sensitivity analysis of the hosting capacity with respect to the assumption of universal adherence to the volt-watt and volt-var functions stipulated by AS4777.2 was performed. The upper limit violation proportions given the assumption that volt-watt and volt-var algorithms are not implemented on any of the PV installations in the system is shown for both of the ISP scenarios Figure 29. Given this pessimistic assumption, the hosting capacity of the network is exceeded even in 2025 in the optimistic Slow Growth scenario.

The significant difference between the results shown in Figure 27 and Figure 28 and the results of this sensitivity analysis highlight the importance of the volt-watt and volt-var functions as they are mandated under the current revision of AS4777.2 and the effectiveness of this standard if it is properly adopted. They also indicate the extent to which the results in this study could worsen if even a subset of the population does not adhere to this standard moving forward. The results shown in Figure 29 in particular should not be considered

realistic; the maximal voltage on all phases of all LV buses in the network for the simulation performed without volt-watt and volt-var active in 2050 in Step Change was 333.48V. This level of overvoltage would trigger disconnection of all solar inverters across the entire network and would never be allowed to occur in practice.

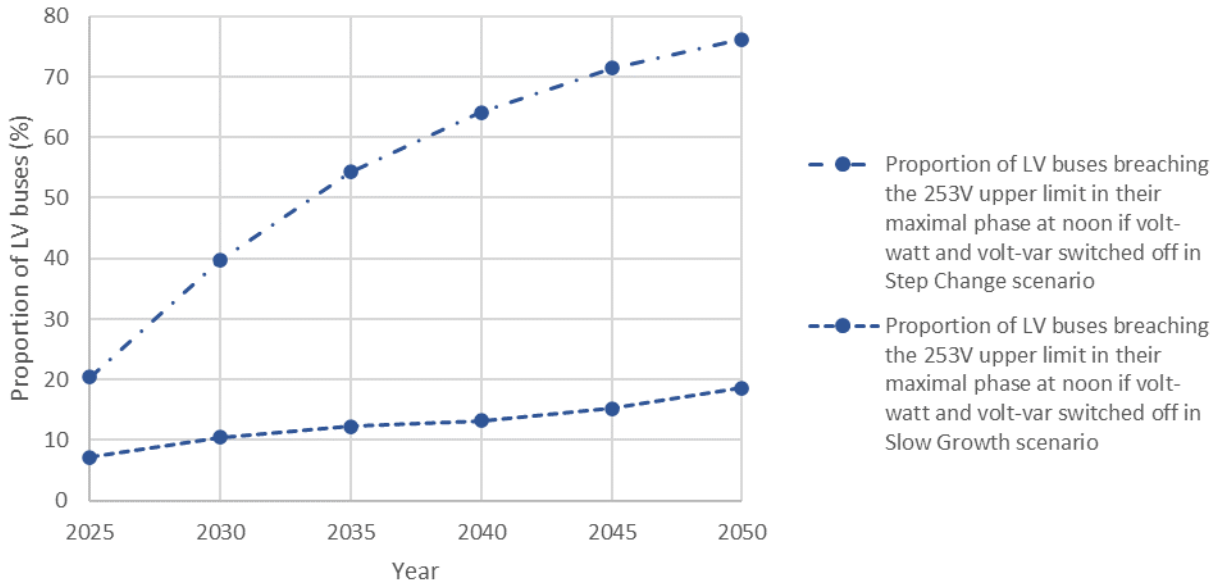

Figure 29 – Proportions of LV bus maximal phase voltages exceeding the upper statutory limit at noon in summer in the Slow Growth and Step Change scenarios for high solar day conditions with volt-watt and volt-var functions deactivated

6.3 BAU conductor and transformer upgrades

The year 2035 in the Step Change scenario was chosen for the purposes of investigating the effectiveness of different voltage management solutions in this study. The Step Change scenario exhibits higher rates of growth in PV and EV and therefore exhibits more severe voltage and curtailment problems that would warrant mitigation in practice. The final year of the scenario was not targeted as only four of the ten 11 kV feeders can be solved for in 2050 (as discussed in the previous section) and a reasonably large population to trial solutions on was desirable.

Even in business as usual (BAU) in which no voltage mitigation strategies are assumed to be employed, upgrades of distribution transformers as well as MV and LV distribution lines would be initiated with the DNSP to mitigate thermal issues caused by the higher current flows in the network generated by increasing amounts of PV generation and EV charging. Investigations of the line and transformer current capacity utilisation factors in the global simulations that had been carried out so far were thus initiated. The thermal limit violations were found to be worse by a significant margin at noon for high solar day conditions than during the evening peak; the investigation was therefore carried out using utilisation factors calculated at noon in summer for high solar day conditions in general.

Different criteria were used to determine thermal overloads for different types of equipment. For distribution transformers, two levels of overload were recorded; if they were found to be exceeding 100% and 150% of their current ratings respectively. The first of these would be of concern but would likely not be addressed immediately in practice, due to the fact that the distribution transformers in Energex's network are generally able to withstand currents higher than their rating for short periods of time, which is referred to as their "cyclic loading" capabilities. The second criterion of 150% utilisation corresponds to the point at which they would be likely to be replaced or see the thermal capacity issue addressed in some other manner, in practice.

In the case of buried LV cable runs, overloads were recorded only when they were found to be seeing more than 120% of their current ratings. The selection policy for buried LV cables in Energex's network permits substantial margin; sufficient that the variability in thermal conductivity of the different soil types occurring in Queensland can be accounted for without additional design effort, and this also allows for cyclic ratings to be considered. Although no actual cyclic rating calculations were undertaken in this study, the experience of senior practitioners indicated that a short-term overload of up to 120% of the continuous rating, for a few hours, would not be likely to cause significant loss of life in buried cable systems. For LV overhead conductor spans, overloads of two types were recorded; those at which the span had exceeded 80% of its current rating and those at which the span had exceeded 100% of its current rating. This was done because both criteria are relevant when DNSP's are considering upgrading LV overhead spans in a given distribution transformer area. Finally, for 11 kV overhead spans and buried cable runs, overloads were recorded wherever currents above 90% of the rating were observed. MV lines would be upgraded sooner than LV lines in general because the number of customers who would have their service interrupted as a result of their failure is significantly greater.

The prevalence of overloads determined using the above criteria, as proportions of the installed counts of each type of equipment, are shown in Figure 30 and Figure 31 for the Slow Growth and Step Change ISP scenarios respectively. The proportion of each type of equipment seeing its thermal capacity exhausted is minor in Slow Growth but concerning in Step Change. Distribution transformers in particular exhibit the highest trends in both scenarios. This indicates that the most common and problematic thermal overloads that will be likely to emerge in the distribution networks in the coming years will be on distribution transformers. For a more detailed view of the thermal utilisation data for the equipment in the network model across the future years of both ISP scenario, including a selection of percentiles for the utilisation factor distributions for each type of equipment, refer to Appendix C.

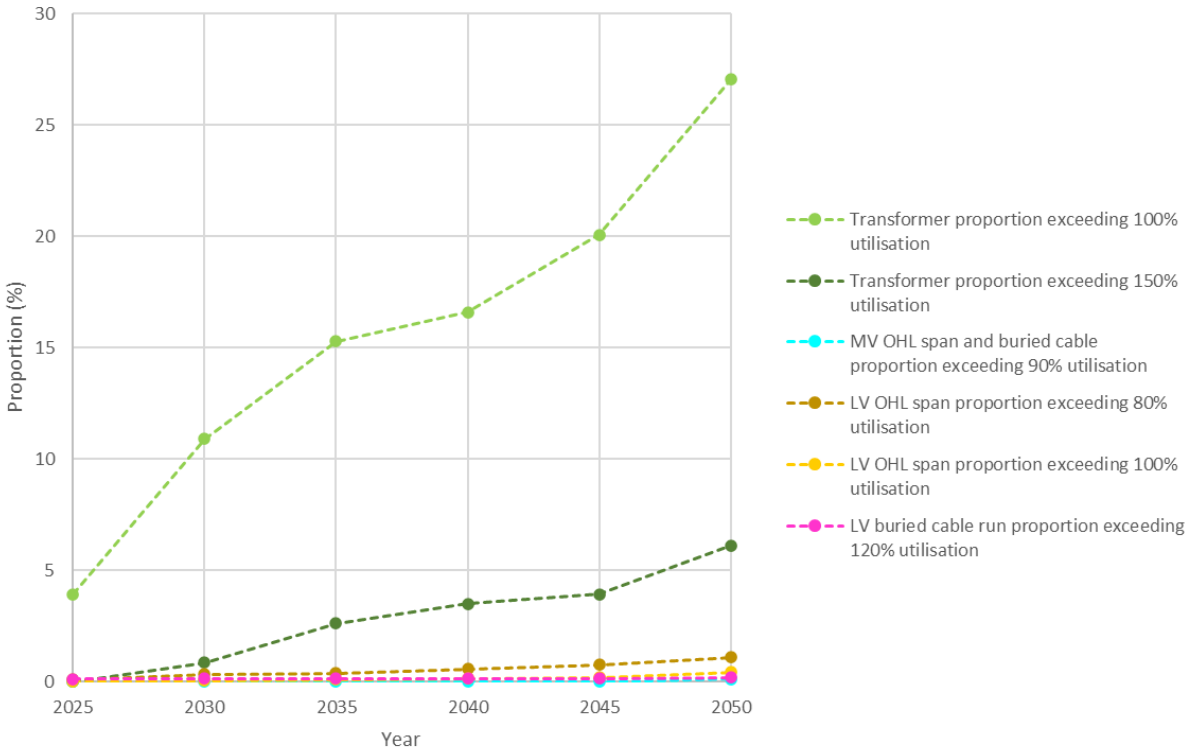

Figure 30 – Proportions of thermal overloads for different equipment types at noon in summer under high solar day conditions for the Slow Growth scenario

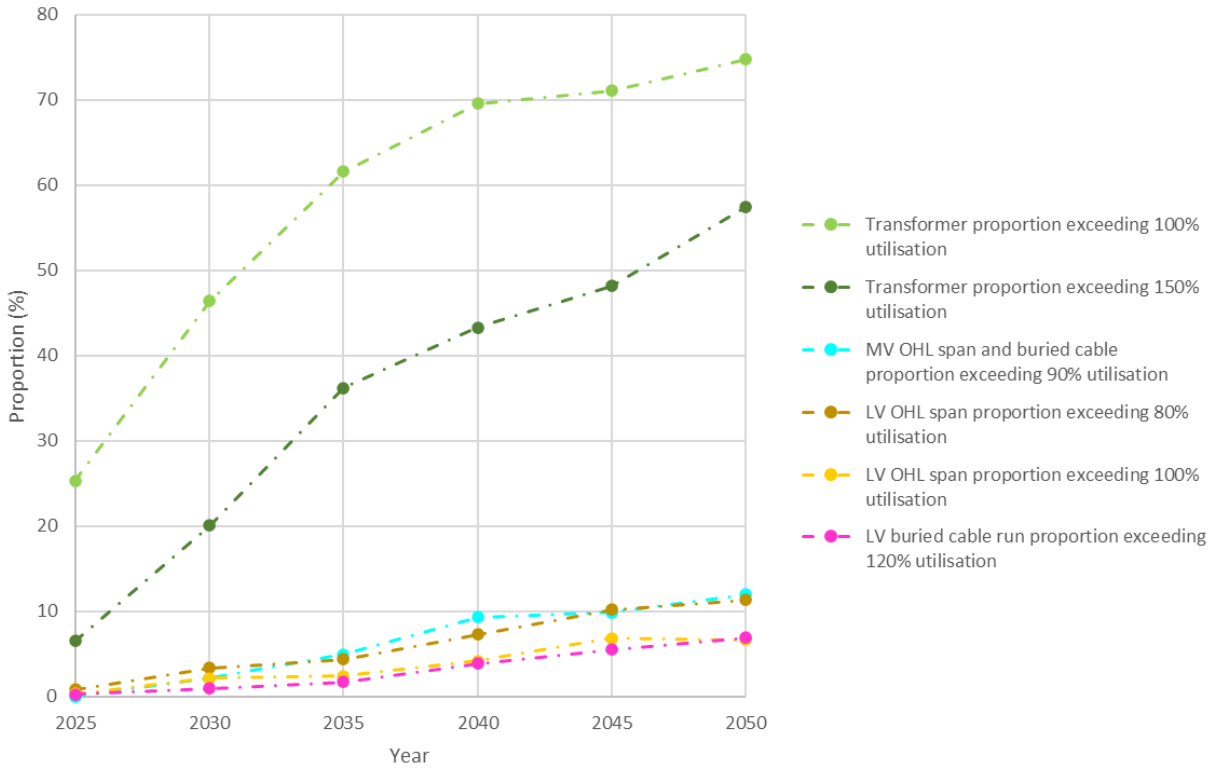

Figure 31 – Proportions of thermal overloads for different equipment types at noon in summer under high solar day conditions for the Step Change scenario

Additional simulations were carried out to see if similar levels of thermal violations were present at 7.30pm during the evening load peak when the largest numbers of EVs are also charging. The violation proportions for 7.30pm in the Step Change scenario in summer given high solar day conditions are shown in Figure 32. It was found that the utilisation proportions are not nearly as high as during noon, which comparison with Figure 31 reveals. This is explained by the numerical details of the inputs for this study; by 2050 in the Step Change scenario, 1.8 electric vehicles per household have been applied to the network model. Application of the after-diversity charging profiles from [18] however, which represents the fact that not all customers would choose to charge during the evening peak on any given day, results in the EV populations for the smaller and larger charger sizes exhibiting average peak load per customer values of only about 1 kW and 2 kW respectively. Furthermore, the number of customers with existing three-phase connections who could be reasonably assumed to use the larger charger size is only about 7% of the total, so that means that the maximal EV charging load during the evening peak in 2050, given 13,535 residential customers in the area, comes out to be only around $(0.07 \times 2 + 0.93 \times 1) \times 13535 \times 1.8 \approx 26$ MW. Compare this to the PV installations, which by 2050 in the Step Change scenario have reached an average installation capacity of 10.978 kW per household and thus in the middle of the day in summer with clear-sky conditions would be producing $10.978 \times 13535 \approx 149$ MW of generation, which is larger than the EV load peak by a significant factor. In simple terms, the practical reality of diverse customer behavior means that EVs don't produce nearly as much load as they could, while the natural and inherent simultaneity associated with rooftop solar generation on a clear-sky day means that it precisely does.

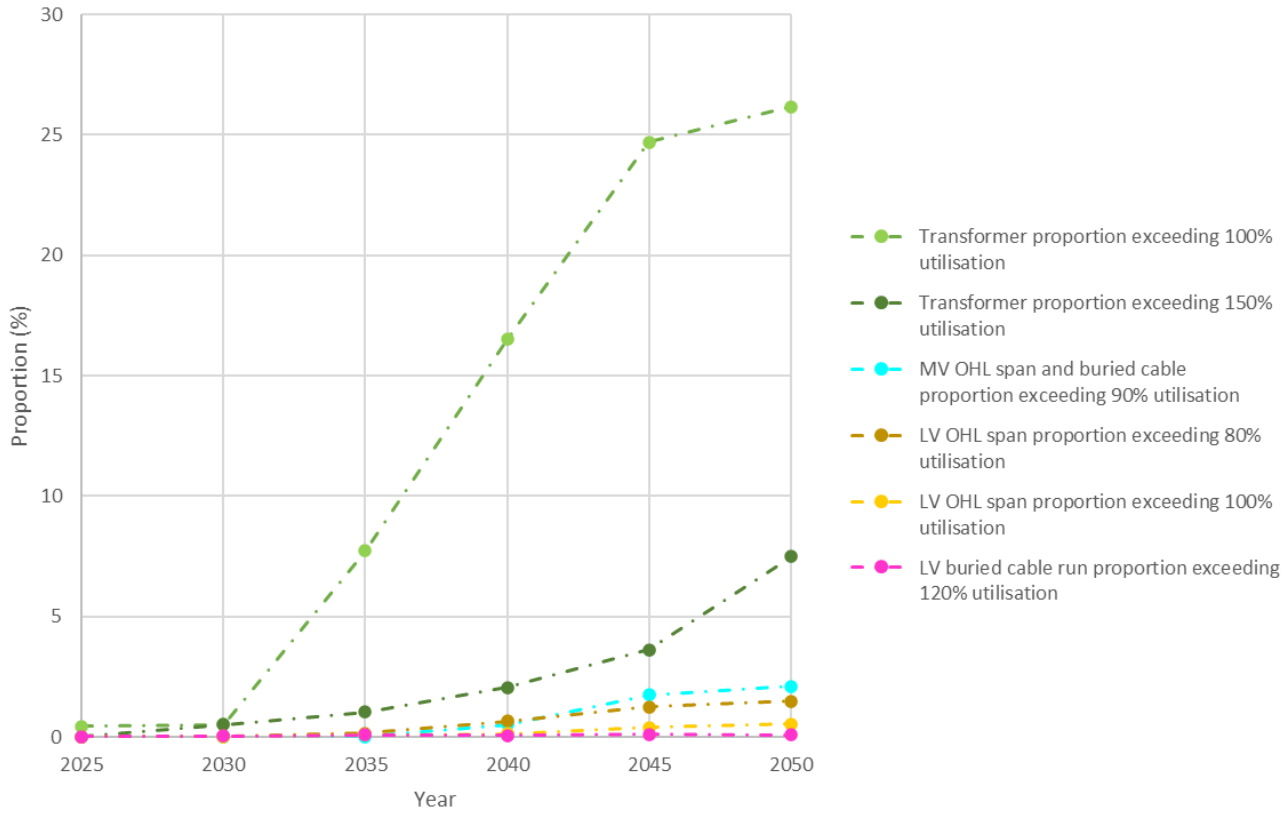

Figure 32 – Proportions of thermal overloads for different equipment types at 7.30pm in summer under high solar day conditions for the Step Change scenario

The number of overloads occurring at noon in the latter years of Step Change would be unlikely to be tolerated in practice. Due to outages that would occur as a result of their emergence, widespread network upgrades and augmentations such as re-conductoring, transformer upgrades, feeder splitting across multiple distribution transformers and possibly the installation of community batteries would be likely to occur. The global voltage management and curtailment results presented for the Step Change scenario thus far in this report should therefore be understood as indicative of what would occur if no action were taken to address them or the thermal violations that would emerge. For the purposes of the voltage management solution investigations however, the results for which will be shown in the sections that follow, reasonable effort was made to apply a series of upgrades to the network so that the BAU context in which these results were formulated were as realistic as possible.

Distribution transformers, MV overhead spans and buried cable runs, and LV buried cable runs were upgraded in the 2035 Step Change version of the model wherever thermal overloads had been identified as per the criteria described above. For LV overhead spans in particular however, upgrades were applied when the spans in each LV area met a particular set of criteria. Specifically, upgrades of all overhead spans in a given LV area were triggered if two conditions were met; (1) at least one of the spans was found to be seeing more than 100% of its rated current and (2) at least 30% of the overhead spans in the area were also seeing more than 80% of their current rating. This assumption is justified on the grounds that upgrades are unlikely to be triggered until an issue is reported (hence (1)) and a key aspect of this issue is that once overhead lines are overloaded there is a risk that statutory ground clearances may be breached, which is a “must avoid” consequence. In addition, once the cost of dispatching workers to the area has been committed to, the decision to simply upgrade all of the overhead spans in the area is often justified to avoid having to return to

the same area in a few years' time as load or generation increases (hence (2)). Note that the LV buried cables in each LV area are not upgraded all together in the same fashion as the cost per unit length of buried cable is significantly higher than it is for overhead conductor in general. Several successive simulations under the same conditions also revealed that the proportion of overhead spans in a given LV area seeing at least 80% of their rating tend to vary by 10-15% due to the randomised EV charging implemented in this study; the first threshold in the second part of the condition triggering overhead span upgrades on a whole LV area was therefore reduced to 15%.

Upgrades were implemented in a successive fashion, e.g., in cases where Mars, Libra, Banana, Mink, 7/.104 or 7/14 copper had been found to be inadequate on LV overhead spans, upgrades would be made to Moon conductor. If Moon were found to be inadequate, upgrades were made to Pluto. In the case of 95mm² ABC, upgrades equivalent to installing a second parallel circuit with the same type of conductor were made. This was facilitated by building a second parallel four-wire 95mm² ABC line with the same length and connecting the same two buses as the first. The more accurate approach of modelling this as an eight-wire coupled geometric system, representing the fact that the second 95mm² ABC circuit is installed on the same poles as the first in practice, was briefly tested and found to yield only very minor changes to the curtailment results for the network; refer to Appendix D for details.

Upgrades to the higher rating of Saturn conductor were not considered for LV or MV spans as this grade of conductor tends to cause pole stress issues, especially in windy conditions. Similarly in the case of buried cable runs, upgrades were made such as from 16mm² copper to 25mm² copper and from 120mm² aluminium to 240mm² aluminium, and from 240mm² aluminium to 300mm² aluminium. Conductor with 300mm² cross-sectional area and 3.5 cores made from aluminium was the highest grade considered as upgrades to 400mm² or higher ratings would generally not be considered for low voltage residential estates due to the fact that they will not pull into the normal conduits used in residential estates. Whether or not the upgrades that were applied to the pole-mounted subset of the transformers that were upgraded would be feasible in practice was not investigated; it is possible that some of the upgrades may have been unrealistic owing to the mass constraints associated with pole structures.

As a result of the investigation, 1424 LV overhead spans, 402 LV buried cable spans, 21 MV buried cable spans, 3 MV overhead spans and 101 distribution transformers were upgraded in the 2035 Step Change version of the network model. The upgrades applied to the 2035 Step Change version of the network model yielded improvements in the thermal limit violation proportions for all types of equipment. These are shown in Table 16 below. Nevertheless, some parts of the network were still found to be showing thermal violations in BAU simulation results despite the large number of upgrades that had been applied to improve the thermal current-carrying capacity of the network.

Table 16 – Thermal violation proportions for the 2035 Step Change version of the model with and without BAU thermal upgrades at noon in summer under high solar day conditions

Thermal violation proportion	Without BAU thermal upgrades	With BAU thermal upgrades
Transformer proportion exceeding 150% utilisation (%)	36.25	1.55
MV OHL span + buried cable run proportion exceeding 90% utilisation (%)	4.96	4.02
LV OHL span proportion exceeding 100% utilisation (%)	2.41	0.40
LV OHL span proportion exceeding 80% utilisation (%)	4.40	1.48
LV buried cable run proportion exceeding 120% utilisation (%)	1.70	0.42

Attempts at applying additional rounds of upgrades identified that the majority of these parts of the network that were still exceeding their thermal limits had been upgraded to the maximum extent that is reasonable. The attempts also identified worsening non-convergence issues in the model as a result of more liberated and thus larger active power flows in some of the offending feeders. It was therefore decided that the upgrades described above were an adequate representation of the majority of upgrades that would occur. In fact, they likely represent a conservative estimate of the number of upgrades that would occur as the high cost of network upgrades would mean that DNSPs would be more likely to address widespread thermal issues like this either by implementing wider-spread and/or more aggressive and universal PV export limits, or by adding additional distribution transformers and splitting low voltage areas. It was clear that several of the LV areas that were still found to have thermal limits being exceeded after the first round of upgrades would need to see their feeders split across multiple distribution transformers in practice. However, such measures are beyond the scope of the present study.

The percentiles of curtailment before and after the upgrades in 2035 in Step Change are shown in Table **17**. The overall effect of the significant amount of conductor and transformer upgrades applied in this study on the global curtailment distribution in 2035 in Step Change was to decrease it only slightly.

Table 17 – Global curtailment percentiles in Step Change in 2035 with and without BAU line and transformer upgrades intended to address thermal issues

Global curtailment metric	Without BAU thermal upgrades	With BAU thermal upgrades
99th percentile (%)	16.25	15.74
95th percentile (%)	6.16	5.93
90th percentile (%)	3.85	3.66
80th percentile (%)	1.63	1.56
50th percentile (%)	0.00	0.00

The reduction of the impedances of many of the lines across the network does indeed have the effect of reducing the voltage rise due to solar generation; the MV voltages across the network are in fact lowered by these upgrades. This is demonstrated in Figure 33 for example, which shows the MV voltage values along the length of the longest 11 kV feeder before and after the upgrades. At all of the buses downstream of the initial ~3km run of buried cable, the voltage is consistently lowered by 10-15V.

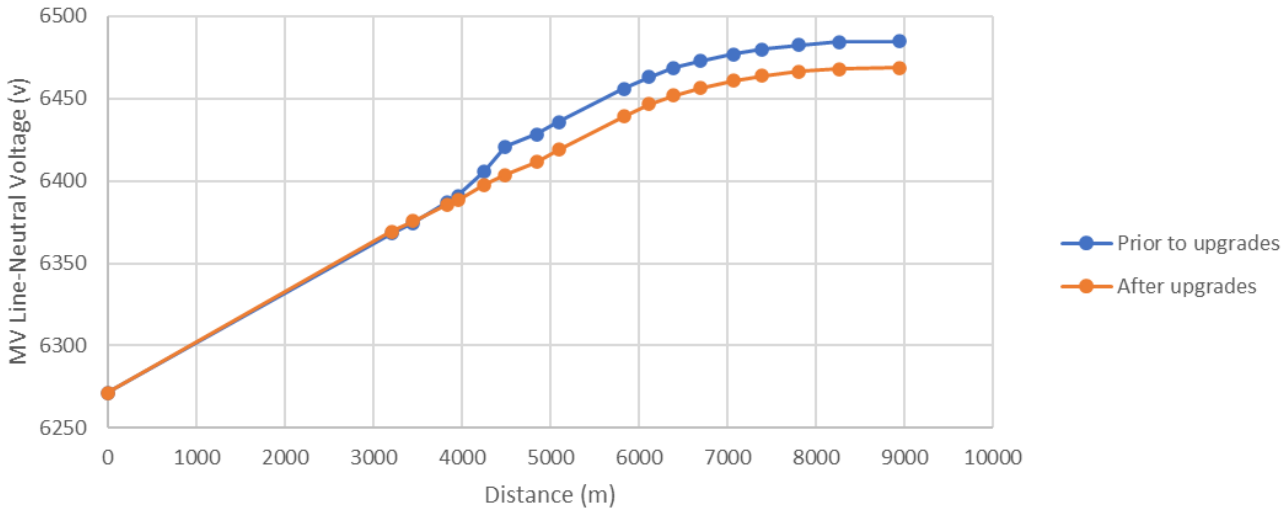

Figure 33 – MV average line-neutral voltage before and after BAU distribution transformer and line upgrades to address thermal issues on the longest MV feeder in summer at noon for high solar day conditions

One of the additional factors that counteracts the reduction in curtailment produced by uprating the distribution lines is the simultaneous increase in impedances that occurs as many of the distribution transformers are uprated. Unlike distribution lines, transformers with higher current ratings generally also have higher inductive impedances. This in turn acts to lift the voltages on many of the LV areas back up higher than they were in the first instance.

Another factor which means that conductor and transformer upgrades don't necessarily improve curtailment across the network in general is that the liberation of greater active power flow from some LV areas that see curtailment improve actually increases the voltage on some of the MV feeders. This in turn increases the voltages on all other neighbouring LV feeders on that MV feeder and worsens their curtailment. An example of an MV feeder that exhibits higher voltage magnitudes following the BAU thermal upgrades is shown in Figure 34.

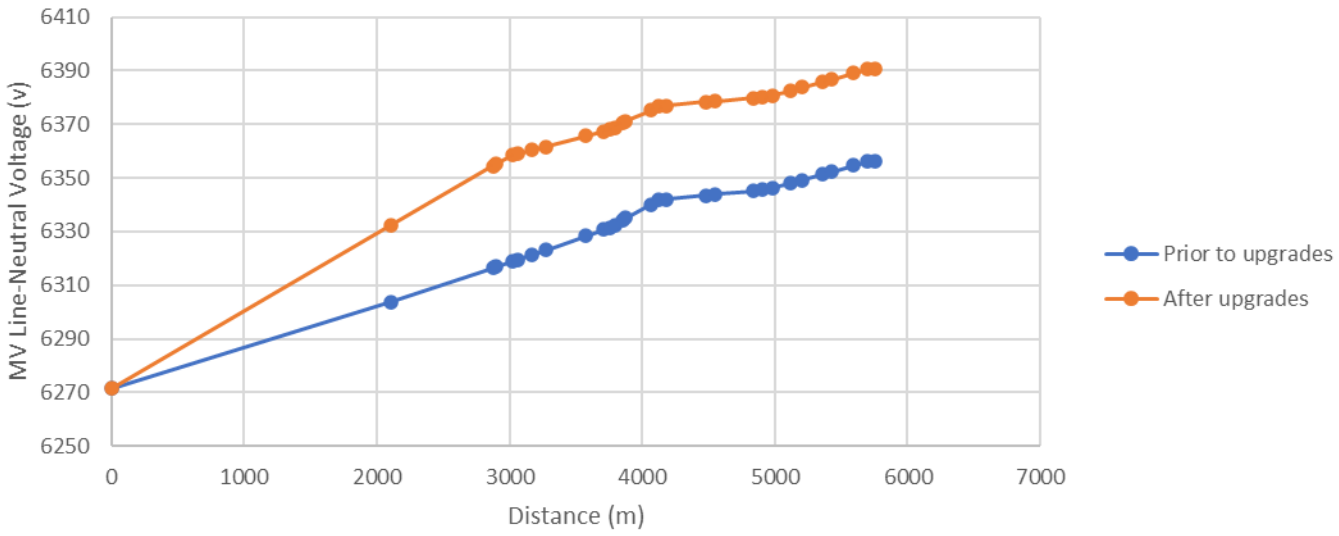

Figure 34 – MV average line-neutral voltage before and after BAU distribution transformer and line upgrades to address thermal issues on the MV feeder exhibiting increase in voltages in summer at noon for high solar day conditions

Thus, the overall effect of combined distribution transformer and conductor upgrades that are intended to address thermal issues is to redistribute curtailment around the network more than it is to reduce it. It is also important to note that the sensitivity of curtailment across the network to changes in network impedances resulting from upgrades to address thermal issues is somewhat reduced by the fact that the LV areas that would hypothetically encounter thermal issues if the upgrades weren't performed are the same LV areas encountering the most significant curtailment in some but not in all cases. In addition, it should also be considered that while conductor upgrades generally imply reduction in resistance per unit length that is directly proportional to the increase in cross-sectional area, the reductions in inductance per unit length that they imply are significantly smaller and hence, the overall change in impedance is not significant.

6.4 Selection of LV areas for application of voltage management solutions

The subset of the 229 LV areas represented in the model selected for the purpose of comparing the effectiveness of voltage management solutions was based on which of them were found to be experiencing the most significant curtailment. Two alternative criteria were adopted tor determination whether a given LV area would fit this description; either (1) the 10th percentile of the curtailment figures for the PV components in the area was 10% or more, or (2) the 5th percentile of the curtailment figures for the PV components in the area was 20% or more. Note that since each individual PV generator component is associated with one customer, these statements are equivalent to "at least 10% of the customers are experiencing at least 10% curtailment" and "at least 5% of the customers are experiencing at least 20% curtailment" respectively. Adoption of such criteria ensured that the LV areas selected were likely to be those experiencing a significant degree of higher curtailment for fewer customers, rather than a small degree of curtailment across many customers. Using these criteria, the LV areas connected to six specific distribution transformers were selected.

It is noted here that the criteria used to determine significant curtailment in this study are not necessarily the most appropriate criteria that a DNSP would necessarily apply as a policy to select LV areas for future voltage management solution. More appropriate criteria may take the number of customers in each area or the number of them which had begun to submit complaints about curtailment into account for example, or they may also incorporate data describing the extent and frequency of over and under-voltage

limit violations. Curtailment has been targeted as the most significant problem needing to be addressed in this study due to the fact that it is a proxy for over-voltage violations as well and the findings that under-voltage violations are less severe and less frequent for the studied network given its current LDC and transformer tap settings, as described in section 6.1.

None of the six LV areas selected for application of voltage management solutions were found to still be meeting the criteria for upgrades of overhead LV conductor spans following the BAU upgrades to address thermal issues. Two of the LV areas were identified as having significant numbers of buried LV cable runs which were still exceeding 120% of their thermal capacity at noon though, despite the fact that they had been upgraded to ratings with 300mm² cross-sectional area, which was the maximum upgrade assumed to be applicable in this study. However, these areas were still treated as valid for the purposes of investigating the effectiveness of STATCOMs and other voltage mitigation options in this study. In practice, buried LV cable overloads may often go unnoticed, or simply have their upgrades avoided for as long as possible due to the significant cost associated with them. Or they may be addressed with more restrictive PV export limits, splitting of LV areas across multiple distribution transformers or installation of LV batteries. Given that this is the case, the number of BAU conductor upgrades that have been considered to address thermal issues in this study is already likely to be relatively conservative. In any case, more of the buried LV spans on the two areas in question were found to be still exhibiting non-zero thermal margin, as well as scope for further upgrades, than those which were appearing overloaded. This implies that reconductoring of these areas to the extent that would still be possible, which is considered in the next section, is still a valid hypothetical voltage management solution.

6.4 STATCOM modelling

The STATCOMs were sized at 50 kVA each as per the plan for the eleXsys pole-mounted dSTATCOM product. They were programmed with linear single-phase V-Q droop controls as shown in Figure 35. The parameters V_i and Q_(S,i) represent the phase-neutral voltage on phase i at the STATCOM terminals and the STATCOM single-phase output reactive power on phase i respectively. The other parameters V_l, V_u and V_sp represent the lower and upper voltage thresholds and voltage setpoint for the droop control law respectively, while the parameter d represents the droop coefficient and Q_r represents the rated reactive power output (or input) per phase of the STATCOM.

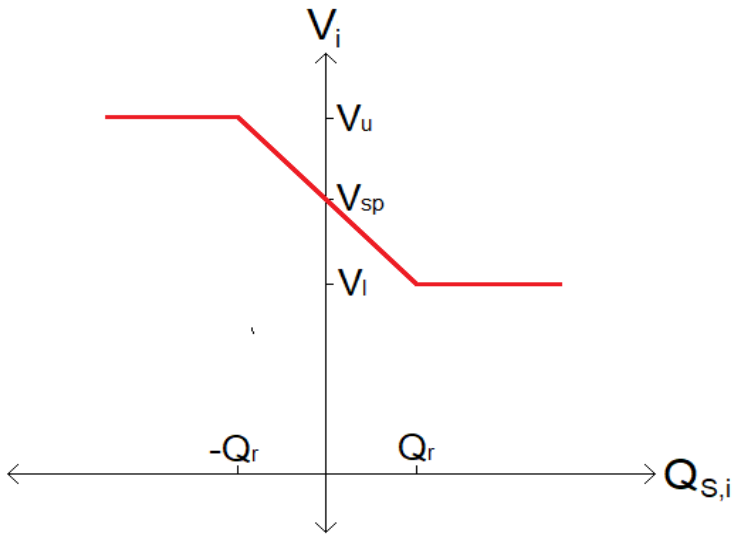

Figure 35 - Graphical depiction of STATCOM linear single-phase V-Q droop control law

A mathematical description of the droop control law is also given by Equation 1. Note that the factor of 100 accounts for the fact that voltages are entered in per unit, while the droop parameter d is entered as a percentage.

$$Q_{S,i} = \begin{cases} -Q_r, & V_i \geq V_u \\ \dfrac{100(V_{sp} - V_i)}{d}, & V_l < V_i < V_u \\ Q_r, & V_i \leq V_l \end{cases}$$

Equation 1 – STATCOM linear single-phase V-Q droop control law

The STATCOMs simulated for the voltage management assessment were programmed with droop coefficients of 2% and voltage setpoints and upper and lower thresholds of 0.92 pu, 0.94 pu and 0.9 pu on a base of 250V respectively. These were intended to be the most useful generic settings as 2% is generally considered to be a STATCOM droop coefficient that is useful but not too aggressive and the two thresholds sit equidistant between 0.88 pu and 0.96 pu at which each of the two separate ends of the volt-var characteristic commences. More useful specific STATCOM settings can often be determined on a case-by-case basis depending on the typical voltage conditions throughout the day occurring beforehand. Attempts at determining these were not made as the majority of the STATCOMs were found to be absorbing reactive power at maximum during summer noon high solar simulations.

6.5 Comparison of voltage management solutions

Apart from application of STATCOMs, two alternative traditional network augmentation solutions were investigated for the purposes of voltage management; upgrades of distribution transformers so that they are equipped with OLTCs and further re-conductoring of the six specific LV areas identified for study. The reconductoring option simply assumed that upgrades would be applied to all of the remaining overhead spans or buried cable runs still exhibiting scope for further upgrades given the maximal ratings assumed to be applicable as discussed in section 6.2. This resulted in 46.88% of the buried cables and 51.7% of the overhead spans in the six LV areas being upgraded. The OLTC option was implemented simply by dropping the distribution transformer taps for the six modelled areas to the lowest available bucking tap, assuming that the OLTC settings would be chosen so as to ensure that this would happen at noon during high solar irradiance conditions in practice. It is noted here that a third traditional network augmentation solution of LDC algorithm augmentation was also considered. In order that such an augmentation would affect significant improvement of the overvoltages across the network at noon under high solar day conditions, a lowering of the voltage thresholds that were discussed in section 3.1 would need to be implemented. It was identified however that the existing settings at the modelled zone substation were sufficiently close to the lowest range that would practically be considered that consideration of a scenario in which they were lowered further would be unlikely to be entertained in practice.

Two cases involving STATCOMs were also considered; one involving only one STATCOM for each of the LV areas identified and one involving multiple STATCOMs for each area. In the case of the first option, the STATCOM was placed either at the bus of whichever PV generator in each LV area that was found to exhibit the highest curtailment in BAU summer noon high solar simulations or, in cases where the conductor out to the largest curtailment PV generator was of a small grade such as 25 or 16mm^2 buried cable, one or two buses upstream from this where the conductor grade was higher. For the multiple STATCOMs option, a number of STATCOMs were placed across each LV area which varied according to the relative size of the area; one area received still only one STATCOM, four of the areas received two STATCOMs each and the single largest LV

area received four STATCOMs placed across its four radial feeders. The STATCOMs were generally placed one or two buses from the end of LV feeders in this case also.

Curtailment results for the different voltage management solutions that were simulated for the six LV areas selected are presented in Table 18. A selection of percentiles of the curtailment distributions have been presented for each case. Note that the curtailment distributions from which the percentiles were calculated here are the distributions for only the PV inverter components on the six specific LV areas selected for the application of voltage management solutions; they are thus referred to as "local" curtailment metrics rather than global ones. Results for the BAU case with conductor and transformer upgrades intended only to address thermal rating violation issues are shown in the first column for comparison. Note that the curtailment reconductoring case, the singular STATCOM case, the multiple STATCOM case and the OLTC case all include the conductor and transformer upgrades implemented to address thermal limit violations in BAU as well. The additional conductor upgrades in the curtailment reconductoring scenario on the other hand are unique to that scenario.

Table 18 – Selection of percentiles for the curtailment distributions for the six LV areas exhibiting significant curtailment given application of different voltage management solutions

Local curtailment metric	BAU with thermal upgrades	Curtailment reconductoring	One STATCOM per LV area	Multiple STATCOMs per LV area	OLTCs
99th percentile (%)	78.83	69.02	53.85	51.63	60.46
95th percentile (%)	34.14	31.64	17.95	10.43	13.20
90th percentile (%)	17.41	17.58	9.80	7.51	5.99
80th percentile (%)	9.41	8.50	6.31	4.91	1.78
50th percentile (%)	0.15	0.00	0.00	0.00	0.00

The local curtailment values in Table 18 are much higher than those which have been presented previously in the global results section previously as the six LV areas selected for study all exhibit relatively high curtailment compared to the rest of the network model. The voltage management solution entailing reconductoring of the six LV areas selected is clearly the most ineffective; while it yields improvements in most of the percentiles calculated they are the smallest of all options presented. The single STATCOM solution on the other hand achieves substantially better results, while the scenario introducing multiple STATCOMs to each area achieves better results still. The OLTC solution achieves curtailment performance that is worse than the single STATCOM case in the 99th percentile, between the single and multiple STATCOM cases in the 95th percentile and better than both in the lower percentiles. That this is the case is to be expected due to the fact that an OLTC directly modulates the voltage that the rest of the upstream network applies to the LV area and hence can lower it across all of the area's constituent buses simultaneously.

It is noted here that the performance of the OLTC option is not as high as it could be because the OLTCs weren't applied to two out of the six LV areas chosen for analysis. The reason for this is that two of the LV areas exhibited such severe phase voltage unbalance in BAU with thermal upgrades that one of their three phases was found to be producing phase-neutral voltages on some of the LV buses that fell below the 216V lower limit. In this situation, OLTCs would not be applied to these distribution transformers as there would be no scope to reduce the phase-neutral voltages on the two phases in overvoltage due to the fact that this would also worsen the undervoltage violation on the other phase. This highlights a major downside of the OLTC option on three-phase distribution transformers; that it cannot fix voltages on networks with phase voltage unbalance that is too severe. This is the case because a three-phase OLTC necessarily applies a uniform downward or upward translation of all of the phase-neutral voltages on the LV simply by virtue of the principle by which it works.

In Table 19, a selection of percentiles of the maximal-phase LV voltage distributions for the six LV areas in which voltage management solutions were employed is shown. Except for the OLTCs case, these voltage metrics are generally reduced moving from left to right across the table indicating the successive effectiveness of the options tested. The OLTC solution does not perform well in terms of the maximal-phase voltage percentile metrics however due to the fact that two of the six areas could not have OLTCs applied, lest they worsen the limit-violating undervoltages already present on one of the phases of their LV areas. The row second from the bottom shows the proportion of the LV buses in the six LV areas that are violating the upper 253V statutory limit in their maximal-voltage phase. Note that using the maximal phase voltage to calculate this metric is universally valid as a customer could be connected to any given phase of the system. Thus, the significance of this metric is that it indicates the extent to which inadequate power quality due to overvoltage is being provided to the customers on the network.

The single STATCOM solution achieves only marginally better performance than the curtailment reconductoring solution in terms of the upper voltage limit violation metric. This is attributable to the fact that the singular STATCOMs installed in each of the LV areas affect significant change in the voltages of only the LV feeders on which they are installed. The other LV feeders in the same area on the other hand, which might also exhibit relatively significant overvoltages, will see changes equivalent to only the small effect that the STATCOM reactive power absorption has on the voltage drop across the distribution transformer. The addition of further STATCOMs in the multiple STATCOMs solution achieves a substantially higher reduction of the upper voltage limit violation metric. Despite its disadvantage in terms of being unable to correct phase voltage unbalance, where it is able to be applied the OLTC solution achieves the best overall performance with respect to reduction of overvoltage violation as it reduces the proportional metric for this to 21.13%.

Table 19 – Upper and lower voltage limit violation proportions and a selection of percentiles for the LV voltage distributions for the six LV areas exhibiting significant curtailment given application of different voltage management solutions

Local LV voltage metric	BAU with thermal upgrades	Curtailment reconductoring	One STATCOM per LV area	Multiple STATCOMs per LV area	OLTCs
99th percentile maximal-phase LV (V)	265.84	259.90	257.88	257.98	264.76
95th percentile maximal-phase LV (V)	260.78	259.27	257.24	256.72	259.91
90th percentile maximal-phase LV (V)	259.69	257.76	256.42	255.77	257.80
Proportion of LV buses with maximal phase voltage over 253V (%)	56.98	52.08	47.17	26.42	21.13

In Figure 36, each of the line-neutral voltages are shown against distance for the longest overhead LV path in the six LV areas studied for high solar day conditions at noon in summer. Dashed curves indicate voltages in BAU with only thermal upgrades applied, while solid curves represent the voltages after application of the single STATCOM solution. It is clear that substantial improvement is affected in all of the phase voltages not just at the remote end of the LV feeder where the STATCOM was installed, but along its entire length. Note that due to the strong phase imbalance in the original network voltages, the B phase component of the STATCOM is heavily generating reactive power to raise the voltage rather than absorbing reactive power to lower it. In fact, the B phase voltages were below the 216V statutory limit prior to STATCOM application, despite the abundance of solar generation.

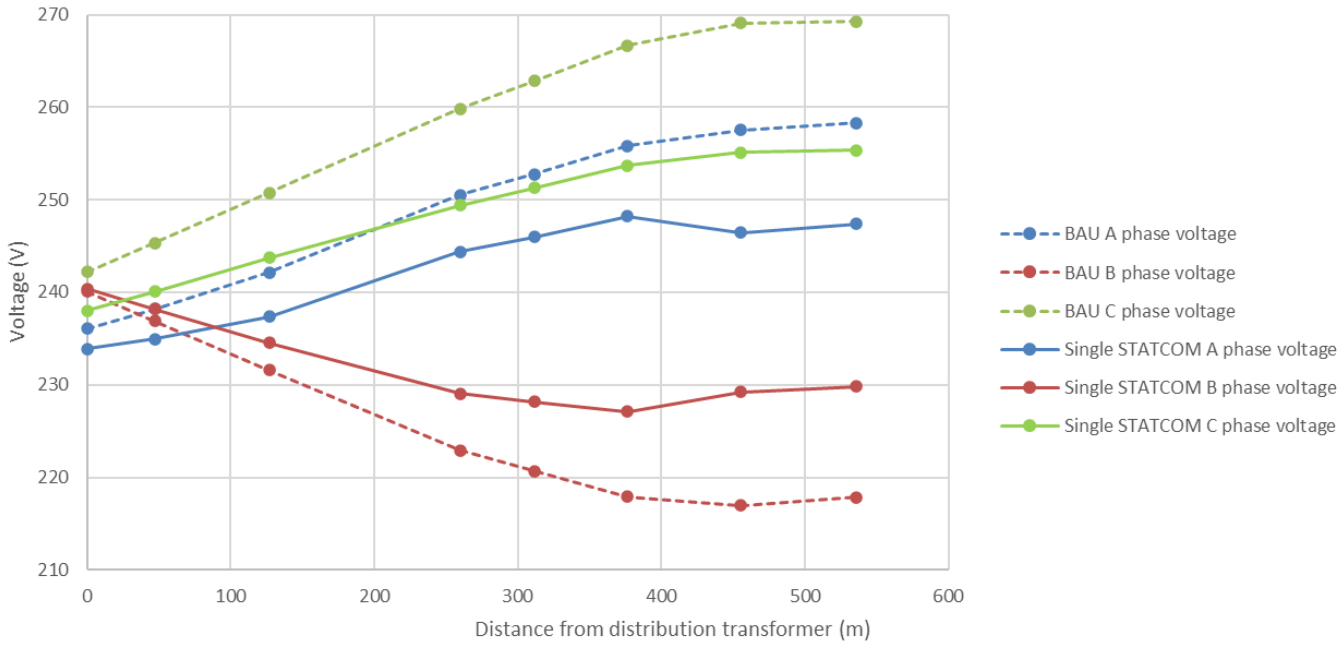

Figure 36 – Phase-neutral voltages against distance for the longest overhead LV path in the six areas studied before and after STATCOM application

The equivalent voltage against distance plot for the same LV feeder with the OLTC solution applied would not be worth showing as an OLTC could not be applied to the distribution transformer for this particular feeder due to the BAU lower limit violating undervoltages present on it. Figure 37 therefore shows a voltage against distance plot for one of the other LV areas on which an OLTC solution could be applied without producing undervoltage violating the lower limit. While the A and B phase-neutral voltages have been pulled down below the upper limit of 253V, the C phase-neutral voltage has been pulled down so far that it encroaches on the lower limit. The minimum phase-neutral voltage value on C phase after application of the OLTC in this case is 220.18V.

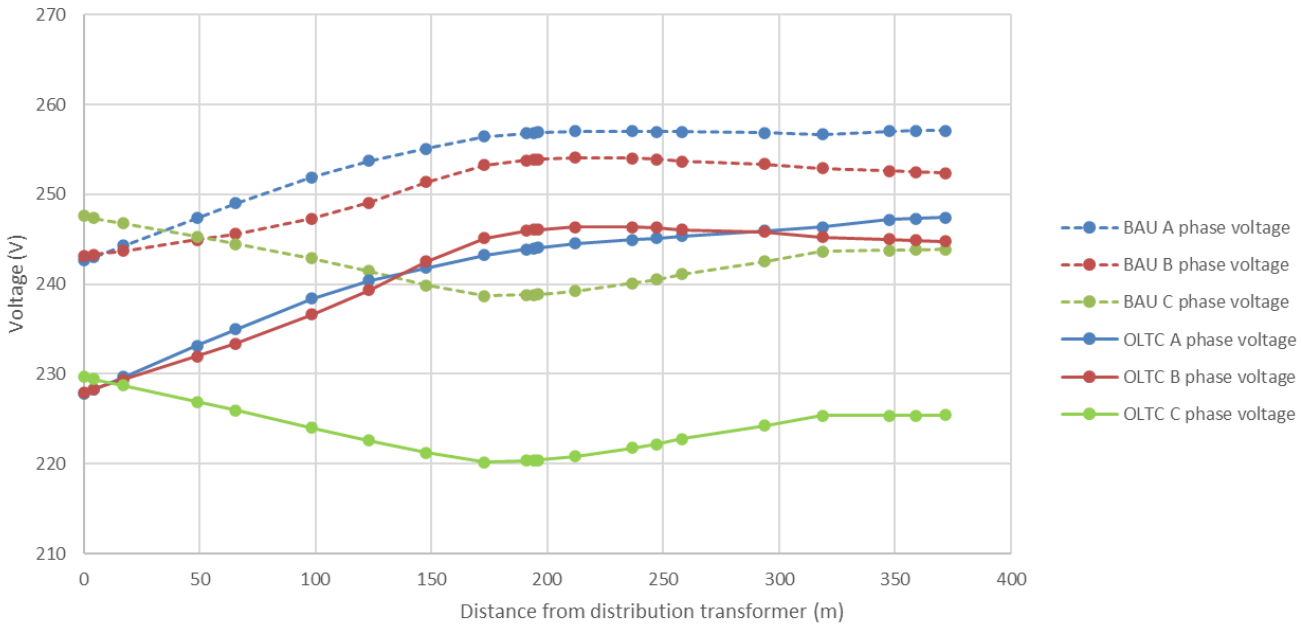

Figure 37 – Phase-neutral voltages against distance for an LV feeder on one of the LV areas for which an OLTC solution could be applied before and after OLTC application

6.6 Cost-benefit analysis

As a further investigation of the benefits provided by dSTATCOMs, a cost-benefit analysis was performed on the voltage management solutions tested in the previous section. The benefit of each solution was quantified using the customer export curtailment value (CECV) metric created by the AER [20]. The CECV represents the value of alleviating the curtailment of solar energy so that it is delivered to the network. It is noted here that CECV is not the only form of financial benefit that would be provided by voltage management solutions. Although the rectification of power quality issues involving voltages exceeding the statutory limits would serve to protecta DNSP's reputation in the eyes of their customers and would therefore hold some significant financial value, it is beyond the scope of the analysis in this report to try and quantify this value.

In the six LV areas for which the effectiveness of voltage management solutions was investigated in this report, 194 customers were identified as owning solar PV installations in 2035 in the Step Change scenario. For each of the solutions investigated and for the baselined scenario with thermal upgrades applied to the network, the curtailed solar energy for these specific PV installations were calculated for each of the half hour periods across a high solar day in each season. Multiple methodologies for the calculation of annual CECV are suggested in [20], including representations using half-hourly data for an entire year and sets of characteristic days spanning triplets of regional load and regional solar generation estimates. For the purposes of this study, the CECV was estimated using extrapolation of the curtailment results for high solar days in each season across the length of the year (noting that curtailment on low solar days is zero in general). This extrapolation was performed using analysis of the solar irradiance data that had been used to delineate high and low solar days in each season in the methodology described in section 4.2. Specifically, the cumulative daily solar irradiance values of the three lowest and three highest solar irradiance days identified in step 3 of this process were collected for each season and each of the MV feeders. These high and low cumulative daily solar irradiance value sets were then averaged to formulate eight "typical" cumulative daily solar irradiance values; one typical high value and one typical low value for each season. The daily cumulative solar irradiance data for the entirety of the baseline year was then analysed to identify what proportion of the days in each season exhibited cumulative solar irradiance values that were closer to the typical high value.

The proportions of high solar days determined for each season using this process were then used to extrapolate the high solar day curtailment results out for the duration of that season. This then allowed the formulation of four seasonal daily curtailed energy curves i.e. curves representing the estimate for the total amount of curtailed solar energy in each half-hour period of the day for that season. Note that the use of solar irradiance data for the baseline year to perform annual extrapolation of curtailment results for the year 2035 is valid because annual solar irradiance patterns are unlikely to change significantly during the years between now and 2035.

To estimate CECV values, scaling factors from the AER's CECV workbook were used [21]. Averages of these scaling factors were taken across the days in each season in the year 2035; separate averages for each half-hour period throughout the day were calculated to form daily curves that were representative of each season. Note that taking averages of the half-hourly scaling factors is reasonable as the value of alleviated curtailment varies with both regional load as well as regional solar generation availability. The scaling factors used were also specific to the NEM region of Queensland. The four seasonal daily curtailed energy curves were then multiplied with these average daily CECV scaling factor curves, then multiplied with the number of days in each season to extrapolate the financial estimates out to form annual CECV figures. The financial benefit of the alleviation profile provided by each solution investigated was then calculated by taking the difference between

the CECV for the baselined scenario with thermal upgrades in 2035 in Step Change and the CECV for each of the individual voltage management solution scenarios respectively.

The costs for the curtailment re-conductoring voltage management solution were estimated using per-unit-length cost estimates for each line type provided. These cost estimates were multiplied with the cumulative lengths of each line type that had been used in the upgrades. Costs estimates for the OLTC and STATCOM options were also based on figures sourced from industry.

The final results for the cost-benefit analysis are shown in Table 20. The differences between annual CECV in each of the voltage management solution scenarios and annual CECV in the BAU with thermal upgrades scenario have been calculated and recorded as annual CECV benefit. It is clear that the solutions involving STATCOMs outperform the other options in terms of cost. In terms of annual CECV benefits, multiple STATCOMs provide the most benefit while OLTCs provide the second highest amount of benefit, singular STATCOMs per LV area provide the third highest benefit while re-conductoring provides the lowest benefit. Note that financial performance metrics such as the payback period or benefit-cost ratio have not been calculated as additional sources of value, such as the protection of Energex's reputation with its customers, would also need to be quantified to make the business cases for any of the options presented below viable.

Table 20 – Cost-benefit analysis final results

Voltage Management Solution/Scenario	Cost ($AUD)	Annual CECV ($AUD)	Annual CECV Benefit ($AUD)
BAU with thermal upgrades	0	3,555	0
Curtailment reconductoring	11,145,753	3,216	339
One STATCOM per LV area	78,000	1,700	1,855
Multiple STATCOMs per LV area	169,000	1,241	2,314
OLTCs	340,000	1,519	2,036

7 Conclusion

This study has investigated the effectiveness of dSTATCOMs in addressing the voltage management issues that are expected to arise in Australian distribution networks in the coming years. It also compared this effectiveness to that of two conventional network augmentation strategies: re-conductoring and OLTC installation. For this purpose, a highly detailed network model of a zone substation area in Brisbane, Queensland was constructed in the power system modelling package PowerFactory. This model included representations of thousands of individual residential and commercial/industrial customer connections. Potential trends in future growth of rooftop solar PV installations and household EVs were also modelled by scaffolding from two of the scenarios included in AEMO's 2022 ISP and the impacts of these on the voltage management of the network, and on curtailment of the solar generation, were studied. The PV and EV projections in the milder Slow Growth scenario were deflated by 20% while the projections in the more extreme Step Change scenario were inflated by 20% for the purposes of this study, so that the envelope of results obtained would be likely to encapsulate all credible future possibilities. Export limits were applied only to the existing PV generators for which records indicated they were in place and were not applied to future PV installations.

The overall level of energy lost throughout the network due to curtailment of solar generation was found to be fairly insignificant. Even in the penultimate year of the Step Change scenario, the ratio of solar energy curtailed to solar energy generated in just the half-hour period around noon on a day with high solar irradiance in summer, was only 2.3%. This figure tends towards much larger values when viewed for particular customers at fringe areas of the network model however, which highlights the fact that the curtailment phenomenon can be expected to remain primarily an issue of social equity, rather than of major opportunity cost to the Australian economy at large.

Despite the effective action of the volt-watt and volt-var functions in existing and future PV installations to manage voltage during the hours of the day with high solar irradiance, overvoltages exceeding the upper statutory limit were still identified in both the Slow Growth and Step Change scenarios. The prevalence of limit-violating over or undervoltages in the maximal and minimal of the phase-neutral voltages (respectively) on each of the LV buses across the network was used to perform a simplified hosting capacity assessment of the network studied. Adopting the rule that having 5% or more of LV bus violating a limit in their most extreme phase was unacceptable, it was found that hosting capacity would be reached due to PV generation at noon in summer shortly after 2030 in the Step Change scenario, but that it would not be reached during the evening peak at any year due to EV charging in either scenario and that it would not be reached at noon either in Slow Growth. If uniform non-compliance with AS4777.2 was pessimistically assumed to be universal across the network however, meaning that volt-watt and volt-var functions were assumed to be inactive, then the hosting capacity of the network was found to be reached immediately at noon in 2025 in both ISP scenarios. This highlights the size of the positive effect on voltage management that is furnished by the volt-watt and volt-var functions throughout the hours of the day that see solar generation active. The voltage unbalance characteristics across the LV network at noon in summer for high solar day conditions were also found to be worsened through the progressive years of both ISP scenarios as further PV is introduced into the system.

The particular PV and EV growth values predicted for 2035 in the Step Change scenario were selected for the investigation of the effectiveness of voltage management solutions. To increase the realism of the study, a large number of upgrades were made to the ratings of distribution transformers and MV and LV distributions lines across the model in this particular year so that the majority of thermal violations that were found to be

flagging in BAU simulations at noon under high solar day conditions would be addressed. It was found that the predominant effect of these upgrades was to redistribute the curtailment around the network and that when this was viewed at a global model scale, the net effect on the curtailment distribution was only a small reduction. Analyses of the thermal overloads that would occur at noon given high solar day conditions were performed across all years of both ISP scenarios; these analyses identified that MV and LV buried cable runs and overhead conductor spans would need replacing in significant numbers, but that the transformers in particular will be likely to see the worst and most rapidly emerging overloads in general. Simulations conducted at 7.30pm found that the levels of thermal violations during the EV charging peak, coincident with the usual evening load peak, would be significantly lower than during noon under high solar day conditions.

Six specific LV areas exhibiting relatively high curtailment were then selected for the purposes of comparing the effectiveness of voltage management strategies. Complete re-conductoring of these LV areas, installation of singular STATCOMs to each of them, installation of multiple STATCOMs to each of them (with variations depending on the size of the area) and OLTC installation on the distribution transformer were then modelled in separate scenarios with the BAU thermal-motivated upgrades already present in each. A third traditional network augmentation solution of LDC algorithm alteration was considered, but then discarded on the grounds that the existing LDC voltage settings are already relatively low.

Re-conductoring was found to be the worst-performing solution, both in terms of curtailment and overvoltage reduction. The single and multiple STATCOMs exhibited progressively better outcomes, while the OLTC option exhibit performance that was slightly better than the multiple STATCOMs option. One downside of the OLTC option however is that it can only affect uniform upward or downward translation of the phase voltages on its connected LV system; it cannot independently correct the individual phase-neutral voltages in the network in the same way that a STATCOM can. As a consequence, the apparent performance of the OLTC option was determined largely by the level of voltage unbalance in the six particular LV areas selected for study; two of the four areas could not have OLTCs installed as they already exhibited voltage on one of their three phases that was encroaching on the lower statutory limit. It is therefore the case that a different selection of LV areas could see significantly higher or lower curtailment and overvoltage reduction performance outcomes for the OLTC solution. This highlights an advantage of the STATCOM solution which, on the other hand, can inherently correct the magnitude of the voltage on separate phases in different directions as needed.

A simple cost-benefit analysis also found multiple STATCOMs to perform better than all other options in terms of both cost and annual CECV benefits. This demonstration of the superior cost-effectiveness of STATCOMs as a solution for distribution network voltage management issues indicates that it will be useful in maximizing the value of investments in the distribution network in a lot of cases. This would make it an instrumental component of future urban renewable energy zones which are intended to hopefully drive a large part of the national energy transformation.

Inadvertently, this study has also revealed that thermal issues, rather than voltage management issues, are likely to be the most severe and rapidly emerging issue for Australian DNSPs. None of the solutions applied for the purposes of dealing with voltage management issues will also cost-effectively deal with the emerging thermal capacity issues. Reasonable efforts were made to incorporate BAU thermal upgrades of distribution transformers and lines in this study; a comprehensive analysis of these fell outside of its scope. It is evident that batteries employed in the LV distribution networks are likely to be a successful and cost-effective strategy for addressing thermal capacity exhaustion, especially as future battery costs are expected to reduce.

Reference List

[1] N. Stringer, A. Bruce, I. MacGill, N. Haghdadi, P. Kilby, J. Mills, T. Veijalainen, M. Armitage and N. Wilmot, “Consumer-Led Transition: Australia's World-Leading Distributed Energy Resource Integration Efforts,” *IEEE Power and Energy Magazine,* pp. 20-36, 2020.

[2] S. Heslop, N. Stringer, B. Yildiz, A. Bruce, P. Heywood, I. MacGill and R. Passey, “Voltage Analysis of the LV Distribution in the Australian National Electricity Market,” Collaboration on Energy and Environmental Markets, Sydney, 2020.

[3] J. Braslavsky, P. Graham, L. Havas, J. Sherman, B. Spak, M. Khorasany, R. Razzaghi, S. Heslop, S. Dwyer, E. Langham, K. Nagrath, J. G. Orbe, J. Hossain, I. Ibrahim and R. Amin, “Low voltage network visibility and optimising DER hosting capacity,” RACE for 2030, 2021.

[4] A. Dinning, D. S. Tan, P. Pradhan, S. Casey, C. Thiris, C. Williams, L. Rakotojaona, M. Kundevski, O. Lacroix, P. Lelong and S. Logan, “Future grid for distributed energy,” ARENA, Melbourne, 2020.

[5] Endeavour Energy, “DER INTEGRATION STRAGEY AND BUSINESS CASE,” Sydney, 2022.

[6] Australian Energy Market Operator, “2022 Integrated System Plan,” AEMO, 2022.

[7] GLOBAL SOLAR ATLAS, “Brisbane City Project detail,” [Online]. Available: https://globalsolaratlas.info/detail?c=-27.469287,153.023758,11&s=-27.468968,153.023499&m=site&pv=small,0,28,1. [Accessed 08 06 2023].

[8] *AS/NZS 4777.2:2020 Grid connection of energy systems via inverters Part 2: Inverter requirements,* STANDARDS Australia; STANDARDS NEW ZEALAND, 2020.

[9] B. Yildiz, S. Adams, S. Samarakoon, N. Stringer, A. Bruce and I. MacGill, “N2 Fast Track Curtailment and Network Voltage Analysis Study (CANVAS),” RACE for 2030, 2021.

[10] Energex, *SUPPLY & PLANNING MANUAL,* 2019.

[11] Energex, “Distribution Annual Planning Report,” 2021.

[12] P. Graham and L. Havas, “Electric vehicle projections 2021,” CSIRO, Australia, 2021.

[13] P. Graham, “Electric vehicle projections 2022,” CSIRO, Australia, 2022.

[14] Australian Bureau of Statistics, *Census of Population and Housing: Housing data summary,* 2021.

[15] Australian Bureau of Statistics, “Transport: Census,” Australian Bureau of Statistics, 28 06 2021. [Online]. Available: https://www.abs.gov.au/statistics/industry/tourism-and-transport/transport-census/latest-release#:~:text=Key%20statistics%201%20The%20average%20number%20of%20motor,reported%20having%20two%20or%20more%20vehicles.%20More%20items. [Accessed 08 06 2023].

[16] P. Heywood, “Historical Market Trends of Distributed Photovoltaic Inverters in Australia,” in *Proceedings of the Asia Pacific Solar Research Conference*, Canberra, 2019.

[17] CLEAN ENERGY COUNCIL, *CLEAN ENERGY COUNCIL GUIDELINES FOR GRID-CONNECTED SOLAR PV SYSTEMS - (NO STORAGE),* 2022.

[18] W. J. Nacmanson, J. Zhu and L. N. Ochoa, “Milestone 8: EV Management and Time-of-Use Tarriff Profiles,” Department of Electrical and Electronic Engineering, The University of Melbourne, Melbourne, 2022.

[19] P. Kundur, Power System Stability and Control, McGraw-Hill, Inc., 1994.

[20] Australian Energy Regulator, “Final CECV Methodology,” Australian Energy Regulator, 2022.

[21] Australian Energy Regulator, “CECV Workbook,” 30 June 2023.

Appendix A - Volt-watt and volt-var QDSL script validation procedure

The QDSL script written to represent volt-watt and volt-var functions on solar PV installations in Queensland for this project were implemented on the "Load Flow Control" component of the QDSL modelling options available in PowerFactory. This means that the script works by reading the phase-neutral voltages calculated by the standard load flow algorithm, then adjusting the active and reactive power outputs of each PV generator according to its own equations, then allowing the load flow algorithm to recalculate the phase-neutral voltages again using this new information. This cyclical process then continues for many iterations. As it constitutes an additional complication to the iterative load flow algorithm, it has the potential to produce non-convergent solutions i.e. network voltages and power flows that are substantially different from the real voltages and power flows that would occur in that network in the real world. This potential for non-convergence meant that the design of the QDSL script for volt-watt and volt-var functionality had to be rigorously tested and the load flow algorithm settings under which it would produce accurate, convergent solutions had to be carefully identified.

The volt-watt and volt-var QDSL script was validated using the same test network as used in section 3.3. Using the final phase-neutral voltages of each of the nodes and active and reactive power outputs of each of the PV generators in the test network for each of the load flow simulations performed in section 3.3, the theoretical curtailment values that each PV generator component should have been operating at were calculated. These theoretical curtailment values are compared to the final curtailment values calculated by the QDSL script instances for each of the six curtailment curves that were presented in section 3.3.

The theoretical curtailment curves do not correspond to error bars for the curtailment results, nor do they correspond to the correct value of curtailment in each simulation case. The correct value of curtailment in each simulation case lies between the final curtailment value calculated by the QDSL script and the theoretical curtailment value implied by the final set of phase-neutral voltages and power flows in the load flow solution. Nevertheless, the close agreement between the QDSL-calculated curtailment values and the theoretical curtailment values shown in to implies good performance of the QDSL script in general; the discrepancy between the two is bounded by $\pm 1.25\%$ in general.

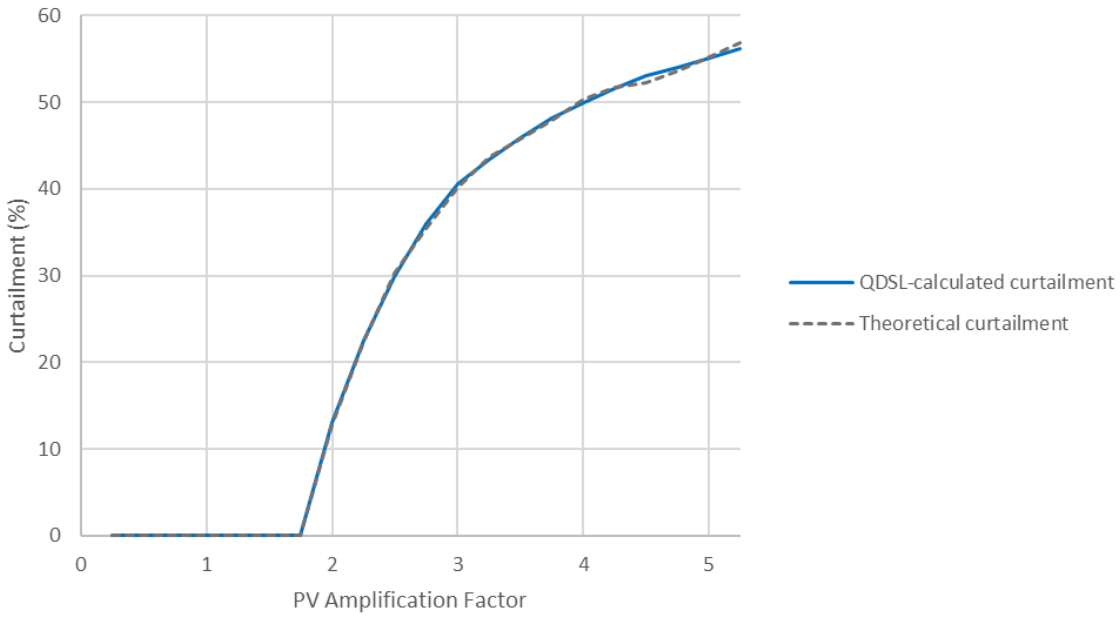

Figure 38 – Comparison of theoretical and QDSL-calculated curtailment curves for 7/.064 copper conductor modelled with sequence network-based lines and 0.96 pu source voltage

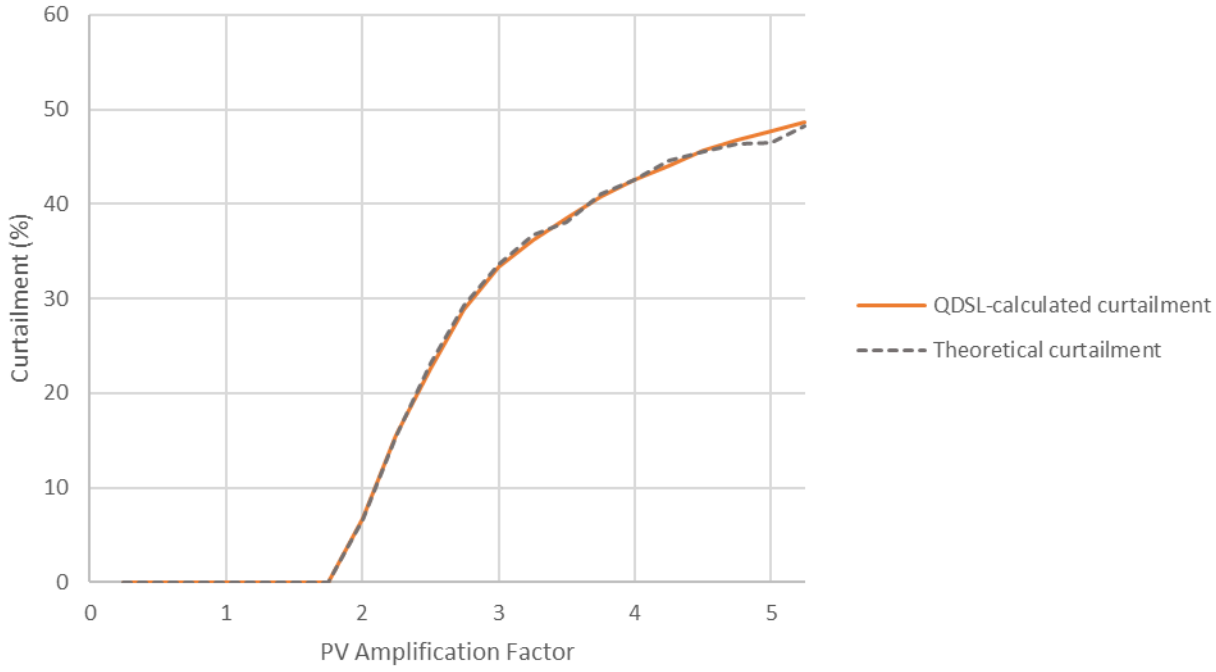

Figure 39 – Comparison of theoretical and QDSL-calculated curtailment curves for 7/.064 copper conductor modelled with coupled geometric lines and 0.96 pu source voltage

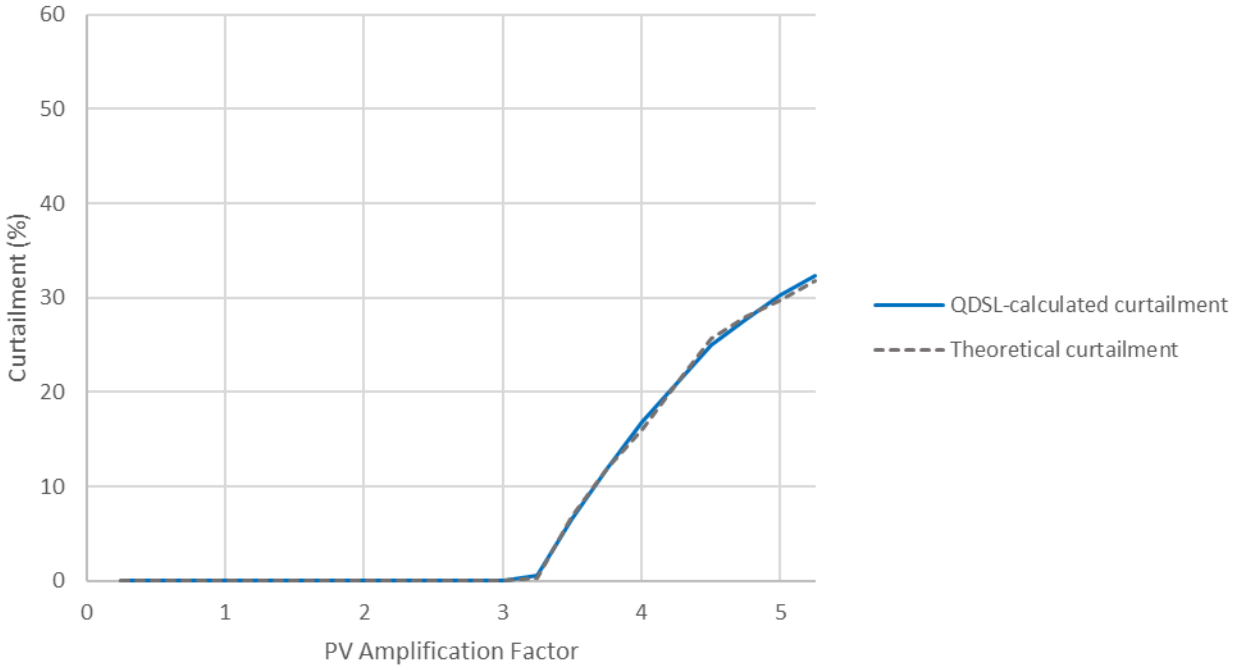

Figure 40 – Comparison of theoretical and QDSL-calculated curtailment curves for 7/.080 copper conductor modelled with sequence network-based lines and 0.96 pu source voltage

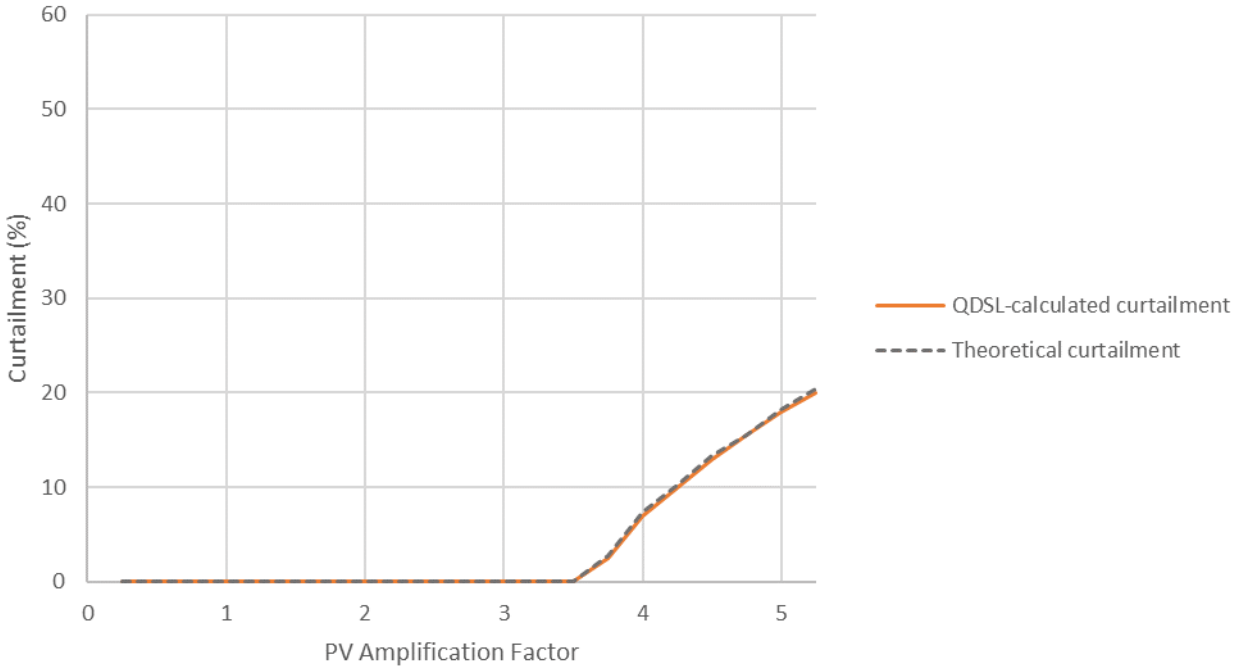

Figure 41 – Comparison of theoretical and QDSL-calculated curtailment curves for 7/.080 copper conductor modelled with coupled geometric lines and 0.96 pu source voltage

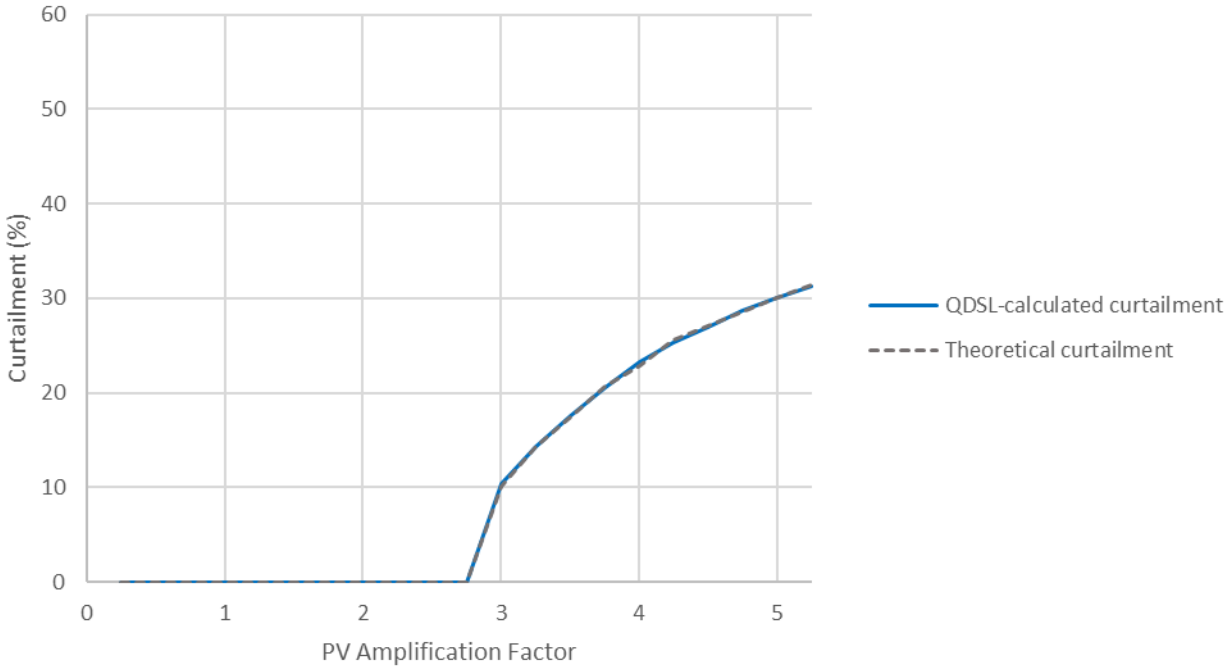

Figure 42 – Comparison of theoretical and QDSL-calculated curtailment curves for Libra conductor modelled with sequence network-based lines and 1.0 pu source voltage

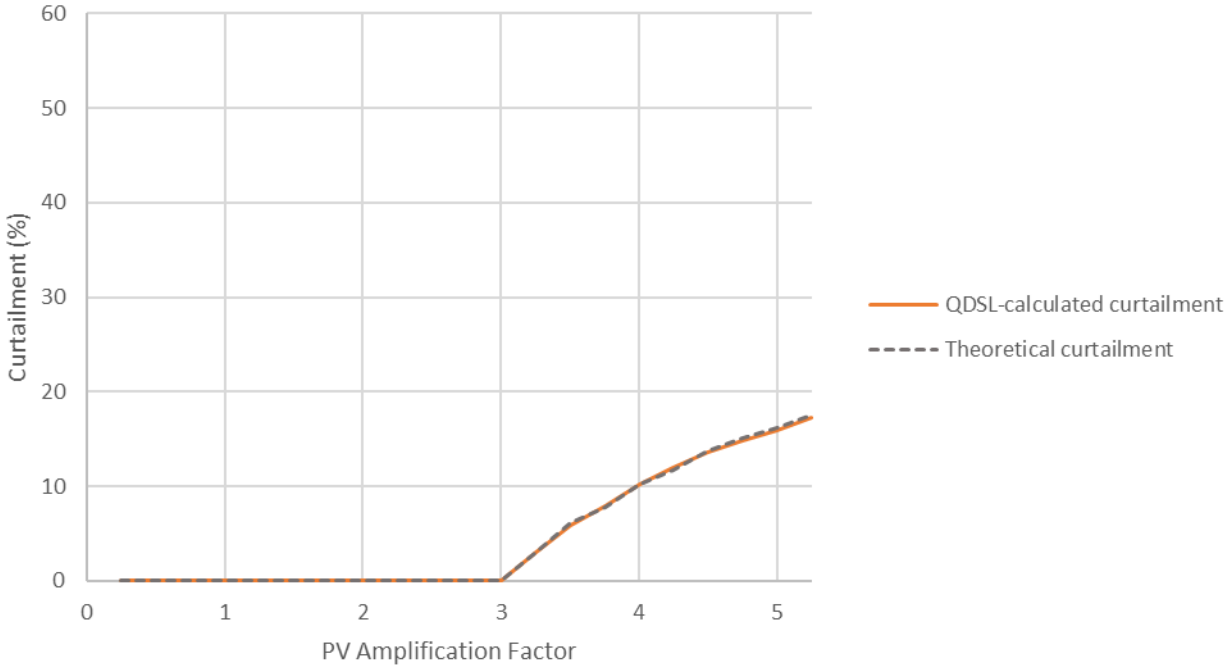

Figure 43 – Comparison of theoretical and QDSL-calculated curtailment curves for Libra conductor modelled with coupled geometric lines and 1.0 pu source voltage

Appendix B – Investigations of line modelling methods

The type of model used for the distribution lines was found to have significant influence on the phase-neutral voltages in the LV networks studied for this project. Correct calculation of these voltages was imperative as many of the LV networks modelled were relatively unbalanced (i.e. in terms of the amount of load and generation they had connected on each phase), and the curtailment results produced by the volt-watt and volt-var QDSL script are sensitive to phase-neutral voltages.

The most detailed and accurate form of line model available in PowerFactory is a coupled geometric model. This type of line model requires input of the geometric position of each the phase and neutral lines relative to each other and the earth (i.e. heights above ground and horizontal distances from each other) as well as the diameter and resistance per unit length of the type of conductor or cable used. PowerFactory uses the geometric position information for each conductor to calculate self-resistances and reactances for each conductor per unit length as well as coupling resistances and reactances between each pair of conductors in the line. While this type of model calculates phase-neutral voltages with a high degree of accuracy, the amount of detail and effort required to build it for buried cable types of lines in particular is non-trivial; detailed information concerning the types of materials and thickness of the sheath, screen and other layers of the buried cables must be entered. The simulation times observed with this type of line model were also found to be longer in general.

The other type of line model available in PowerFactory is the sequence network-based line model. Three-phase line with neutral models which represent the self and coupling impedances of the neutral wire separately are available as well as equivalent three-phase models that incorporate the impedances of the neutral into the positive and zero sequence impedances of the network. Of these, the former is a more accurate representation of the lines and was studied for incorporation into this project. The resistances and reactances for the positive and zero sequence networks for these models, as well as the self and coupling resistances and impedances for the neutral wire representation, were formulated using four by four impedance matrices generated for each conductor type by running geometric conductor spacing and thickness information through the alternative (electromagnetic) transient program ATP.

Simulations with coupled line models were observed to be slower than those with sequence network-based line models; there was thus a motivation to save simulation time by using the second type of line model. However, since the coupled geometric model represents the four-by-four impedance matrices that characterise each conductor type precisely, whereas the sequence network-based models represent the lines with an approximation of these, the validity of the second type of model had to be tested before its use in this project could be justified. This testing was carried out by calculating the maximal curtailment results for a simple radial LV test network. The test network was designed using data from one of the LV networks studied in the project. Two of the three radial spurs of this system were disconnected from the distribution transformer for the network and reconnected together in a daisy-chain fashion, to create a radial system with only one spur. The three most remote buses in this system were then removed to bring the total length of the LV feeder below 400 meters to maintain a realistic representation of the longest credible LV feeder lengths in lightly loaded areas of the Energex network.

Versions of the test network with both coupled geometric and sequence network-based line models were developed. The conductor types 7/.064 copper, 7/.080 copper and Libra were used in multiple separate sequences of simulations. The voltage magnitude of the grid source component representing the connection

up into the 11 kV network was set to 0.96 pu for simulations with the smaller gauges of 7/.064 copper and 7/.080 copper and to 1.0 pu for simulations with the larger gauge of Libra.

In order to investigate the worst-case curtailment conditions due to over voltages, the curtailment during the half-hour time period of noon alone was calculated. The load was set to the value that it would have had in the original network at noon. The solar PV generators in the test network were set to a cumulative peak generation value of 44.44 kW; 70% of the installed inverter capacity. The total capacity and active power output of the PV generators in the test system were then scaled up using a gradually increasing amplification factor and many simulations investigating the maximal curtailment in the test network were carried out. The largest distribution transformers connected to residential load systems in the modelled network tend to have capacities of 500 kVA. As a conservative estimate, it was decided that a cumulative installed PV inverter capacity of twice the distribution transformer rating was likely to be the largest amount of PV that a DNSP would permit to have installed on any of their LV networks in general. It is noted here that some residential load systems in the modelled network are connected to distribution transformers with ratings of 750 kVA and even 1000 kVA. These are rare however and would likely have their cumulative installed PV inverter volumes limited more strictly than to twice the transformer capacity. For the most part, 750 kVA and 1000 kVA distribution transformers are connected to commercial or industrial loads with significantly shorter LV feeder lengths, which would not be likely to produce the highest PV curtailment conditions throughout any given area of the network.

The amplification factor was therefore not increased beyond a value of 15.75 in general, which corresponds to a total installed PV inverter capacity of ~1000 kVA, although the load flow simulations were often found to be non-convergent at amplification factors smaller than this. The maximal curtailment values identified on any PV inverter in the test system for both sequence network based and coupled geometric 7/.064 copper lines are plotted against PV amplification factor in Figure 44. Owing to the high resistance of this type of conductor, the curtailment reaches values upwards of 50% for high PV amplification factor. The sequence network based and coupled geometric line models yield similar results, with a maximum discrepancy of ~7.5%. Relative to maximal curtailment values on the order of 50%, this level of error was deemed to be tolerable in general.

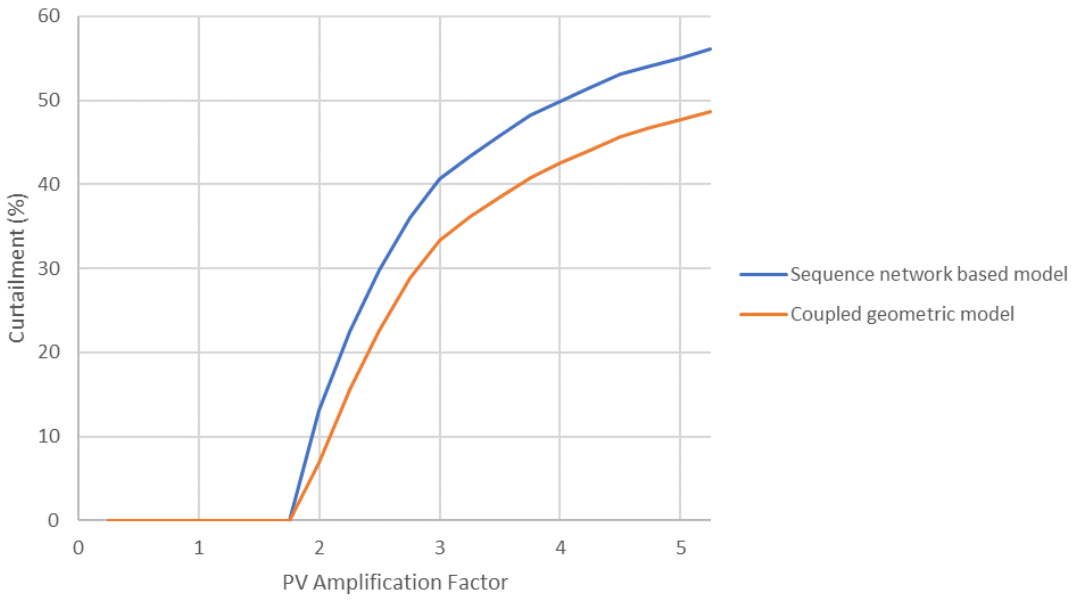

Figure 44 – Maximal curtailment vs PV amplification factor across test network with 7/.064 copper lines modelled with sequence network-based models and coupled geometric models with 0.96 pu source voltage

The maximal curtailment values identified on any PV inverter in the test system for both sequence network based and coupled geometric 7/.080 copper lines are plotted against PV amplification factor in Figure 45. Owing to the lower resistance of this type of conductor relative to 7/.064 copper, non-zero curtailment only commences at amplification factors around 3.25-3.5 and only reaches values around 20-30%. The discrepancies between the sequence network based and coupled geometric line models are larger in this case, with a maximum discrepancy of ~12%. Relative to maximal curtailment values on the order of 20-30%, this level of error is more significant.

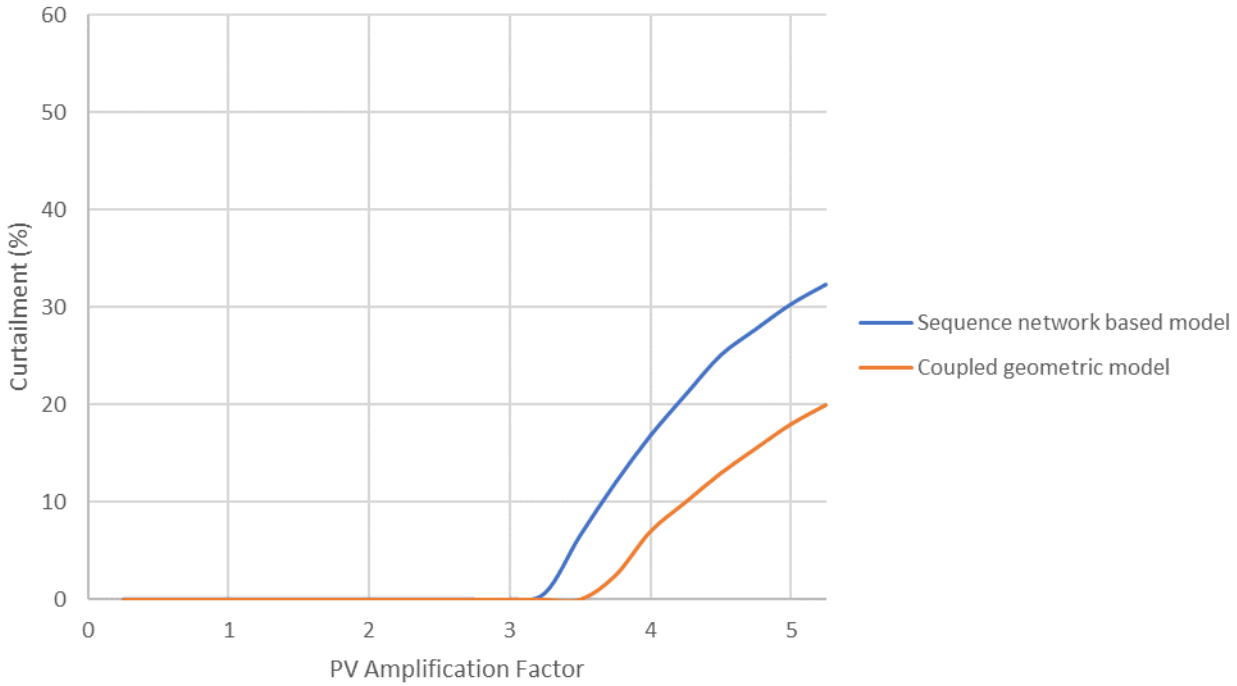

Figure 45 – Maximal curtailment vs PV amplification factor across test network with 7/.080 copper lines modelled with sequence network-based models and coupled geometric models with 0.96 pu source voltage

The maximal curtailment values identified on any PV inverter in the test system for both sequence network based and coupled geometric Libra lines are plotted against PV amplification factor in Figure 45. The grid source component representing the connection to the 11 kV network was increased to 1.0 pu for this conductor type. Even still, non-zero curtailment only commences at amplification factors around 3.25-3.5 and only reaches values around 17-31% due to the significantly lower resistance of this type of conductor relative to both 7/.064 and 7/.080 copper. The discrepancies between the sequence network based and coupled geometric line models in this case are also similar to those shown in Figure 45 for 7/.080 copper conductor.

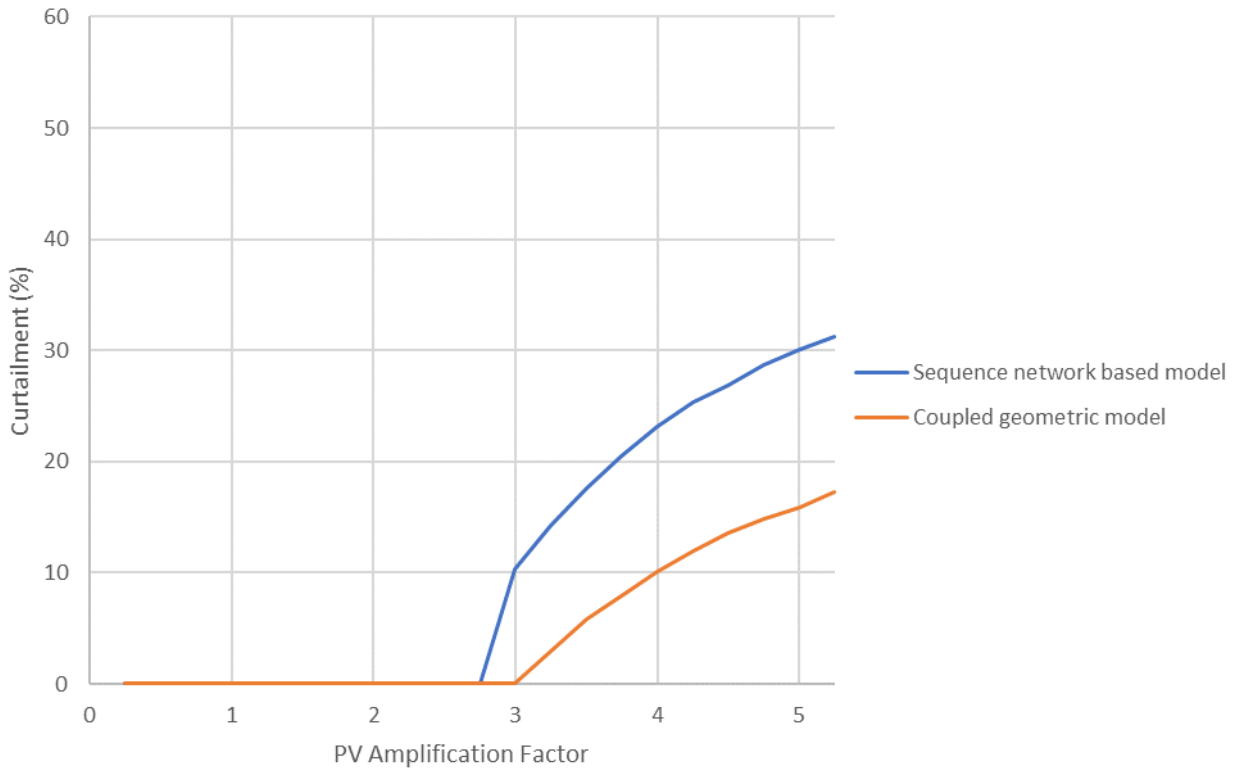

Figure 46 – Maximal curtailment vs PV amplification factor across test network with Libra lines modelled with sequence network-based models and coupled geometric models with 1.0 pu source voltage

These results demonstrate the trend that for conductor types with larger ratings and hence lower resistances per unit length, the curtailment results predicted by simulations with sequence network-based line models and coupled geometric line models will differ by larger relative amounts, with sequence network-based lines predicting more pessimistic results in general. The results predicted by coupled lines are expected to be more accurate in general.

It was therefore decided that the final version of the PowerFactory simulation model for this project should be developed using coupled geometric line models. The detailed geometric information needed to produce such models for the buried LV cables in the modelled area of the network was not available at the time that the baselining of the model was to be carried out, however. Since the baselining process depends only on positive sequence voltage magnitudes and total three-phase current values in general, it was decided that the baselining would be conducted on an initial version of the model built using sequence network based lines and that this model would be re-built using coupled geometric lines before it was to be used for simulating futuristic scenarios in which high levels of curtailment would be expected.

Appendix C – Detailed thermal utilisation data for network model

Table 21 – Transformer thermal capacity utilisation data for noon in summer under high solar day conditions in the Slow Growth scenario

Transformer thermal capacity utilisation metric	2025	2030	2035	2040	2045	2050
99th percentile (%)	110.91	147.7	160.4	176.88	191.87	199.05
95th percentile (%)	95.25	119.53	130.55	135.87	141.74	155.3
90th percentile (%)	85.66	104.7	112.47	116.71	122.99	137.78
80th percentile (%)	67.75	78.99	89.4	93.16	99.68	116.06
50th percentile (%)	38.82	46.43	53.97	54.66	57.99	67.81
Proportion exceeding 100% utilisation (%)	3.93	10.92	15.28	16.59	20.09	27.07
Proportion exceeding 150% utilisation (%)	0	0.87	2.62	3.49	3.93	6.11

Table 22 – Transformer thermal capacity utilisation data for noon in summer under high solar day conditions in the Step Change scenario

Transformer thermal capacity utilisation metric	2025	2030	2035	2040	2045	2050
99th percentile (%)	193.06	294.83	342.68	420.00	432.01	496.35
95th percentile (%)	158.40	243.94	267.23	323.91	339.63	424.14
90th percentile (%)	138.20	202.70	235.76	280.08	296.44	357.70
80th percentile (%)	113.19	149.38	194.04	216.13	232.07	268.14
50th percentile (%)	63.90	95.20	123.71	135.49	145.34	169.42
Proportion exceeding 100% utilisation (%)	25.33	46.39	61.57	69.59	71.08	74.77
Proportion exceeding 150% utilisation (%)	6.55	20.10	36.24	43.30	48.19	57.41

Table 23 – MV overhead span and buried cable run thermal capacity utilisation data for noon in summer under high solar day conditions in the Slow Growth scenario

MV overhead span and buried cable run thermal capacity utilisation metric	2025	2030	2035	2040	2045	2050
99th percentile (%)	36.52	41.58	48.78	52.91	56.14	63.05
95th percentile (%)	25.43	30.03	34.50	37.42	40.87	45.36
90th percentile (%)	20.36	23.11	26.23	28.09	30.84	35.22
80th percentile (%)	11.46	14.69	16.02	16.89	18.30	21.32
50th percentile (%)	3.25	3.81	4.15	4.31	4.80	5.07
Proportion exceeding 90% utilisation (%)	0.00	0.00	0.00	0.00	0.00	0.13

Table 24 – MV overhead span and buried cable run thermal capacity utilisation data for noon in summer under high solar day conditions in the Step Change scenario

MV overhead span and buried cable run thermal capacity utilisation metric	2025	2030	2035	2040	2045	2050
99th percentile (%)	66.54	106.13	130.83	160.22	176.56	203.83
95th percentile (%)	44.43	71.48	88.95	111.04	126.21	136.29
90th percentile (%)	34.65	56.55	65.98	82.94	89.07	95.67
80th percentile (%)	21.64	36.35	42.16	56.88	65.37	66.51
50th percentile (%)	4.97	8.55	9.62	13.41	16.13	19.39
Proportion exceeding 90% utilisation (%)	0.00	2.17	4.96	9.35	9.88	12.01

Table 25 – LV overhead span thermal capacity utilisation data for noon in summer under high solar day conditions in the Slow Growth scenario

LV overhead span thermal capacity utilisation metric	2025	2030	2035	2040	2045	2050
99th percentile (%)	46.91	60.76	63.62	70.08	73.18	81.59
95th percentile (%)	27.40	34.12	36.69	38.60	41.45	45.24
90th percentile (%)	20.22	24.61	27.53	28.65	30.36	33.79
80th percentile (%)	13.57	16.62	18.35	19.11	20.25	22.29
50th percentile (%)	4.36	5.84	6.52	6.92	7.28	7.95
Proportion exceeding 100% utilisation (%)	0.00	0.05	0.10	0.15	0.21	0.43
Proportion exceeding 80% utilisation (%)	0.10	0.33	0.39	0.59	0.76	1.11

Table 26 – LV overhead span thermal capacity utilisation data for noon in summer under high solar day conditions in the Step Change scenario

LV overhead span thermal capacity utilisation metric	2025	2030	2035	2040	2045	2050
99th percentile (%)	75.67	119.70	139.88	177.51	210.20	213.58
95th percentile (%)	45.44	66.94	75.33	93.16	116.98	116.07
90th percentile (%)	33.36	48.73	56.68	70.21	80.48	83.17
80th percentile (%)	22.92	33.29	37.81	46.08	52.79	55.16
50th percentile (%)	8.06	10.60	13.79	16.37	17.20	19.22
Proportion exceeding 100% utilisation (%)	0.32	2.14	2.41	4.19	6.84	6.67
Proportion exceeding 80% utilisation (%)	0.81	3.38	4.40	7.30	10.23	11.32

Table 27 – LV buried cable run thermal capacity utilisation data for noon in summer under high solar day conditions in the Slow Growth scenario

LV buried cable run thermal capacity utilisation metric	2025	2030	2035	2040	2045	2050
99th percentile (%)	52.22	59.92	66.62	70.19	75.51	79.38
95th percentile (%)	36.01	38.67	43.21	46.10	48.94	53.23
90th percentile (%)	26.75	30.62	34.15	35.28	37.18	40.65
80th percentile (%)	16.74	19.94	22.64	23.86	26.04	28.89
50th percentile (%)	5.21	6.21	6.94	7.31	7.97	9.00
Proportion exceeding 120% utilisation (%)	0.13	0.14	0.14	0.14	0.16	0.20

Table 28 – LV buried cable run thermal capacity utilisation data for noon in summer under high solar day conditions in the Step Change scenario

LV buried cable run thermal capacity utilisation metric	2025	2030	2035	2040	2045	2050
99th percentile (%)	79.40	119.41	136.70	159.57	179.18	190.10
95th percentile (%)	52.04	77.09	90.76	112.61	123.07	133.78
90th percentile (%)	39.90	61.81	69.74	87.38	100.17	104.96
80th percentile (%)	28.54	42.14	47.68	60.15	69.22	71.71
50th percentile (%)	8.87	13.86	18.07	21.25	23.61	26.15
Proportion exceeding 120% utilisation (%)	0.26	0.94	1.70	3.88	5.50	6.93

Appendix D – Eight-wire coupled tower geometry modelling for doubled 95mm² ABC

The upgrades which were made to the BAU model to represent attempts to address thermal rating violations, as well as those which were performed to represent re-conductoring for the purposes of addressing curtailment, were done by adding a second parallel circuit to the first. In practice however, 95mm² ABC conductor would be upgraded by adding a second parallel circuit to the same series of poles on which the first were installed. In physical principle, this differs from the first approach as the closer proximity of the two four-wire circuits implies a greater amount of inductive coupling and hence a different mutual inductance matrix for the overall double 95mm² ABC circuit.

In order to test the significance of this effect, an eight-wire coupled geometric tower model for double 95mm² ABC representing the true orientation of the second circuit above the first on the same system of poles was created in PowerFactory and used to re-calculate the global curtailment percentiles presented in Table 16 in this study. The results are shown in Table 29; it is clear that the effect on the curtailment distribution is negligible when compared to the effect of applying the BAU thermal upgrades in general. This justifies the use of a second separate four-wire coupled geometric circuit to represent upgrades of 95mm² ABC to double 95mm² ABC in the BAU thermal upgrades and curtailment reconductoring upgrades applied in this study.

Table 29 – Global curtailment percentiles in Step Change in 2035 with two different modelling methods used for doubled 95mm² ABC conductor

Global curtailment metric	Without BAU thermal upgrades	With BAU thermal upgrades; 95mm² ABC represented with a second parallel four-wire coupled geometric tower model circuit	With BAU thermal upgrades; 95mm² ABC represented with eight-wire coupled geometric tower models
99th percentile (%)	16.25	15.74	15.42
95th percentile (%)	6.16	5.93	5.90
90th percentile (%)	3.85	3.66	3.64
80th percentile (%)	1.63	1.56	1.57
50th percentile (%)	0.00	0.00	0.00

www.racefor2030.com.au

RACE for 2030

Australian Government
Department of Industry, Science, Energy and Resources

AusIndustry
Cooperative Research Centres Program